Addis Ababa University

HYDROPOWER GENERATION AND OPERATION PLANNING FOR ETHIOPIA

Doctoral Dissertation of:
Firehiwot Girma Dires

A dissertation submitted to the Graduate School of Electrical and Computer Engineering in partial fulfillment of the requirements for the Degree of Doctor of Philosophy (Ph.D.) in Electrical Engineering (Electrical Power Engineering).

December 2023
Addis Ababa, Ethiopia

Addis Ababa University

School of Graduate Studies

Addis Ababa Institute of Technology

School of Electrical and Computer Engineering

HYDROPOWER GENERATION AND OPERATION PLANNING FOR ETHIOPIA

Doctoral Dissertation of:

Firehiwot Girma Dires

dires@kth.se / firehiwotgirma@gmail.com

Supervisor

Dr. Getachew Bekele, School of Electrical and Computer Engineering
Addis Ababa Institute of Technology/Addis Ababa University

Co-Supervisor

Prof.Mikael Ameline, School of Electrical Engineering and Computer Science
KTH Royal Institute of Technology

HYDROPOWER GENERATION AND OPERATION PLANNING FOR ETHIOPIA

Author

Firehiwot Girma Dires _____

Examination committee:

Examination chairperson

Dr.Libsework Negash _____

Addis Ababa Institute of Technology

External Examiner

Prof.Viktoria Martin _____

KTH Royal Institute of Technology

Internal Examiner

Prof.N.P.Singh _____

Addis Ababa Institute of Technology

Supervisor

Dr.Getachew Bekele _____

Addis Ababa Institute of Technology

Co-Supervisor

Prof. Mikael Amelin _____

KTH Royal Institute of Technology

Declaration

This Ph.D. dissertation is a presentation of my own work and any material used from other sources has been clearly identified and properly acknowledged and cited.

Abstract

The Ethiopian power system is highly dominated by hydropower plants. Almost 90% of the generation is covered by hydropower. Although the total generation capacity in the power system is sufficient enough to cover the peak demand, it is common to see load shedding and power rationing in the country, especially in the dry seasons of the year. The absence of a suitable and appropriate generation planning tool makes the current planning dependent on historical generation patterns.

Recent literature has shown different models for hydropower planning for long-term and short-term operation in a deterministic, stochastic, stochastic dynamic, etc., with different levels of details and mathematical formulations. However, most of the models are concerned with profit maximization and cost minimization in a competitive electricity market. In addition, no previous studies have been conducted, and no models have been developed for the planning of the unique Ethiopian power system. The Ethiopian power system is a system dominated by hydropower generation, which is dependent on seasonal rainfall. The electricity market is a vertically integrated market where the government determines the electricity price. Therefore, there is no price uncertainty and less concern about cost or profit. The primary concern for the planning of the Ethiopian power system will be the proper scheduling of the power plants to use the stored water in the rainy season through the dry season with minimum load shedding to increase system reliability while keeping the balance between load shedding now and in the future. In principle, load shedding can be avoided by using all the water available right now, but then, if there is a poor rainy season with low inflow the following year, the power system may get into a massive problem supplying the demand for that year. Before the market deregulation, the electricity market in developed European countries was almost similar to what is practiced in Ethiopia now. The difference is they have much more details of measurements and statistics about inflows, run time between reservoirs, etc.

This thesis develops different hydropower planning tools, including deterministic and stochastic, risk-neutral, and risk-averse models for the Ethiopian power system based on the limited available data, intending to utilize the water stored in the rainy season throughout the year with minimum load shedding. It further studies and tests the models in a rolling horizon framework for long-term operation.

The Methodology used to develop the hydropower planning tool is, first, all the necessary data for the planning is collected from Ethiopian Electric Power (EEP), inflow is scaled from the mean annual energy (MAE) of each reservoir using the publicly available precipitation data from NASA. Then, the deterministic model is developed and compared with the historical generation data. In hydropower generation, inflow is an uncertain stochastic process. To consider the uncertainties in the inflow, the deterministic model is further developed into a two-stage stochastic model. To run the stochastic model, we formulate a method to prepare a synthetic historical inflow series from the available data on hand and derive a method to estimate the stochastic process that mimics the synthetic historical series. We use Monte Carlo simulation to generate random inflow scenarios from the estimated stochastic process. The stochastic planning model is then tested both in a risk-neutral and a risk-averse version. We use Conditional Value-at-Risk (CVaR) risk measure to develop the risk-averse model. Finally, the performance of the models developed is compared using a rolling horizon framework for a one-year planning period.

The results show that the Ethiopian power system has a great deal of flexibility to be operated more efficiently to minimize load shedding. The results also show that by using stochastic models, we can better manage the water in the reservoirs in the form of slightly lower load shedding without compromising the energy we reserve for the next planning period. We could also avoid large load shedding events so that the load shedding is evenly distributed throughout the year instead of having massive load shedding in a short period, which could be very valuable when we have higher load demand in Ethiopia. When testing the hydropower planning tools for current load demand, there is a very good generation capacity to supply the demanded load. However, there was significant load shedding in the actual operation, even though the planning model suggested no need for load shedding. It is concluded that it will be an improvement if the planning is supported by stochastic planning tools instead of using the method depending on historical data.

Keywords

Hydroelectric power generation, power system planning model, Deterministic model, Stochastic model, Rolling horizon, Time series analysis, Uncertain inflow.

Acknowledgements

First and foremost, I would like to express my heartfelt gratitude to the Almighty God for making my dream a reality and providing me with the strength to complete this journey.

I am incredibly thankful to my supervisors, Dr. Getachew Bekel and Prof. Michael Amelin, for their unwavering support, patience, and dedication in reviewing my work. Without them, this endeavor would not have been possible. Additionally, I am thankful to the EEP staff, Ato Andarge Eshete (Head of Generation planning) and Ato Mikiyas Wondimu (Dispatch center), for providing me with critical data on the Ethiopian power system. Their support, coupled with the generous assistance from SIDA, laid the foundation for my research work.

I would also like to extend my appreciation to my childhood friends, Dr. Yenesew Mengiste, Dr. Tigis Fetene, Workaferahu Abebe, and all my friends and siblings around me that I can't finish describing the names for their moral support and encouragement, and to my office-mates and KTH friends, Dr. Evelin Blom, Dr. Stefan Stankovic, Dr. Priyanka Shinde, Dr. Lars Herre, Dr. Elis Nycander, Saeed Nordin, Luigi Viola, and all members of the PEM research group, for their continuous support and experience sharing. Most of all, I am indebted to my AAIT colleagues, including Kena Likasa, Teshome Hambisa, Mesfin Tessema, Yared Bekele, and many others, for making me feel at home and taking care of me when I needed it.

Finally, I cannot forget to mention my family, especially my loving husband, Michael Mitiku, and my children, Saron, Eliana, and Kaleab Michael. Your belief in me, your emotional support, and your love have kept me motivated throughout this process.

Contents

List of Figures

List of Tables

Acronyms

ACF	auto-correlation function. 35, 45, 46
ARIMA	autoregressive integrated moving average. 47
CVaR	Conditional Value-at-Risk. iv, 29, 30, 65
EEA	Ethiopian Energy Authority. 14
EEP	Ethiopian Electric Power. iv, 14, 17, 19, 21
EEU	Ethiopian Electric Utility. 14
EVPI	Expected value of perfect information. 27
GERD	Grand Ethiopian Renaissance Dame. 1, 2, 13, 14, 65
GHG	greenhouse gas. 1
GIS	The current and future geographic information systems. 11
GTP	Growth and Transformation plan. 2
HE	Hour Equivalent. 20
IHA	International Hydropower Association. 2
LBQ	Ljung-box Q-test. 45, 46
MAE	mean annual energy. iv, 33, 37
MAI	Mean Annual Inflow. 20, 33
MILP	A stochastic mixed-integer linear program. 10, 11
MOWIE	Ministry of Water Irrigation and Energy. 14
NEXRAD	Next Generation Weather Radar. 11
PAR	periodic autoregressive. 11

PARMA periodic autoregressive-moving average. 11, 12

PRMS Precipitation-Runoff Modeling System. 11

SARIMA seasonal autoregressive integrated moving average. 34, 45

SDDP stochastic dual dynamic programming. 11

SWAT Surface Water Assessment Tool. 11

VRES variable renewable energy resources. 1, 24, 65

VSS Value of the Stochastic Solution. 25, 27, 28

1 Introduction

1.1 Background

Hydropower has been the most flexible, affordable, clean, and renewable energy resource worldwide for the last several decades. It is the third largest power source, next to coal and natural gas. In 2020, one-sixth of the global electricity demand was supplied from hydropower. Today, hydropower plants constitute 30% of the world's capacity of flexible electricity supply, with almost 60% untapped potential worldwide [1]. The flexibility and controllability of hydropower plants play an important role in the transition of the energy system towards more variable renewable energy resources (VRES) and the reduction of greenhouse gas (GHG) emissions. One of the disadvantages of VRES in the power system is the frequency stability due to the uncontrolled variable generation. In order to keep the power system stable, there must be a balance between generation and consumption (load). This will not be the case in the event of continuous load variation as well as wind and solar power generation variations in the system. These variations lead to a change in system frequency. The frequency decreases when a load increases or a loss of production from one power source is not compensated by a corresponding increase from another source in the system. The active power production must be regulated to keep the frequency within the acceptable limit. To achieve this, the system needs flexible resources such as hydropower. Hydropower is an excellent flexible resource because it can rapidly increase or decrease, and the energy can be stored in reservoirs. There will be no loss of energy by regulating the hydropower. The stored water can be used later to increase hydropower generation when there is a shortage of wind or solar power in the system.

The global hydropower expansion is expected to slow down because of the growing concern about the availability of sites for large projects in developed countries and environmental impacts such as displacement of habitats in the area, resource displacement, and reservoirs being a barrier to the free movement of fishes. However, to meet the net zero GHG emissions target, expanding hydropower plants and other renewable energy resources, solar and wind, is essential. On the other hand, the fast growth of hydropower plants is observed in Southeast Asia and Africa. Sub-Saharan Africa is expected to record the third-largest growth over the next decade, which is driven by the growth of electricity demand, the need for electricity access at a low cost, and the abundant availability of untapped hydropower resources. This growth includes the nation's largest hydropower plant, the Grand Ethiopian Renaissance

Dame (GERD), under construction with an installed capacity of approximately 6 GW, and the KOYESHA hydropower plant, with an installed capacity of 2.16 GW, also under construction.

Hydropower is the most dominant power source in Ethiopia and many other countries in Africa. According to the International Hydropower Association (IHA) 2022 hydropower status report, Africa's energy generation by hydropower is 146 TWh in 2021, with 21% of this generation being from Eastern African countries, of which 45% is from Ethiopia [2]. Hydropower constitutes 90% of the country's electricity generation, with an overall national potential of as much as 45 GW [3]. To harness this considerable national potential, the government is working on further expansion of hydropower capacity with mega projects like GERD.

Currently, Ethiopia is in the third period of Economic reform following Growth and Transformation plan (GTP)-II, which is a ten-year plan applied to the period from 2020-2030. Some of the targets in the energy sector include boosting the annual per capita electricity consumption from 86 kWh to 1,269 kWh, upgrading the power generation capacity from 4,180 MW to 17,208 MW, of which 75% of the generation comes from hydro, and the rest 25% generation will be covered from other energy resources. This increases the share of solar from zero to 6.2%, wind from 5.9% to 10.2%, and Geothermal from 0% to 11.3% in 2030 [4].

To ensure the timely provision of reliable and sufficient electricity access and to address the ambitious plans, the power sector should have all the facilities, recent technologies, and power system planning tools for a reliable system operation. The current method of generation and operation planning in the Ethiopian power system is performed based on the historical generation of the power plants and the historical water level of the reservoir, putting the growth of demand into consideration; this will be further explained in Chapter 2, Section 2.3. This method of operation planning is open to various errors, especially when there is no accurate forecast about future demand, when the system expands, and when the number of renewable resource integrations increases. At this point, we need to have a proper generation and operation planning tool in the system.

1.2 Problem statement

The total generation capacity in the Ethiopian power system is sufficient enough to cover the peak demand of the system. However, it is an energy-deficient system because of the hydropower dominance and lack of planning tools. The absence of a suitable and appropriate generation planning tool makes the planning dependent on historical generation patterns, and it does not account for the uncertainties in the inflows of the reservoir in the different seasons. With the help of a proper planning model, the water management in the reservoirs could be improved to minimize or avoid repeated load shedding and power rationing, especially towards the dry season and the end of the planning year in Ethiopia and most African countries' power systems. This leads to the two main research questions of this thesis:

Q1: What should a long-term hydropower planning look like? This is how we can optimize the generation scheduling among the hydropower plants to manage the water in the reservoirs in such a way that the excess water in the rainy season is utilized in the dry season. This can be broken down to the specific objectives as follows.

a) How long should the time resolution and planning horizon be? The time resolutions can be hourly, daily, weekly, or monthly, depending on the planning horizon. and the planning horizon can be for days, weeks, months, or years, depending on the type of planning, short-term, mid-term, or long-term planning.

b) How do we deal with the objective of the planning model? Load shedding now or later? How To find an appropriate trade-off between using the available water now (risking future energy shortage) or starting load shedding to a smaller or lesser extent now? If we focus only on reducing load shedding, we might drain the reservoirs, and we may not have sufficient water for the next planning period. If the focus is to store water for the next planning period, we may end up shedding unnecessary loads and spilling water at the end of the year.

c) What type of model should it be, deterministic or stochastic, risk-neutral or risk-averse? This is how we can deal with the uncertainty of parameters in the planning.

Q2: How to generate inflow scenarios when there is a lack of well-organized data? Here, we need to prepare Synthetic historical inflow data and identify the stochastic process to generate random inflow scenarios. This can be broken down to specific objectives:

a) How can we use time series analysis to generate synthetic historical inflow series?

b) How should the statistical process be identified and the model be formulated to generate random inflow scenarios for each reservoir?

1.3 Research objectives

The main objective of this research is to develop a long-term hydropower generation and operation planning model for the Ethiopian power system. The planning model will be utilized to simulate the Ethiopian power system to properly schedule the hydropower plants to find an appropriate trade-off between using the available water now (risking future energy shortage) and starting load shedding to a smaller or lesser extent now.

This research answers the two questions described in section-1.2 to fulfill the main objective of the project through the three specific objectives below.

Objective 1: To develop a deterministic hydropower planning model for the long-term operation of the Ethiopian power system and compare the result with the actual operation of the system. To simulate the model further to see how the system reacts to increased demand. (Research question Q1)

Objective 2: To develop synthetic historical inflow time series, identify the stochastic process that mimics the historical inflow series, and generate inflow scenarios that can be used in stochastic models. (Research question Q2)

Objective 3: To develop a long-term stochastic hydropower model for the Ethiopian power system considering the uncertainty of the inflow and the risk associated with the worst scenarios in the system. (Research question Q1)

1.4 Scientific Contributions

The main scientific contributions of this work, which are used to answer the two research questions, are summarised here. These contributions are addressed in the publications of this Ph.D. project. Table 1.1 describes the relationship between research questions, contributions, and publications.

Cont-I: To apply a standard hydropower planning model for the Ethiopian power system to minimize load shedding by optimizing the hydro scheduling so that the excess water

Table 1.1: Scientific contributions and research questions with corresponding publications, J* represent journal and C* conference publications

Research Questions	Contributions					
	I	**II**	**III**	**IV**	**V**	**VI**
Q1	C1	C1				
Q2			J1	J1	J2	J2

in the rainy season can be utilized in the dry season.

Cont-II: To investigate the flexibility of the Ethiopian hydropower system for better operation and how the existing power plants could be used more efficiently and effectively to avoid the load shedding encountered in the dry season.

Cont-III : To derive a method for generating a synthetic historical time series by combining the available data at hand. And identify the stochastic process that mimics the synthetic historical inflow time series by applying existing methods.

Cont-IV: To generate random but realistic inflow scenarios. The method is applied to the Ethiopian power system to demonstrate how the generated scenarios can be applied in Ethiopia's long-term deterministic hydropower planning model.

Cont-V: To develop a long-term stochastic hydropower planning model for the Ethiopian power system considering the uncertainties in the inflow and the risk associated with the worst inflow.

Cont-VI: To test the planning model in a rolling horizon framework for the long-term stochastic model in which only a subset of the time horizon decision is considered at a time. The model rolls in a fixed horizon, with the first period updated in each roll.

1.5 Publications

All publications are included in the dissertation.

[C1] Dires, F.G.; Amelin, M.; Bekele, G. Deterministic Hydropower Simulation Model for Ethiopia. 2021 IEEE Madrid PowerTech, 521 PowerTech 2021 Conference Proceedings 2021. https://doi.org/10.1109/PowerTech46648.2021.9494862.

Summary: This paper presents a long-term deterministic linear simulation model for the Ethiopian hydropower system, intending to utilize the water stored in the rainy

season throughout the year with minimum load shedding. Two cases are simulated and compared to historical data. It is shown that the Ethiopian hydropower system has a great deal of flexibility to be operated in a more efficient way to minimize load shedding

[J1] **Dires, F.G.**; Amelin, M.; Bekele, G. Inflow Scenario Generation for the Ethiopian Hydropower System. Water 2023, 15(3). 484 https://doi.org/10.3390/w15030500.

Summary: This paper presents a method of developing synthetic historical inflow time series and techniques to identify the stochastic process that mimics the behavior of the time series and generates inflow scenarios. The methodology was applied to the Ethiopian power system. The time series were analyzed using statistical methods, and the stochastic process that mimics the inflow patterns in Ethiopia was identified. It is shown that the generated inflow scenarios give a realistic output of generation scheduling and reasonable reservoir content based on the actual operation.

[J2] **Dires, F.G.**; Amelin, M.; Bekele, G. Long-Term Hydropower Planning for Ethiopia: A Rolling Horizon Stochastic Programming Approach with Uncertain Inflow. Energies 2023, 16, 7399. https://doi.org/10.3390/en16217399

Summary: This paper compares deterministic as well as stochastic models for a weekly rolling horizon framework considering inflow uncertainty. The stochastic model is tested both in a risk-neutral and a risk-averse version. The Conditional Value at Risk (CVaR) risk measure is used to develop the risk-averse stochastic model. The results show that the risk-neutral and the best risk-averse models perform almost similarly and are better than the deterministic model.

Contributions of authors

Firehiwot G. Dires is the main author of the three papers C1, J1, and J2. For these publications, Firehiwot G. conducted the research, developed the models, and wrote the papers under the supervision of Professor Mikael Ameline and Dr. Getachew Bekele. The two supervisors also reviewed, edited, and provided their feedback on all three papers.

1.6 Thesis Outline

The rest of the dissertation is organized into five chapters as follows:

Chapter 2 Introduces the concept of hydropower generation and operation planning and presents a review of the literature written on the topic. Then discusses the current method of generation and operation planning in the Ethiopian power system.

Chapter 3 Describes the different Methodologies conducted in the research work and introduces the different types of mathematical models formulated for each planning method developed in the Ph.D. project.

Chapter 4 Compares the simulation results from each model to the actual operation and discusses the results of the various case studies conducted in the model development process.

Chapter 5 Concludes the thesis and identifies topics for future work in the research area of long-term hydropower planning.

2 Hydropower Generation and Operation Planning

Hydropower generation is the conversion of the potential energy and the kinetic energy of fast-flowing elevated water to mechanical energy through turbine blades and the turbine's mechanical energy to electrical energy through generators.

There are three types of hydropower plants: reservoir, pumped storage, and run-of-river. Reservoir hydropower plants include dams that enable water storage for extended periods to be released based on demand.

Fig 2.1 illustrates the main components of a typical hydroelectric generating unit. Water flows from an elevated area called the forebay at a certain speed (U) through an intake structure called the penstock. The penstock is used to convey water from the forebay to the turbine. Wicket gates are adjustable and pivot open around the periphery of the turbine to control the amount of water admitted to the turbine [5]. The turbine is coupled with the generator through the shaft to produce electrical power.

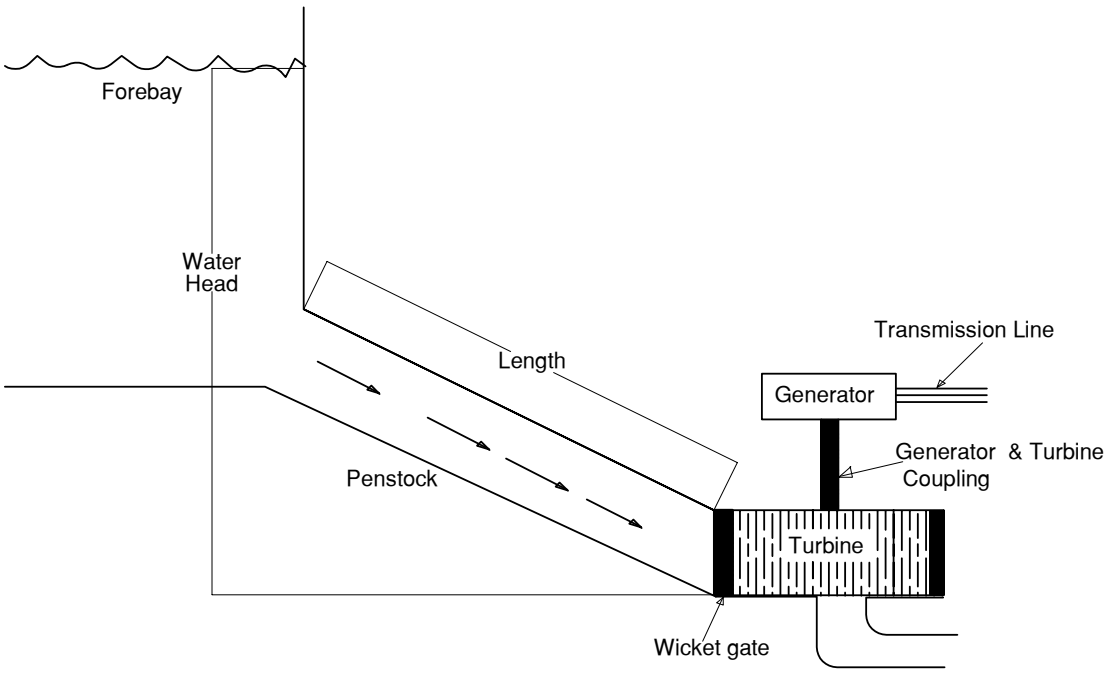

Figure 2.1: Simplified schematic of hydropower plant

Pumped storage hydropower plants consist of two reservoirs, upper and lower. The water released from the upper reservoir will be captured in the lower reservoir and pumped to the

upper reservoir to store energy. The stored water will be released through turbines based on demand. Run-of-river hydropower plant generates electricity based on the natural water flow with limited or temporary storage capacity.

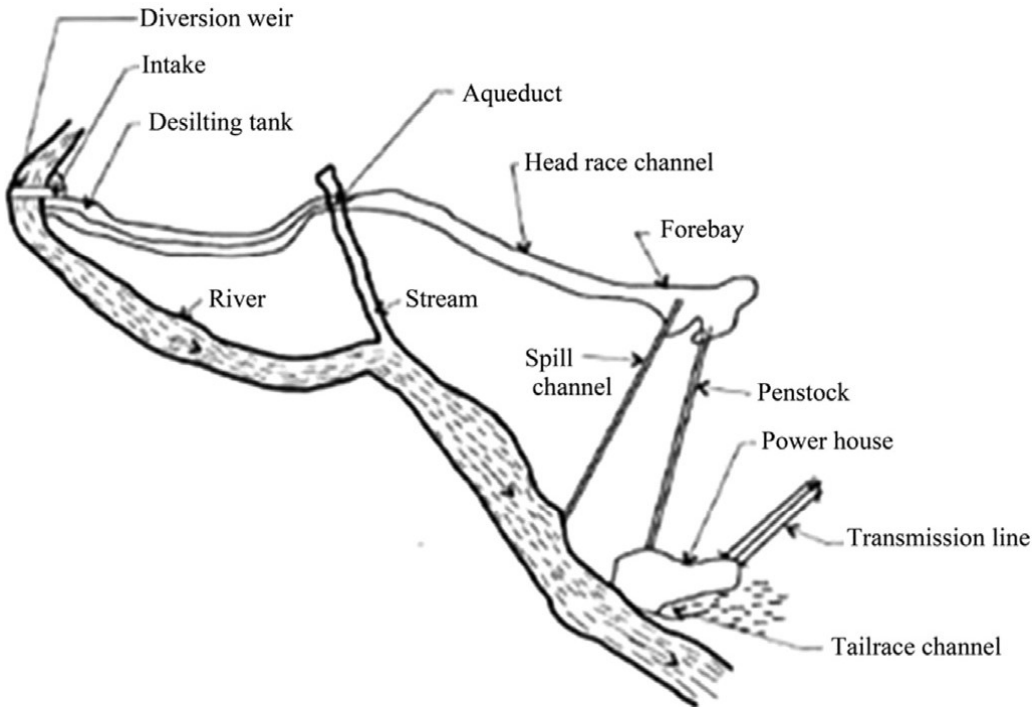

Figure 2.2: Simplified schematic of run-of-river hydropower plant [6]

Fig2.2 shows the schematic of a run of the river hydropower plant. In this scheme, water is diverted from the river by the diversion weir. The weir is constructed across the river, maintaining continuous flow through the intake. Water is then passed through the desilting tank, where sand particles are settled. The water from the desilting tank goes to the forebay tank through a channel. From the forebay tank, water is passed to the turbine through the penstock and strikes the turbine blades, the turbine is connected to the generator through a shaft to produce electrical power [6].

The majority of the hydropower plants in the Ethiopian power system have large reservoirs, which allow water to be stored for extended periods and used when the demand is high or when other generation sources are scarce in the system. There are also a few run-of-river power plants in the system.

Hydropower operation is expected to be reliable and economical. It should generate

as much energy as possible with optimum operating cost. For the proper operation of hydropower plants and utilization of the water stored in the reservoirs as efficiently as possible, considering both technical and economic aspects, hydropower planning is required. Typically, there are a few shorter periods with substantial inflow each year, and the task of hydropower planning is to decide during which periods this water should be used. In a country like Ethiopia, where hydropower plants highly dominate power generation, the water stored in the rainy season should be planned for long-term use, depending on the seasonality of the inflows to the reservoirs.

Hydropower Planning can be divided into three categories based on the time in the planning horizon. Planning for short time frames, weeks, or days (Short-term planning), planning for months (Mid-term planning), and planning for several months, seasons, or years (Long-term planning).

2.1 Hydropower planning in the literature

Hydropower planning models have been developed and well-investigated for several decades [7–10] and [11]. There is a wide range of ways to model hydropower for short-term, mid-term, and long-term, including deterministic, stochastic, and dynamic models, for example, [12–16] and [17–21]. Some of them use linear models; others use non-linear models, deterministic models, stochastic models, and dynamic models. A linear programming approach for hydro scheduling and power flow algorithm is applied to a long-term problem but with short-term phenomena in [13], and the challenges of short-term hydropower scheduling are presented for the Norwegian power system in [19]. The effect of uncertain wind power and large wind power in the system on short-term hydropower planning is addressed in[20].

Algorithms such as deterministic optimization, stochastic dynamic programming, sampling stochastic dynamic programming, and a scenario tree approach are compared with ensemble streamflow prediction for a hydropower reservoir operation in [22]; the results show that methods based on scenarios prove superior to methods based on probability distribution. A stochastic mixed-integer linear program (MILP) for a yearly self-scheduling model is formulated in [23], considering uncertain streamflow and residual demand curve using a three-stage scenario tree with 90 scenarios for a price maker hydropower producer in the Greek power system. In [24], a sensitivity analysis of short-term hydropower planning for a

price-taker hydropower producer is presented with uncertain volume inflow and spot market price. A stochastic MILP model is developed in [25] with the idea of exploring the effects of including uncertainty explicitly into optimization by comparing the stochastic approach to a deterministic approach for a Norwegian hydropower producer. A stochastic model for a hydro-thermal system with uncertain reservoir inflow is presented in [26].

In long-term hydropower planning, the water coming to the reservoirs at different times of the year, which is the inflow to the reservoirs, needs to be estimated. Hydrologists use watershed models to estimate stream flow, surface run-off, water quality, flood management, and water management. The review of different watershed modeling, the use of AI techniques, artificial neural networks (ANN), fuzzy logic (FL), and genetic algorithms (GA) to improve upon or replace traditional physically-based watershed modeling techniques, and detailed discussions of individual watershed models are presented in [27]. Precipitation-Runoff Modeling System (PRMS) is one of the watershed modeling software used to simulate precipitation and snow melt-driven movement of water to produce the daily system response and streamflow for a basin [28]. The current and future geographic information systems (GIS) trends and remote sensing technologies in watershed modeling are reviewed in [29]. It is demonstrated in [30] that the Surface Water Assessment Tool (SWAT) provides a better streamflow estimate with Next Generation Weather Radar (NEXRAD) precipitation input than rain gauge inputs. The accuracy of the model results suggests that NEXRAD is a good alternative to rain gauge data and can be extremely valuable in large watersheds without readily available rain gauge data. To utilize the watershed modeling tools, for example, SWAT, we need to have input about soil, land use and management, elevation, and daily rainfall to predict daily stream flow. In addition, we need expert knowledge of hydrology and the use of watershed models, which is beyond the scope of this thesis.

There are also other methods proposed in the literature to generate random inflow time series, for example, stochastic processes. In [31], a stochastic process estimation based on the concept of aggregation is presented, and the aggregation of periodic autoregressive (PAR) and periodic autoregressive-moving average (PARMA) models for the seasonal and annual flows of the Niger River is used to illustrate the concept. Inflow is modeled as a stochastic variable by first-order autoregressive model AR(1) in [32] for a stochastic dual dynamic programming (SDDP)to solve optimal medium-term scheduling in the Norwegian hydropower system. In [33], a non-parametric simulation model is applied to generate

synthetic monthly flows from the Beaver River, Australia. A maximum likelihood procedure for estimating the PARMA model of a monthly average river flows time series is presented in [34]. A non-linear periodic autoregressive model (PAR(p))scenario generation method based on the vine coupula model is presented in [35]. A monthly stream flow simulation method based on the vine coupula model is proposed in [36] for a catchment of the Yellow river basin upstream of the Tangnaihai hydrological station in north China. The ARFIMA model, an extension of the Box& Jenkins family, where the differentiation can take fractional values to capture the long-memory effect present in the time series, is used in [37] for generating synthetic hydrological scenarios for the Brazilian hydropower system.

We need to generate inflow scenarios using existing methods to develop stochastic long-term hydropower planning models. The stochastic model can be considered risk-neutral or risk-averse as in [38–40]. Moreover, the rolling horizon framework has long been used to solve stochastic programming models of different applications. To mention some of the works, A rolling horizon framework is used in [41–46], for unit commitment problems, for production decision, for load shedding strategy, and so on. In general, hydropower planning models minimize operation costs or maximize profits with different levels of detail and mathematical formulations. Thus, there is a wide variety of possible models for hydropower planning to choose between. The challenge is to find a model that provides good results in an Ethiopian context, where the primary goal of the planning is to supply uninterrupted power to the end users and to utilize the water in the rainy season throughout the year with minimal load shedding. However, the load shedding during the planning period has to be balanced against the risk of large load-shedding in the future if not enough water is stored in the reservoirs at the end of the planning period.

2.2 Hydropower power plants in Ethiopia

Ethiopia is a country located in the horn of Africa between latitudes of 3.8°N to 14.5°N and longitudes of 33°E to 48°E with a varied topology ranging from the lowest point of 120.00 m below sea level and the highest point about 4620.00 m above sea level [47]. The country is endowed with a substantial amount of water body, which is divided into twelve basins, eight of which are river basins, one lake basin, and the remaining three are dry basins as shown in Fig. 2.3, [48].

The Ethiopian power system has around thirteen larger operational hydropower plants as of

2019 located in different river basins. Additionally, there are three wind power plants and one waste-to-energy plant. These are connected to the national grid. After 2019, the Genale Dawa and two units of the GERD hydropower plants became operational and connected to the grid. However, these two new additions are not considered in this thesis.

Figure 2.3 shows the locations of the Ethiopian hydropower stations in the corresponding river basin.

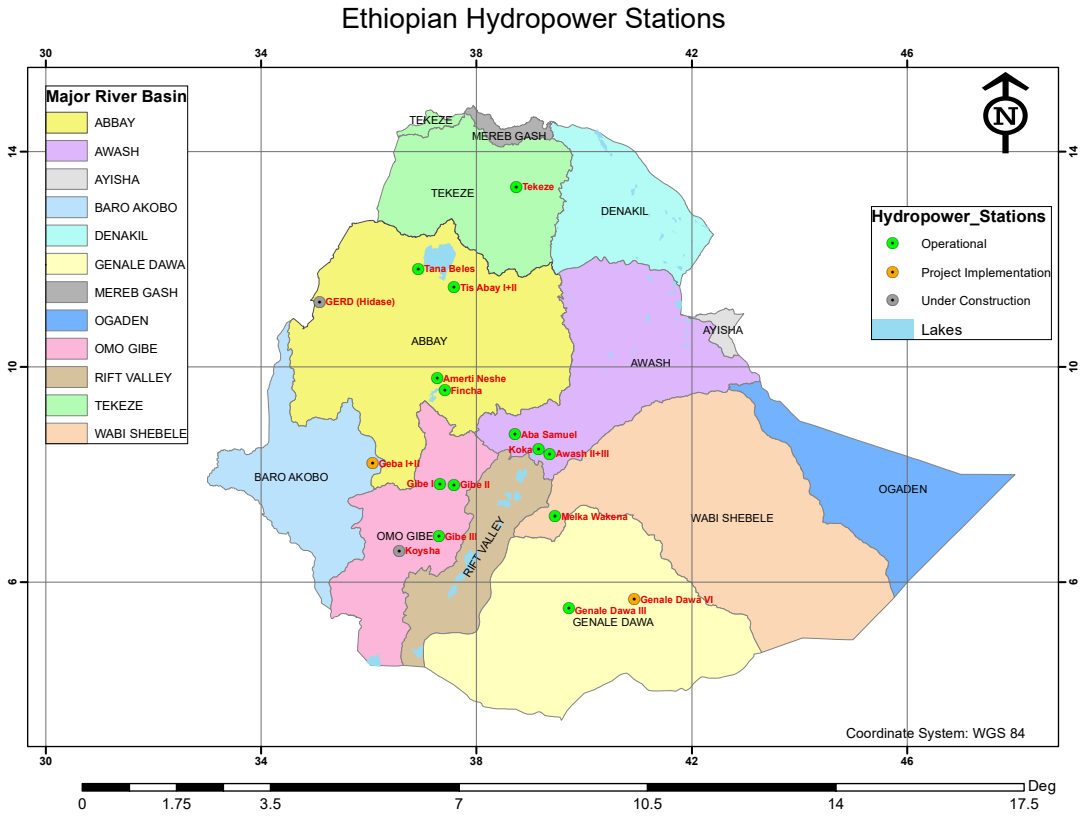

Figure 2.3: Map of Ethiopian Hydropower stations and River Basins.

Most of the reservoirs are constructed in the different river basins. Cascaded hydropower plants in the Omo-Ghibe river basin are Gibe-I and Gibe-II, with Gibe-I at the upper stream. Gibe-III and KOYESHA (under construction) are the other two cascaded power plants in the same river basin. There are Koka, Awash-II, and Awash-III cascaded power plants in the Awash River basin, with Koka at the upper stream. In the Abbay (Blue Nile) river basin, there are Beles, sometimes called Tana Beles, Tis-Abbay I, and Tis-Abbay II power plants that source Lake Tana. Lake Tana is the largest lake in Ethiopia, the source of the Blue Nile River, located in the northwestern highlands of the country with a surface area of 3200 km^2 and an elevation of 1787 m. The lake serves as the reservoir of the Beles hydropower plant

with seven spillway gates called Charachara Gates. The spilled water at Charachara is used partly for the Tis-Abbay fall (Tis Esat, tourist attraction) and partly for power generation at Tis Abbay-I and II. However, there is yet to be available data about the percentage of water that will be used for power production. Therefore, we treat the Tis-Abbay I and II power plants as run-of-the-river plants in this thesis. Fincha, Amerti Neshe, and GERD (under construction) are the other power plants in the Abbay River basin. The rest of the power plants are located in different river basins in the country.

The hydropower generation data and the general information about the reservoirs understudy are collected from Ethiopian Electric Power (EEP). Table 2.1 shows the geographical location and general information about the thirteen Ethiopian hydropower plants connected to the national grid and included in this study. This study excludes reservoirs that were out of operation during the study, small reservoirs with incomplete information and insignificant effect in operation, and reservoirs under construction during the study time 2018-2019, which is our base year for the actual operation data.

Table 2.1: Reservoirs generation information and geographical location.

Power plant	**Coordinates ^{o}N , ^{o}E**	**Dam Height (m)**	**Maximum Level (m a.s.l)**	**Storage (Mm^3) at Max.level**	**Installed Capacity (MW)**	**Maximum Discharge (m^3/s)**	**Average Energy (GWH)**
Beles	11.82, 36.92	35.00	1,787.00	37,307.00	460.00	160.00	1,867.00
M.Wakena	7.225, 39.462	42.00	2,522.90	875.00	153.00	60.00	543.00
Fincha	9.789, 37.269	22.20	2,219.00	964.00	134.00	29.68	760.00
Gibe I	7.831, 37.322	41.00	1,671.55	863.00	210.00	100.00	722.00
Gibe II	7.757, 37.562	46.50	Diversion Weir	-	420.00	98.12	1,635.00
Gibe III	6.844, 37.301	243.00	892.00	15,500.00	1,870.00	2,200.00	6,500.00
Koka	8.468, 39.156	23.80	1,599.00	4,250.00	42.00	144.00	110.00
Awash II	8.468, 39.156	river	run-of-river	-	32.00	65.60	182.00
Awash III	8.468, 39.156	river	run-of-river	-	32.00	66.20	182.00
Tekeze	13.348, 38.742	188.00	1,140.10	9,310.00	300.00	184.00	1,393.00
Am. Neshe	9.789, 37.269	38.00	2,232.50	526.10	97.00	18.70	35.00
Tis-AbbayI	11.486, 37.587	river	run-of-river	-	12.00	114.00	33.70
Tis-AbbayII	11.486, 37.587	river	run-of-river	-	72.00	114.00	359.00

The generation distribution and administration of the listed power plants are handled by the government. There are three government institutions involved in the Ethiopian power system under the Ministry of Water Irrigation and Energy (MOWIE). The first institution is EEP, which is responsible for power generation and transmission; the second one is Ethiopian Electric Utility (EEU), which is responsible for selling and distributing the energy generated for the end users; and the third one is the Ethiopian Energy Authority (EEA). Therefore, the Ethiopian power system is operated in a vertically integrated market with no electricity

market competition, and the energy tariff is set by the government. This is one of the characteristics that makes the Ethiopian power system a unique power system.

2.3 Current hydropower planning practice in Ethiopia

The generation and operation planning in the Ethiopian power system is highly dependent on the seasonal rainfall and the maximum reservoir level attained during the rainy season. The seasonal rainfall is driven mainly by the Intertropical Convergence Zone migration (ITCZ), tropical upper easterlies, and local convergence in the Red Sea coastal region [49]. There are four different seasons in Ethiopia; heavy rain *Kiremt* (July to September), small rain *Tseday* (October to December), and dry season *Bega* (January to March), and small rain *Belg* (April to June),

The generation planning in the Ethiopian power system is performed in two stages. The first stage comprises the rainy season from the beginning of July to the end of September when there is considerable rainfall in almost all regions of the country. The second stage comprises the small rainy seasons and the dry season, from the beginning of October to the end of June.

The planning is based on the historical generation data recorded for several years and the demand growth following the economic growth of the country and export demands. The demand growth is forecasted based on the percentage increase of the demand served at the end of the planning year compared to the previous year. The generation planning will be performed for a one-year time horizon from July to June, and the system will be operated based on this plan for the first stage (July to September). At the end of the first stage, the information about the status of the reservoir content and the load demand will be updated, and the generation plan will be revised for the next stage (October to June) based on the water level of the reservoirs, the historical generation pattern of the power plants, and the specific characteristics of the power plants.

For example, Fig.2.4 shows the five-year history of the reservoir levels for Gibe-I, Gibe-III, Koka, and Tekeze reservoirs. As can be seen from the figures, the reservoir levels increase from July to the end of September and start to drop and reach the lowest point around May. The water levels are different for the different planning years. For example, Gibe-I has almost the same historical water level pattern with a small variation in the water level. The 2015–2016 planning year is the year for the commissioning of Gibe-III, whereas the Tekeze

and Koka reservoirs start the year with low water in the reservoir.

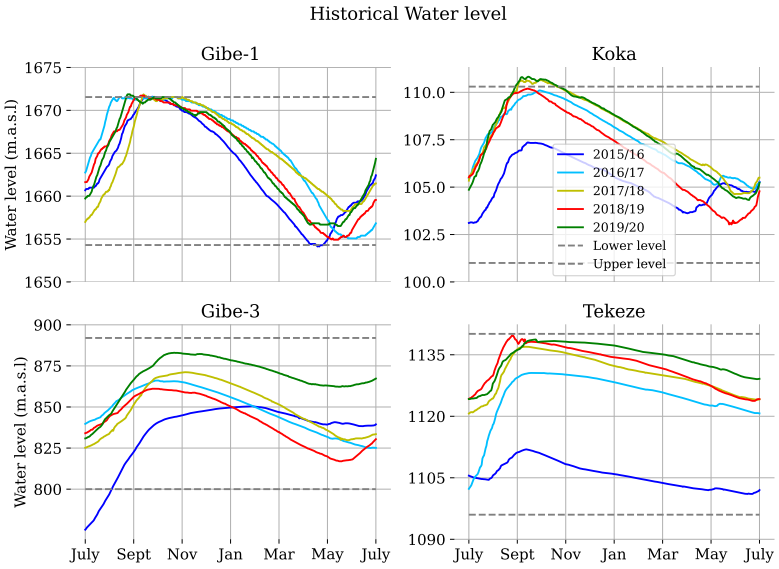

Figure 2.4: Historical pattern of water levels for Gibe1, Gibe3, Koka and Tekeze reservoirs source: EEP

The first planning period is from the beginning of July to the end of September when there is considerable rainfall in almost all regions of the country. It can be seen from the figures that the reservoirs attain their maximum levels around the end of September. The water management planning for the dry season starts in October when the reservoir begins to decrease, which is the second and the main planning period. The generation schedule considers the three conditions for each generating station.

- Plant unique characteristics in relation to water level(Gibe-I, Gibe-II, Gibe-III)
- Load forecast and history of the generation.
- Downstream facilities (Beles, Fincha, and Koka)

Based on these three conditions, the generation is scheduled following the historical relationship between the reservoir's water level and power generation. The information in the water level recording can tell us when the reservoir is full and when it starts to drop, which is a precaution to begin water management of the reservoirs. However, it could not tell us the inflows to the reservoir or how much is expected in the future. This leads to unnecessary load curtailment at some time of the year, spilling of more water at other times in case of a wet year, and draining of reservoirs in case of a dry year.

Based on the data collected from EEP, the actual power generated, the demanded load, and load shedding for the July 2018 to June 2019 planning year are shown in Fig.2.5. As can be

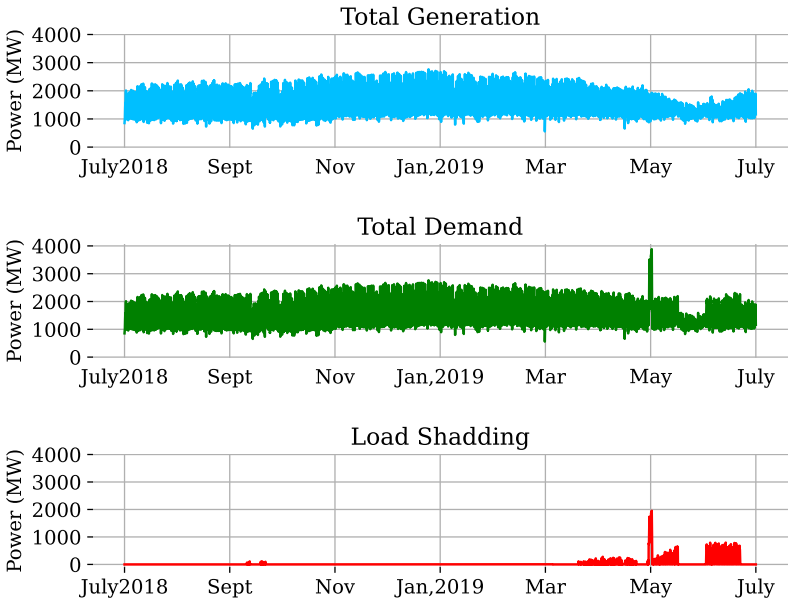

Figure 2.5: Actual generation, demand, and load shedding for the 2018-2019 planning year in hourly time resolution.

seen from the figure, there was significant load shedding starting from the end of March to mid-May, which is the end of the dry season, and again in the month of June, the beginning of the rainy season. Different reasons can be given for the load shedding during these periods. The first reason can be the water shortage in the reservoirs during the periods. When we see Fig.2.4 in the year 2018–2019, most of the reservoirs are at their lowest point in May and June, and the planners may prefer load shedding to withhold some reserve or to store a little bit more water for the next planning period. The other reason can be the historical generation, as the planning follows the historical pattern, and if there is less generation at the same time as the previous years, load shedding is preferred. However, the load shedding could have been reduced using the water in the reservoirs, but that could also mean less water in the reservoirs for the next planning period. That is the main challenge to deal with: should we do load shedding now? or should we use the water now and hope there will be more inflow and lower load in the future, or take the risk of massive blackouts?

This challenge could have been mitigated by better scheduling of reservoirs and stored water management using a proper planning model. The main objective of this thesis is, therefore, to develop a hydropower generation and operation planning model suitable for the Ethiopian power system.

3 Hydropower Planning Models

This chapter describes the methodologies and the mathematical formulations for the different hydropower planning models developed in this thesis. A detailed description of how we formulate the hydropower planning model, both in deterministic version and stochastic version, and how to generate inflow scenarios based on available data are presented in this chapter.

The different models developed in this methodology are discussed in the following subsection.

Model Assumptions

The production of power from a hydropower plant can be calculated using the equation,

$$H_i = Q_i * \rho g h \eta \tag{1}$$

Where:

H_i	Generation of hydropower plant i,
Q_i	Discharge from power plant i,
h	Water head,
g	Acceleration of gravity,
ρ	Water density ,
η	Efficiency ratio.

The efficiency depends on the water head and the discharge through the turbine. The relation between power generation, discharge, and head is a non-linear function. To develop a linear hydropower model, this non-linear behavior needs to be approximated by a linear or piecewise linear function. The impact of the head is rather small for most of the hydropower plants, and therefore, we will neglect this factor. Then will find a linear approximation of the power generation as a function of discharge, $H(Q)$.

When calculating the power generation in a hydropower plant, it is important to understand the difference between the following three notions. [50].

The production equivalent (γ) is the quota between the energy generation and the

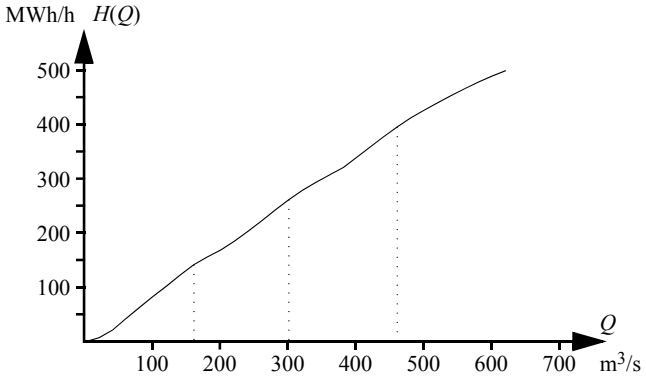

Figure 3.1: The electricity generation of a particular hydropower plant (H-Q) curve.[50]

discharge through the turbines. It is measured in MWh/HE. Where (HE) is the hour equivalent, which corresponds to the water flow m^3/s during one hour. Given the generation and the discharge, the production equivalent is calculated by

$$\gamma(Q) = \frac{H(Q)}{Q}$$

The marginal production equivalent(μ) is a measure of how much the power generation will increase for a small change of the discharge, i.e.,

$$\mu = \frac{dH(Q)}{dQ}$$

It is also measured in MWh/HE.

The relative efficiency(η) refers to the production equivalent for some discharge compared to the maximal production equivalent of the power plant. The relative efficiency shows how much energy can be extracted from each (m^3/s) of water compared to the maximum possible.

$$\eta(Q) = \frac{\gamma(Q)}{\gamma_{max}}$$

In order to approximate the power production using the marginal production equivalent, we need to have the (H-Q) curve of all power plants, which is one of the information about the power plants that we could not access from EEP. Therefore, from the data available at hand,

we approximate the hydropower generation as a linear function of production equivalent and discharge:

$$H_{i,t} = \gamma_i Q_{i,t} \tag{2}$$

The other assumptions taken in this thesis are zero water delay time between cascaded hydropower plants, one area of generation and consumption, no transmission limitations, and only power exports to neighboring countries are considered.

The data for the Mean Annual Inflow (MAI) of each reservoir is approximated from the average annual energy generated and the rated discharge of the reservoirs. All volume units are converted to Hour Equivalent (HE), which is defined as 1 m^3/s of water released during one hour, i.e., 1 HE = 3600 m^3.

All the assumptions and approximations are considered for all the models developed in this thesis.

3.1 Deterministic planning model

A Deterministic Model is a model that allows us to calculate an exact future event without any randomness. If something is deterministic, that means we have all the data necessary to predict (determine) the outcome with certainty. Deterministic models assume that known average rates with no random deviations are applied to large populations. The first model to be formulated in this thesis is the deterministic hydropower planning model.

This subsection presents the model overview and the mathematical formulation of the deterministic planning model for the Ethiopian power system. The simulation results are compared with the actual operation of the year 2018–2019. The results of the model will further be discussed in Chapter 4. This subsection is based on [C1].

3.1.1 Model Overview

The deterministic model is developed considering the existing thirteen larger hydropower plants. The generation from the three wind power plants and the waste-to-energy plant is taken as a constant value from historical generation data. The inflow to the reservoirs is scaled from ten-year average satellite precipitation data and the mean annual inflow of the reservoirs (MAI). The model considers perfect information. The model is realized in an

hourly time resolution and a one-year planning horizon. It is considered that the stored water will be used for electricity generation at the best efficiency.

The data for the hourly load demand forecast for the period from July 2018 to June 2019 and the starting content of reservoirs are collected from EEP. Values are assigned for the electricity price and the penalty cost of load shedding. The value of the electricity price is assigned close to the current electricity price in the country, which is set by the government so that we can estimate how much is the value of the stored water. The value of stored water is calculated from the electricity price and the amount of energy that could be generated out of the stored water, and the penalty cost for each megawatt of load shedding is set much higher than the electricity price so that the model prioritizes generation than storing water. In practice, if the value of future electricity price is much higher than the penalty cost of load shedding, that means we are prioritizing storing water. The choice of reasonable values will depend on what we want to achieve and how to balance load shedding and stored water.

3.1.2 Matematical Model

The deterministic optimization model maximizes the value of stored water and minimizes the penalty cost of load shedding. The mathematical model is, therefore, a maximization of the difference between the value of stored water and the penalty cost of load shedding subjected to hydrological balance, load balance constraints, and the various variable limits.

$Objective function$:

$$Maximize \quad (Value\ of\ stored\ water - Cost\ of\ load\ shedding)$$

$Subjected\ to$:

$$Constraints : Hydrological\ balance, and\ Load\ balance,$$

$$Limitations : Reservoir\ content,\ Discharge,\ and\ Spillage.$$

Indices:

i Index for export area: $m = \{1, 2..., M\}$,

n Index for wind power plants: $n = \{1, 2, ..., N\}$,

t Planning period, one year with hourly time resolution : $t = \{1, 2..., T\}$,

Parameters:

C	Penalty cost of load shedding,
D_t	Load forecast during Hour t,
$\bar{H}_i$	Maximal generation in power plant i,
I	Number of reservoirs,
K_i	Index set of all power plants downstream to reservoir i,
L_i	Index set of power plants upstream to reservoir i,
$M_{i,0}$	Start content of reservoir i,
$\bar{M}_i$	Maximal content of reservoir i,
$\underline{M_i}$	Minimal content of reservoir i,
$\underline{M}_{i,T}$	Minimal content of reservoir i, at the end of the planning period T,
$P_{m,t}$	Power export to area m, during hour t,
M	Number of the export areas,
N	Number of wind power plants,
PR_t	Power generation of waste to energy plant during Hour t,
$\underline{Q_i}$	Minimal discharge in power plant i,
$\bar{Q}_i$	Maximal discharge in power plant i,
T	Number of times in the planning horizon,
$V_{i,t}$	Local inflow to reservoir i, during Hour t
W_t	Total wind power generation during Hour t,
γ_i	Production equivalent for power plant i,
λ	Vale of future electricity generation,

Variables:

$H_{i,t}$	Generation of hydropower plant i, during hour t,
$M_{i,t}$	Content of reservoir i, at the end of hour t,
$Q_{i,t}$	Discharge from power plant i, during hour t,
$S_{i,t}$	Spillage from reservoir i, during hour t,
U_t	Load shedding during hour t,

The objective function consists of two sub-functions. The first function maximizes the value of the stored water (3), and the second function minimizes the penalty cost of load shedding (4). Therefore, the overall objective function maximizes the difference between the value of

stored water (Z_1) and the cost of load shedding (Z_2).

$$Z_1 = \lambda\left(\sum_{i=1}^{I}\sum_{j\in K_i}\gamma_j M_{j,T}\right) \tag{3}$$

$$Z_2 = C\sum_{t=1}^{T} U_t \tag{4}$$

The first constraint is the hydrological balance (5), i.e., the reservoir content at time t equals the sum of all the inflows minus the sum of all outflows at the same time t. The next constraint is the load balance constraint (6), i.e., the total generation from all power plants should satisfy the local demand plus export; if the demand exceeds the generation, the excess load will be the load shedding. It is to be noted that the local demand and export include the transmission losses. Finally, there are different variable limits as described in equations (8 - 12).

Objective function:

$$Maximize \quad Z = Z_1 - Z_2 \tag{5}$$

$$Subjected\,to: \quad M_{i,t} = M_{i,t-1} + V_{i,t} - Q_{i,t} - S_{i,t} + \sum_{j\in L_i}(Q_{j,t} + S_{j,t}) \tag{6}$$

$$U_t = D_t + \sum_{m=1}^{M} P_{m,t} - \left(\sum_{i=1}^{I} H_{i,t} + \sum_{n=1}^{N} W_{n,t} + PR_t\right) \tag{7}$$

$$H_{i,t} = \gamma_i Q_{i,t} \tag{8}$$

$$0 \le U_t \le (D_t + \sum_{m=1}^{M} P_{m,t}) \tag{9}$$

$$\underline{M_i} \le M_{i,t} \le \bar{M}_i \tag{10}$$

$$\sum_{i=1}^{I} M_{i,T} \ge \sum_{i=1}^{I} M_{i,0} \tag{11}$$

$$\underline{Q_i} \le Q_{i,t} \le \bar{Q}_i \tag{12}$$

$$0 \le S_{i,t} \tag{13}$$

The optimization problem for this model is analyzed using the JULIA scientific programming tool. Julia is an open-source, high-level, and high-performance dynamic

programming language developed specifically for scientific computing [51].

3.2 Stochastic planning model

A Stochastic Model is a model that has the capacity to handle uncertainties in the inputs applied. Stochastic models possess some inherent randomness. The same set of parameter values and initial conditions will lead to an ensemble of different outputs. A stochastic model will allow us to calculate random scenarios with a range of possible outcomes for the future. This is particularly useful when there are known uncertain parameters in the planning.

Many hydropower plants have large reservoirs, which allow water to be stored for an extended period of time. This water is used when the demand is high or other generation sources are scarce in the system. In many cases, there are a few short periods with substantial inflow each year. The task of long-term hydropower planning is to decide during which periods this water should be used. In a country like Ethiopia, where hydropower plants highly dominate power generation, the challenge is to decide how to use the inflow from the rainy season while considering the uncertainty of future inflow. The hydropower planning will, therefore, have to find an appropriate trade-off between using the available water (risking future energy shortage) or starting load shedding to a smaller or lesser extent now. Therefore, all long-term planning problems require a forecast of the inflow during the planning period. However, it is challenging to accurately forecast the inflow to hydropower reservoirs with a reasonable time resolution (preferably not longer than one week) for one year or more. Therefore, it is common to use stochastic planning models, where the planning is based on several possible scenarios.

Depending on the type of the power system, the uncertain parameters to be considered in the stochastic models could vary. For example, for a power system with a competitive electricity market, the electricity price will be uncertain; for a power system with VRES integration, the power production from VRES will be uncertain; for a power system with a lot of hydropower, inflow will be uncertain, and the load demand could also be an uncertain parameter. For a vertically integrated electricity market dominated by hydropower plants, where the government determines the electricity prices without any competition, like in Ethiopia and most African countries, there is no price uncertainty, but the most determining factor in the proper hydropower scheduling is the inflow uncertainty. Therefore, the deterministic model

in section 3.1 is reformulated to a two-stage stochastic model considering the uncertainties in the inflow.

This subsection presents the method to develop the stochastic planning model, the quality metric Value of the Stochastic Solution (VSS), to determine the benefits of solving the stochastic model over the deterministic model, the mathematical formulation of the stochastic model both as risk-neutral and risk-averse and finally the rolling horizon framework are presented. These methods are published in the journal [J2], and the model results will further be discussed in section 4.3.

3.2.1 Model Overview

The stochastic model in this sub-section is the updated version of the deterministic model in the previous subsection to account for the uncertainties in the inflow. The stochastic model is developed in two stages in a weekly time step for a one-year planning horizon. The first stage comprises some part of the planning period, and the second stage comprises the rest of the year. The time horizon for the first stage can be selected based on the data available for the planning period; it could be days, weeks, or months. In this thesis, we selected one week for the first stage and the rest of the year for the second stage. Fig.3.2 shows The scenario tree for the particular two-stage stochastic model.

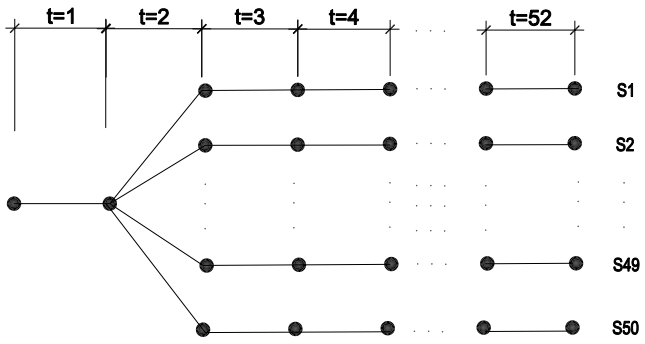

Figure 3.2: Scenario tree.

3.2.2 Mathematical Model

The stochastic optimization model maximizes the value of stored water and minimizes load shedding, considering the uncertainty in the inflow of the reservoirs. Therefore, we will have

a range of different possible model outcomes.

The additional indices, parameters, and scenario-dependent variables for the stochastic model are listed below.

Indices:

ω Index of inflow Scenarios: $\omega = \{1, 2, \ldots, \Omega\}$,

Parameters:

$V_{i,t}^{\omega}$ Local inflow to reservoir i, during time t, Scenario ω,

α Confidence level of conditional value at risk (CVaR),

β CVaR risk factor,

γ_i Production equivalent for power plant i,

Ω Number of scenarios,

π^{ω} Probability of inflow scenarios ω.

Variables:

$H_{i,t}^{\omega}$ Generation of hydropower plant i, during time t, scenarios ω,

$M_{i,t}^{\omega}$ Content of reservoir i, at the end of time t, scenario ω,

$Q_{i,t}^{\omega}$ Discharge from power plant i, during time t, scenarios ω,

$S_{i,t}^{\omega}$ Spillage from reservoir i, during time t, scenario ω,

U_{t}^{ω} Load shedding during week t, scenarios ω,

ζ, η^{ω} Auxiliary variables for calculating CVaR.

The random parameters may have a continuous probability distribution. In most cases, we will need to use a discrete approximation, where each scenario ω occurs with the probability π^{ω}. In this thesis, it is assumed that there are equally probable inflow scenarios.

The two sub-objective functions of the deterministic model (4 and 5) are then updated to (14 and 15) to account for the uncertainty of the inflow.

$$Z_1^w = \lambda \sum_{i=1}^{I} \sum_{j \in K_i} \gamma_j M_{j,T}^{\omega}, \qquad \forall \omega \in \{1, 2, ..., \Omega\} \tag{14}$$

$$Z_2^w = C \sum_{t=1}^{T} U_t^{\omega}, \qquad \forall \omega \in \{1, 2, ..., \Omega\} \tag{15}$$

$$Z^w = Z_1^w - Z_2^w, \qquad \forall \omega \in \{1, 2, ..., \Omega\} \tag{16}$$

The overall objective function for the stochastic model will then be expressed as:

Objective function:

$$Maximize \quad \sum_{\omega=1}^{\Omega} \pi^{\omega} Z^{w} \tag{17}$$

$$Subjected\,to: \quad M_{i,t}^{\omega} = M_{i,t-1}^{\omega} + V_{i,t}^{\omega} - Q_{i,t}^{\omega} - S_{i,t}^{\omega} + \sum_{j \in L_i} (Q_{j,t}^{\omega} + S_{j,t}^{\omega}) \tag{18}$$

$$U_t^{\omega} = D_t + \sum_{m=1}^{M} P_{m,t} - \left(\sum_{i=1}^{I} H_{i,t}^{\omega} + \sum_{n=1}^{N} W_{n,t} + PR_t \right) \tag{19}$$

$$H_{i,t}^{\omega} = \gamma_i Q_{i,t}^{\omega} \tag{20}$$

$$0 \leq U_t^{\omega} \leq (D_t + \sum_{m=1}^{M} P_{m,t}) \tag{21}$$

$$\underline{M_i} \leq M_{i,t}^{\omega} \leq \bar{M}_i \tag{22}$$

$$\sum_{i=1}^{I} M_{i,T}^{\omega} \geq \sum_{i=1}^{I} M_{i,0}^{\omega} \tag{23}$$

$$\underline{Q_i} \leq Q_{i,t}^{\omega} \leq \bar{Q}_i \tag{24}$$

$$0 \leq S_{i,t}^{\omega} \tag{25}$$

The non-anticipativty constraint for the first stage is given by:

$$Q_{i,t}^{\omega} = Q_{i,t}^{(\omega-1)} \quad \forall i, \quad t = 1, \;\; \omega = 2, ...\Omega, \tag{26}$$

That is, the discharge at time t scenario (ω) and $(\omega - 1)$ will always be equal and will not be scenario-dependent for the first stage. Then, for the second stage, the discharge will be scenario-dependent.

3.2.3 Value of stochastic solution

There are two types of quality metrics used to compare the deterministic and stochastic models. The Expected value of perfect information (EVPI), which compares the profits of decisions based on perfect information to decisions made considering uncertainty, tells us the value of perfect information about the future. Value of the Stochastic Solution (VSS) is

the other quality metric that determines the benefits of solving the stochastic model over the deterministic model.

VSS is the value of the difference between the result of using the expected value solution (EEV) and the recourse problem solution (RP) [52]. The VSS compares the profit of decisions based on uncertainty to those based on expected value. For a two-stage maximization stochastic problem, the VSS can be calculated as:

$$VSS = Z^{RP} - Z^{EEV} \quad (For\ Maximization\ problem) \tag{27}$$

Where:

z^{RP} = optimal value of the stochastic problem(recourse problem)

z^{EV} = optimal value of the stochastic problem when the first-stage variables are fixed to the values provided by a deterministic problem using expectation values for all uncertain parameters.

We use the quality metrics VSS in this thesis to compare the two models. The results will further be discussed in Section 4.2.

3.2.4 Risk measures in stochastic models

Risk measures are used to characterize the risk associated with a given decision. The main advantage of considering risk measures is that it is possible to avoid the very low cost experienced in some unfavorable scenarios in profit maximization. A risk measure can be incorporated either into the objective function of the problem or as an additional set of constraints in the problem formulation [53].

In this paper, we consider two types of risk. The first risk is the load-shedding risk, which is concerned with the occurrence of load shedding in the process of water value maximization, which is included in the objective function as a penalty cost of load shedding weighted by a cost factor $C \in [0, \infty]$.

The second risk considered is the risk of having empty reservoirs or low reservoir content at the end of the planning period while minimizing load-shedding penalty costs. In order to

avoid this risk, we introduce a variable bound for the end content of the reservoir.

$$\sum_{i=1}^{I} M_{i,T}^{\omega} \geq \sum_{i=1}^{I} M_{i,0}^{\omega} \tag{28}$$

For an equiprobable scenario and a given confidence level α, the Conditional Value-at-Risk (CVaR) is defined as the expected profit in the $(1-\alpha)*100\%$ worst scenarios [53].

$$CVaR = max\left(\zeta - \frac{1}{1-\alpha}\sum_{\omega=1}^{\Omega}\pi^{\omega}\eta^{\omega}\right), \ \forall \ \alpha \ \in \ (0,1) \tag{29}$$

$$Subjected\,to: \ \ \zeta - Z^{\omega} \leq \eta^{\omega} \tag{30}$$

$$0 \leq \eta^{\omega} \tag{31}$$

The variable ζ represents the highest profit in the $(1-\alpha)$ worst scenario such that the probability of experiencing a profit less than ζ is less than or equal to $(1-\alpha)$ [54]. TheCVaR risk measure is included in the objective function weighted by a risk factor $\beta \ \in \ [0,1]$. Therefore, the overall risk-averse equation will become:

$$Max \ \ (1-\beta)\sum_{\omega=1}^{\Omega}\pi^{\omega}\left(\lambda_f\sum_{i=1}^{I}\sum_{j\in K_i}\gamma_j M_{j,T}^{\omega} - C\sum_{t=1}^{T}U_t^{\omega}\right) + \beta\left(\zeta - \frac{1}{1-\alpha}\sum_{\omega=1}^{\Omega}\pi^{\omega}\eta^{\omega}\right) \tag{32}$$

This objective function will be subject to the same constraints as (5-13). In addition to those, it will be subjected to a risk measure constraint. In this paper, we will investigate three possible formulations of the CVaR risk measure constraints:

$$\zeta - \left(\lambda\sum_{i=1}^{I}\sum_{j\in K_i}\gamma_j M_{j,T}^{\omega}\right) \leq \eta^{\omega} \tag{33a}$$

$$\zeta - \left(-C\sum_{t=1}^{T}U_t^{\omega}\right) \leq \eta^{\omega} \tag{33b}$$

$$\zeta - \left(\lambda\sum_{i=1}^{I}\sum_{j\in K_i}\gamma_j M_{j,T}^{\omega} - C\sum_{t=1}^{T}U_t^{\omega}\right) \leq \eta^{\omega} \tag{33c}$$

$$0 \leq \eta^{\omega} \tag{34}$$

CVaR risk measure could be considered to account for the risk of low stored water (33a) and high load shedding (33b) separately or in combination, i.e., when the risk measure is considered for the entire objective function (33c). It is to be noted that only one of the constraints (33a) to (33c) should be applied at the same time. The consequences of choosing different risk measure constraints will be analyzed in section 4.3.2.

3.2.5 Stochastic models in rolling horizon framwork

It is computationally difficult to plan a stochastic model in the long term as the time step is shorter and the number of scenarios gets larger. In addition, it is difficult to get an accurate forecast for long-term planning. Forecast information should be updated intermittently through the planning horizon. Therefore, there is a need to test all the planning models developed in this thesis in a rolling horizon framework for long-term planning, in which only a subset of the time horizon decisions is considered at a time. This framework allows us to see how a model will perform not just in one snapshot but also how it will perform in the long run.

A rolling horizon framework is developed to simulate the two-stage stochastic model described in the previous section. The stochastic model is simulated in a weekly rolling horizon as shown in Fig.3.3.

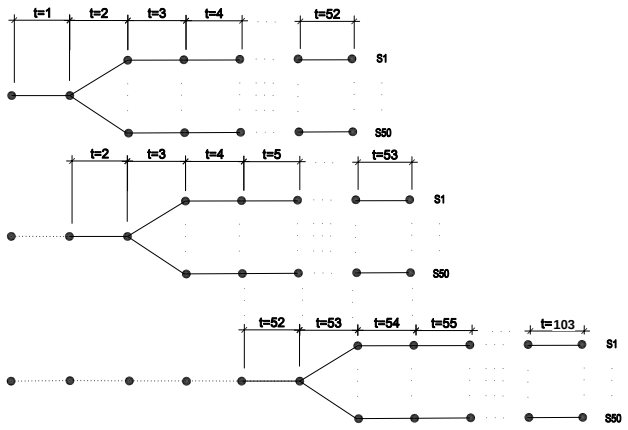

Figure 3.3: Scenario tree in a weekly rolling horizon.

The first week's (week –r) operation is based on the stochastic model output for the period ($t = r : T$), where r is the rolling time step (one week in this case) and T is the planning horizon (one year or 52 weeks in this case). For the first week, the system will be operated to generate the sum of the total power scheduled in each plant. This will help to allocate

the power scheduled to the run-off of the rivers during the model simulation in case there is no sufficient inflow during the actual operation. At the end of the week, all the information, such as the inflow, the reservoir content at the end of the week, the load shedding, and the spillage, will be updated and recorded. Then, the model will be simulated for the next period ($t = r + 1 : T + r$) using the updated information. This will continue rolling until the end of the planning period ($t = T : 2T - 1$), which is one year in this case.

The algorithms for the risk-neutral and risk-averse stochastic rolling horizon models are described as follows.

Algorithm 1 Risk neutral stochastic rolling horizon model

1: **for** $r = 1 : T - 1$
$t = (r + 1) : (T + r)$
$V^{\omega}_{i,r} = V_{act_{i,r}}$
$M_{i,0} = M_{i,r} \ldots$ **do**
2: Maximize: (4)
3: Subjected to: (5 – 12), and

$$\sum_{i=1}^{I} H^{\omega}_{i,t} = \sum_{i=1}^{I} H_{avg_{i,r}} \quad \forall i, \quad t = r, \ \ \omega = 1, 2, ...\Omega, \tag{35}$$

$$Q^{\omega}_{i,t} = Q^{(\omega-1)}_{i,t} \quad \forall i, \quad t = r + 1, \ \ \omega = 2, 3, ...\Omega, \tag{36}$$

4: **end for**

where:

$V_{act_{i,r}}$	The inflow for the first week r of the planning horizon.
$M_{i,r}$	The result of the reservoir content at the end of week r.
$H_{avg_{i,r}}$	The average value of generation of power plant i week r of the planning horizon.

Algorithm 2 Risk averse stochastic rolling horizon model

1: **for** $r = 1 : T - 1$
$t = (r + 1) : (T + r)$
$V^{\omega}_{i,r} = V_{act_{i,r}}$
$M_{i,0} = M_{i,r} \ldots$ **do**
2: Maximize: (18)
3: Subjected to: (5 – 12), (33a ,33b or 33c), and (34 – 36)
4: **end for**

The information about the inflow $V^{\omega}_{i,t}$ will be updated to the actual inflow of $V_{act,r}$ in the rolling week. (21) is used to set the total generation for the rolling week to be equal to the

scheduled total generation for the week. At the end of the week, we will be able to know the actual reservoir content, which will be used as start content for the next rolling week. Finally, (22) is the non-anticipativity constraint for the stochastic model of the next rolling horizon.

The problem is analyzed using JULIA scientific programming tool version 1.7.2, with JuMP mathematical optimizer of version 0.22.3 and Gurobi solver version 0.10.3.

3.3 Inflow scenario generation

In order to simulate the stochastic models, we need random scenarios of the stochastic parameter as input to the model. In a hydropower system, inflow is an uncertain stochastic process that depends on the meteorology of the reservoir's location. To properly utilize the stored water in reservoirs, it is necessary to have a good forecast or historical inflow record. In the absence of these two pieces of information, which is the case in Ethiopia and most African countries, the derivation of synthetic historical inflow series with appropriate time resolution will be a solution. This subsection presents the methodology to develop synthetic historical inflow time series and techniques to identify the stochastic process that mimics the behavior of the time series and generates inflow scenarios that can be used in a stochastic hydropower planning model.

3.3.1 Methodology

The NASA POWER Data Access Viewer (DAV)[55] is used to access the satellite precipitation measurement data based on the geographical location of each reservoir. Ten years of historical precipitation time series from July 2010 to July 2020 is extracted from the DAV for each reservoir in a daily time resolution. The Matlab Econometric Modeler Application of Version 5.1 (R2018b) [56] is used to perform time series analysis and statistical model identification tests.

We have developed two steps of processes to generate the inflow scenarios. The first step is to combine the available historical data about hydropower generation and precipitation to estimate synthetic historical inflow time series. As a straightforward solution, we could have used the estimated synthetic historical inflows as scenarios for the future. However, the limited data to estimate the historical series may lead to a series that misses significant variations, and the data might not be sufficient for planning models. Therefore, the second

step is to identify a stochastic process that can generate random inflow scenarios, which follow the same pattern as the synthetic historical inflow series. The second step allows us to generate as many scenarios as needed that are not limited by historical data.

3.3.2 Estimation of historical inflow time series

A method to generate a synthetic inflow series from the data available for all the reservoirs is derived. The method used to derive synthetic historical inflow series to the reservoirs is scaling down the mean annual inflow (MAI) of each reservoir based on the percentage precipitation of each reservoir. First, the data for the individual reservoir precipitation measurement is extracted from the NASA data access viewer based on the geographical location of the power plants in a daily time resolution. Then, the percentage of precipitation over a year is used to distribute the MAI in the same proportion as the precipitation, neglecting delays, topology, and such factors.

$$V_i = \frac{P_i}{P_{annual_i}} MAI_i \tag{37}$$

where:

V_i Volume inflow of reservoir i in (HE),

P_i Daily precipitation per location of reservoir i in (mm),

P_{annual_i} Annual precipitation per location of reservoir i.

However, there are no statistics for the MAI of each reservoir. Therefore, we need to estimate the MAI using the available information at hand. The mean annual energy (MAE) generation and the production equivalent are used to approximate MAI to the reservoirs. The approximation considers electricity generation at the best efficiency and generation approximated as a linear function of discharge. Therefore,

$$MAI_i = \frac{MAE_i}{\gamma_i} \tag{38}$$

$$\gamma_i = (H_{imax})/(Q_{imax})$$

where:

γ_i	Production equivalent of power plant i, (MW/HE).
MAE_i	Mean annual Energy generation of power plant i in (MWh).
MAI_i	Mean annual inflow to power plant i in (HE).
HE	Hour equivalent, m^3/s of water released during one hour.

Ten years of synthetic historical inflow time series are estimated using Eq.37 for each reservoir in a daily and weekly time resolution.

3.3.3 Time series analysis and stochastic model estimation

The most prominent and frequently used method for time series analysis for all applications, such as finance, business, and engineering research, is the Box-Jenkins methodology [57]. We follow this methodology to identify the stochastic process that mimics the inflow time series. The seasonal autoregressive integrated moving average (SARIMA) model from the Econometric Modeler Matlab tool is used to estimate the stochastic model.

The time series analysis is performed for the individual reservoir in two sets of inflow time series: one with daily time resolution and the other with weekly time resolution. The objective is to see which resolution best captures the behaviors of the synthetic series and transforms them into the future.

In the selected methodology, the time series are checked for stationarity. For a non-stationary series, there is a need for differencing the original series (y_t) to reduce the process to a mixed autoregressive-moving average process of the form,

$$\phi(B)\omega_t = \theta_0 + \theta(B)\epsilon_t \tag{39}$$

as stated in[57],
where:

$$\omega_t = (1-B)^d y_t = \Delta^d y_t$$

B Backward shift operator defined by $B^m y_t = y_{t-m}$.

$\phi(B)$ Autoregrasive operator.

θ_0 Constant term.

$\theta(B)$ Moving average operator.

Δ^d Backward difference operator of order d

ϵ_t White noise process.

Then, the analysis will be performed in the differenced series (ω_t).

3.3.4 Residual diagnosis

After the time series analysis and estimation of the stochastic model, there is a need to perform a residual diagnosis to make sure that the model fits the synthetic series. The property expected from a good fit is to have uncorrelated residuals with zero mean [58]. In addition to these properties, having residuals with zero variance and normal distribution indicates a good model fit. We can test those properties by visually inspecting the auto-correlation function (ACF) and histogram plots of the residuals or applying various test methods. The test method proposed by [57, 58] is the portmanteau test, which tests whether the first K autocorrelations are significantly different from what would be expected from a white noise process. The most used test method and the modified version of the portmanteau test is the Ljung-Box Q-test, which is incorporated in the Matlab Econometric Modeler tool based on the equitation,

$$\tilde{Q} = n(n+2)\sum_{k=1}^{K}(n-k)^{-1}r_k^2(\hat{a}) \tag{40}$$

The modified statistic has, approximately, the mean $E[\tilde{Q}]$ of the $\chi^2(K-p-q)$ distribution [57]. This modified form of the portmanteau test statistic has been recommended for use because it has a null distribution much closer to the $\chi^2(K-p-q)$ distribution for typical sample sizes n.

4 Results and discussion

This section discusses the results of the study based on the steps followed in the methodology. Section 4.1 discusses the results of the deterministic model. The results from the stochastic models and their comparison are discussed in section 4.2 and finally, the results of the time series analysis and scenario generation are discussed in section 4.3.

4.1 Deterministic model

The deterministic model has been used to simulate two cases: a base case (Case-1) representing the current load levels in Ethiopia and Case-2, for a 50% load level increase from the base case. These two cases are compared to the actual historical generation and operation of 2018-2019.

4.1.1 Historical data

In the Ethiopian power system, the method of generation and operation planning is based on historical data. The planning is performed in two stages. The first planning stage starts from the beginning of July to the end of September when there is a considerable amount of rainfall in almost all regions of the country, and the second stage is the rest of the year. Before planning for the second stage, the reservoir levels at the end of the first stage will be collected and compared with the historical water levels at the same time, and the generation schedule of each plant will be performed based on the pattern of the previous years.

Based on the data collected from Ethiopian Electric Power (EEP), the actual power generated, the demanded load, and load shedding for the Ethiopian planning year July 2018 to June 2019 are shown in Fig.4.1, on the left side. As can be seen from the figure, there was significant load shedding from mid-March to mid-May, which is the end of the driest season, and again in June, the beginning of the rainy season. These were the periods when power was rationed for the end-users in the country. This was mainly due to the water shortage in the reservoirs during the period. This load shedding could have been mitigated by better scheduling and managing stored water. It should be noted that there could be possible errors in the data collection that could not be tracked, which may explain the unexpectedly high demand for some hours and a low demand towards the end of the year.

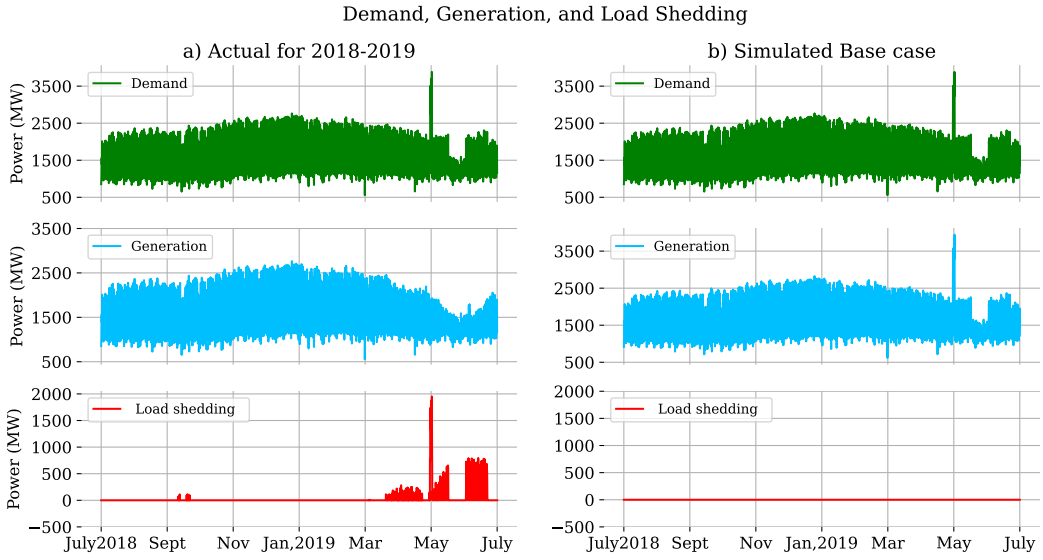

Figure 4.1: Generation, Demand, Load shedding, Historical and Base case.

4.1.2 Base Case (Case-1).

The demand for the base case is taken from the historical load demand of 2018–2019, which is the same as the historical data described above. The inflow is scaled from the MAE using the precipitation data of 2018–2019 from NASA. The start content of reservoirs is set to the average start content of the previous ten years. The minimum discharge($\underline{Q_i}$) from all reservoirs is assumed to be zero except for *Tana Beles, Fincha*, and *Koka* reservoirs with downstream sugar-cane plantation.

The simulation results for the base case are shown in Fig.4.1, on the right side. When we compare the base case with the actual scenario, the simulation result indicates the possibility of operating the hydropower plants in a more efficient way to eliminate the load shedding. The simulation result also indicates the possibility of using the water in the reservoirs throughout the year with minimum spillage. The simulation result of the reservoir content and spillage for the planning year in Fig. 4.2 shows that, the reservoirs start filling up in the rainy season and reach their maximum at the end of September. Then, they start dropping from mid-October throughout the dry season. And then start filling up again at the beginning of the rainy season. Most of the spillage occurred in the rainy season, especially from the smallest reservoirs. This shows that the model optimizes the generation scheduling so that the water in the reservoirs can be used throughout the year with minimum water spilled. However, it should be noted that the model assumes perfect information, neglects

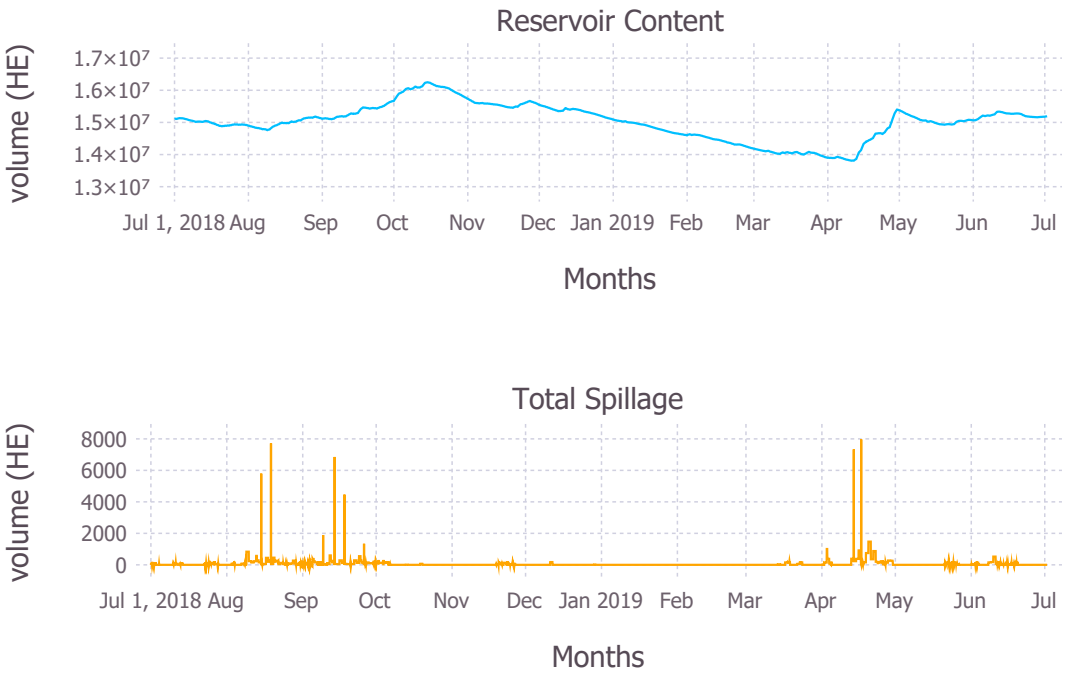

Figure 4.2: Simulation result for aggregate Reservoir content and spillage

transmission limitations, and uses a simplified model of hydropower generation as a function of discharge. Moreover, the inflow data used in the simulation are approximations. Thus, the results could change if more reliable data were available for the power system. Even though the data are uncertain, we can conclude from the result that the power system is flexible enough to be operated efficiently, which indicates that better water management could improve the situation for the power system. Maybe not as good as in this model, but at least an improvement compared to how it is now.

4.1.3 50% Load Level Increase (Case-2).

In this case, the demanded load level is increased by 50% compared to the base case, with an adjustment of unexpected pick demands like the very high demand shown around the beginning of May in Fig.4.1. To develop the model for the case, a ten-year average rainfall data from the NASA satellite and a start content of the reservoirs from the end content of the simulation period for the base case are taken. The simulation result in Fig. 4.3 shows with optimum generation scheduling, the system can support the 50% load increase with a minimum load shedding in the system. Load shedding is observed where there is more load demand than the system's generating capacity. The model can be utilized to forecast the

appropriate time to perform system expansion by considering the load demand increase in the system.

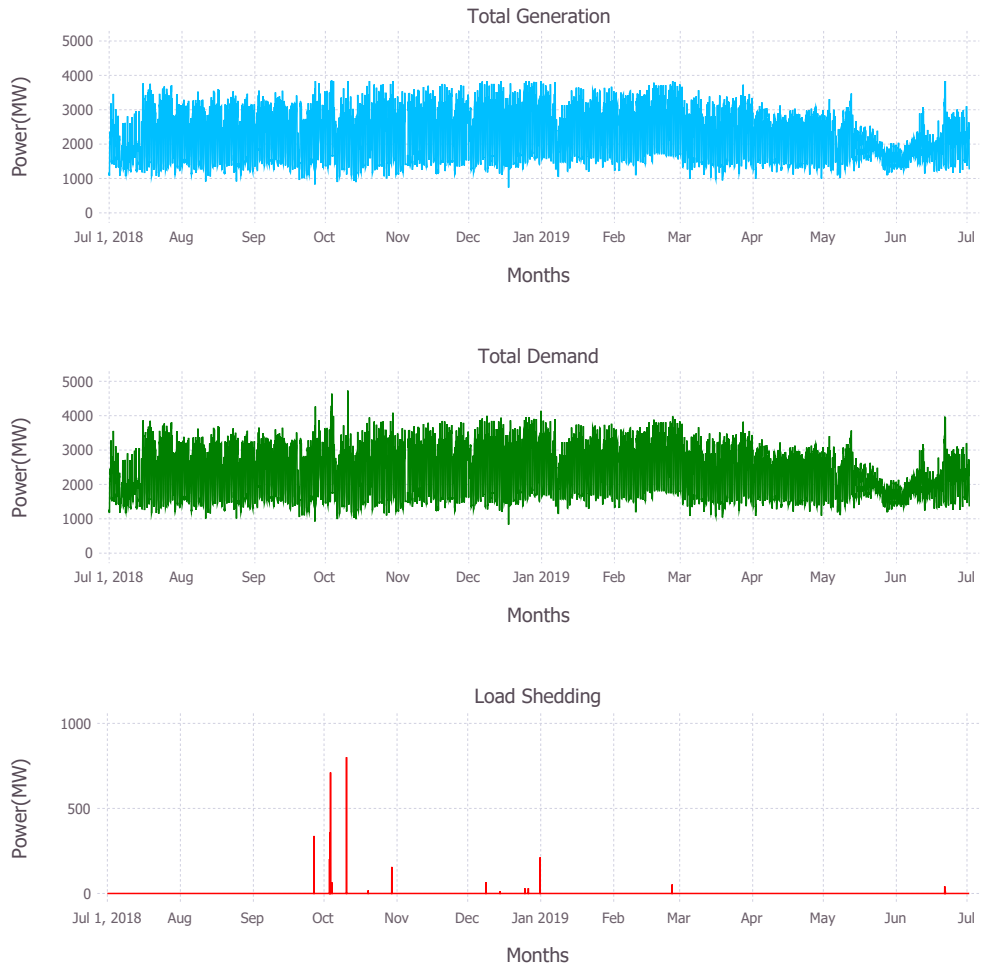

Figure 4.3: Generation, Demand, and Load shedding for case2

To see the hourly scheduling in the power plants, the simulation result of the bigger hydropower plants for the first ten days or 240 hours is shown in Fig. 4.4 as an example. The figure shows the share of the power plants in the generation schedule. The model distributes generation arbitrarily between hydropower plants as long as no reservoir limits are exceeded. The biggest power plant supplies the majority of the demand and the peak demand.

The generation schedule could be an indicator of the operation and maintenance schedule of the power plants. The model can also be used to see the capacity of the system to supply the increased load without shedding any load. In general, the simulation results show that the Ethiopian power system has a great deal of flexibility. However, how much of this flexibility can be utilized depends on the uncertainty of inflows, load forecasts, and trading

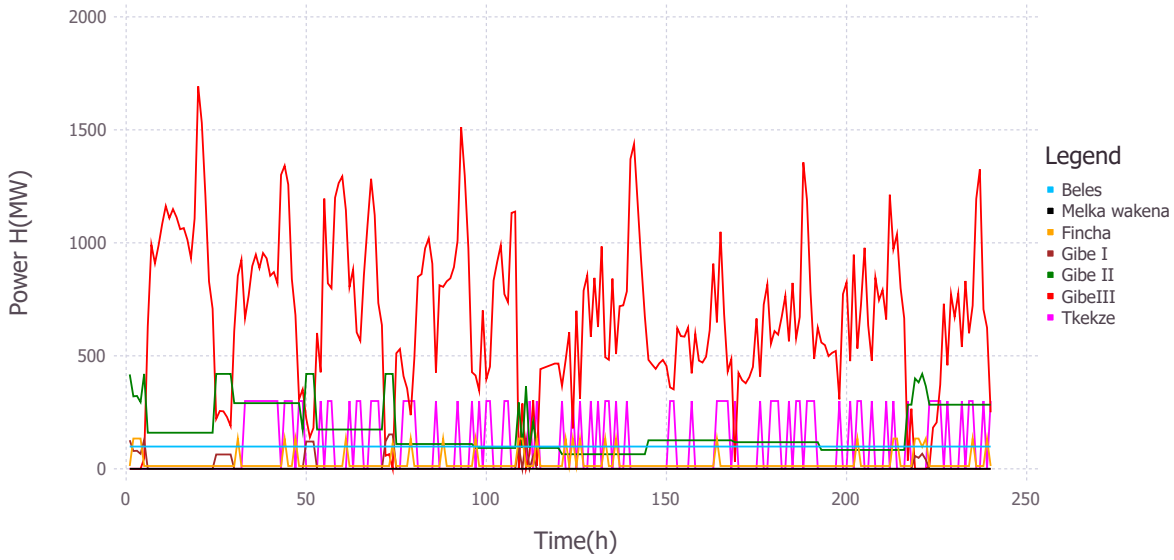

Figure 4.4: Generation schedule for ten days.

with neighboring countries. Therefore, there is a need to further develop the deterministic model into a stochastic model to consider the uncertainties of the parameters.

4.2 Inflow scenarios

For a power system like Ethiopia, dominated by hydropower plants, the most determining uncertain parameter is the inflow to the reservoirs. Therefore, to develop the stochastic model, we need to first deal with inflow scenarios that will be the input to our stochastic model.

The objective of this section is to discuss the results of the derivation of the synthetic historical inflow time series, time series analysis, stochastic model estimation that best fits the synthetic series, and the generation of realistic inflow scenarios that can be used in hydropower planning models.

4.2.1 Synthetic historical inflow time series

Synthetic historical inflow time series for the past ten years, from July 01, 2010, to Jun 30, 2020, is derived in a daily time resolution for each reservoir based on the method described in section 3.3. The aggregate inflow time series of all the reservoirs in a daily time resolution and a one-year planning period is shown in Fig.4.5 below. The result in the figure shows that

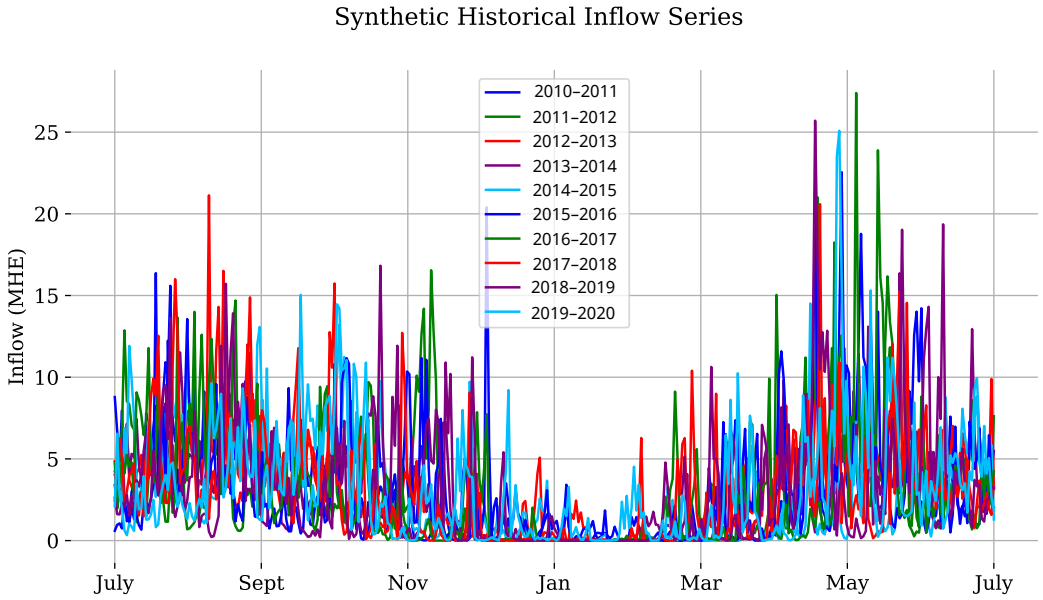

Figure 4.5: Synthetic historical inflow time series for the Ethiopian power system.

there are seasonal variations in the inflows. Most of the reservoirs get a considerable inflow during the same season. The reservoirs' geographical location variation creates a slightly different precipitation pattern.

In general, all reservoirs get considerable rain in the rainy season, July–September, and attain their maximum level around September and October. When we compare the actual water level and the synthetic inflows for Gibe 1 and Tekeze reservoirs using historical water levels and synthetic inflows for 2015–2016 and 2018–2019 shown in Fig.4.6, the water levels of Gibe 1 in 2015–2016 and 2018–2019 have an almost similar pattern. The maximum level is at the beginning of September for both years, and it starts dropping from October throughout the dry season; the water level reached its lowest point around April for 2015–2016 and around mid-May for 2018–2019. After that, the level started rising relatively fast, starting from the end of April on the blue curve and rising relatively slowly from June on the red curve. It can be seen from the same figure that there is a high inflow from July to October in both years, and the inflow starts to lower from November and very little inflow in the dry season in both years. In the dry season, the inflow was better in 2018–2019 than in 2015–2016. However, at the end of the planning year, May to June, we saw a higher inflow in 2015–2016 than in 2018–2019, which corresponds to the water level pattern of each year.

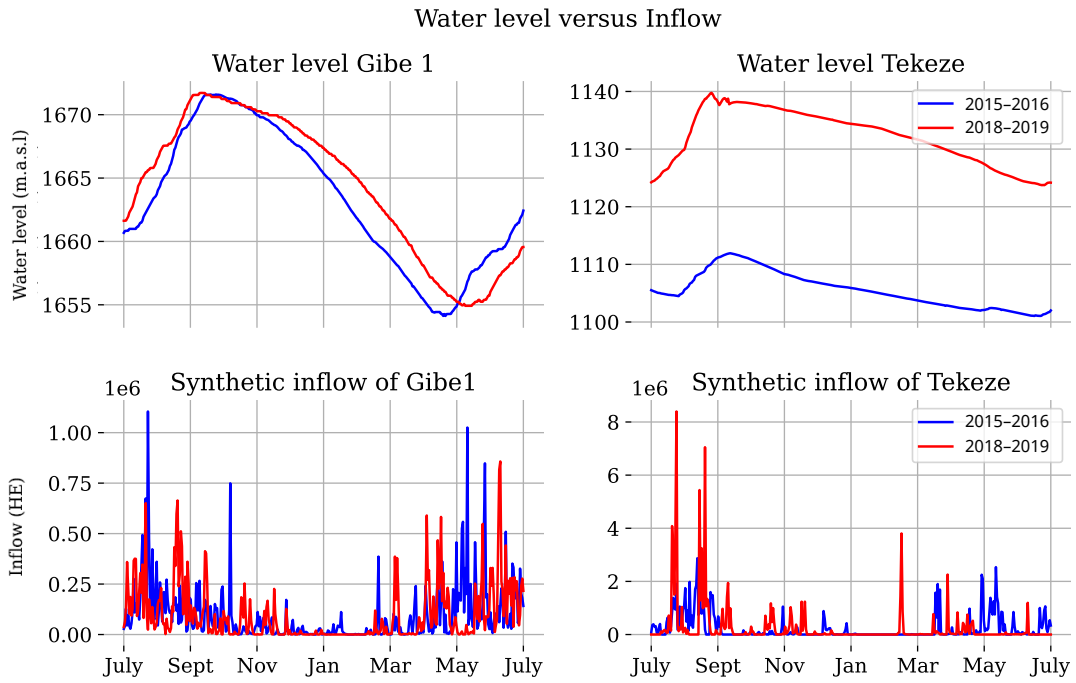

Figure 4.6: Actual water level versus synthetic inflow in 2015–2016 and 2018–2019 for Gibe1 and Tekeze reservoirs

The Tekezé reservoir water levels for 2015–2016 and 2018–2019 in Figure 4.6 have similar patterns, but there are big differences in water levels between the two years. When we compare the increase in the water level from July to September and the inflow for the same time, we can see that in 2015–2016 (blue curve), the level increase is only around 6 m.a.s.l, which corresponds to the lower inflow. On the other hand, in 2018–2019 (the red curve), the level increase is around 15 m.a.s.l during the same time, which corresponds to the higher inflow. Therefore, the inflow can justify the variation of the water levels for the two different years; in 2018–2019, the Tekezé reservoir had the highest rainfall in August and September and a small inflow throughout the dry season. On the other hand, in 2015–2016, the year started with a low water level, and it had a lower inflow during the wet and dry seasons.

Water levels and inflows varied in a logical pattern in the two reservoirs, which held for the rest of the reservoirs, implying that the generated time series are realistic. Therefore, we can further analyze the developed inflow time series to estimate the stochastic process and generate a random but realistic inflow scenario.

4.2.2 Time Series Analysis and Stochastic Model Estimation

Once we get a realistic historical inflow time series, we can further analyze the developed inflow time series to estimate the stochastic process and generate a random but realistic inflow scenario. The two sets of inflow time series developed are in daily and weekly time resolution.

Daily time resolution

The time series in a daily time resolution is the first set of time series approximated from the available information. The analysis indicates that the reservoirs' inflow time series in the daily time resolution are non-stationary processes. The analysis of the differenced time series shows that the stochastic processes are seasonal autoregressive integrated moving average processes of various orders.

For example, the differenced time series for Gibe 3 shows that the stochastic process is an autoregressive integrated moving average process (ARIMA) (0,1,3) seasonally integrated with MA(730)(SARIMA(0,1,3)(0,1,2)[365]).

$$(1-B)(1-B^{365})y_t = (1+\theta_1 B+\theta_2 B^2+\theta_3 B^3)(1+\Theta_{365}B^{365}+\Theta_{730}B^{730})\epsilon_t \quad (41)$$

and for the rest of the reservoirs the process is SARIMA(0,1,2)(0,1,2)[365],

$$(1-B)(1-B^{365})y_t = (1+\theta_1 B+\theta_2 B^2)(1+\Theta_{365}B^{365}+\Theta_{730}B^{730})\epsilon_t \quad (42)$$

where:

$\Theta =$ Seasonal Moving average operator.

Weekly time resolution

The second set of time series analyzed is the same series reduced to weekly time resolution. The analysis shows that the time series for all the reservoirs are stationary autoregressive models of various orders, AR(1), AR(2), and AR(3) process with the consideration of seasonality equal to the number of weeks in a year (52). For example, the model for Gibe 3 is estimated as SARIMA(2,0,0)(2,0,0)[52] (an ARIMA(2,0,0) model seasonally integrated

with Seasonal AR(104)(Gaussian distribution)).

$$(1-\phi_1 B-\phi_2 B^2)(1-\Phi_{52}B^{52}-\Phi_{104}B^{104})(1-B^{52})y_t=\epsilon_t \tag{43}$$

The models for Gibe 1, Koka, and Tekeze are estimated as SARIMA(3,0,0)(3,0,0)[52].

$$(1-\phi_1 B-\phi_2 B^2-\phi_3 B^3)(1-\Phi_{52}B^{52}-\Phi_{104}B^{104}-\Phi_{156}B^{156})(1-B^{52})y_t=\epsilon_t \tag{44}$$

Where:

Φ = Seasonal autoregressive operator.

Fig.4.7 shows the model fit for Gibe-1 and Gibe-3 time series in a weekly time resolution. From visual inspection, the models follow the patterns of the synthetic time series and capture the information in the time series for both Gibe 1 and Gibe 3.

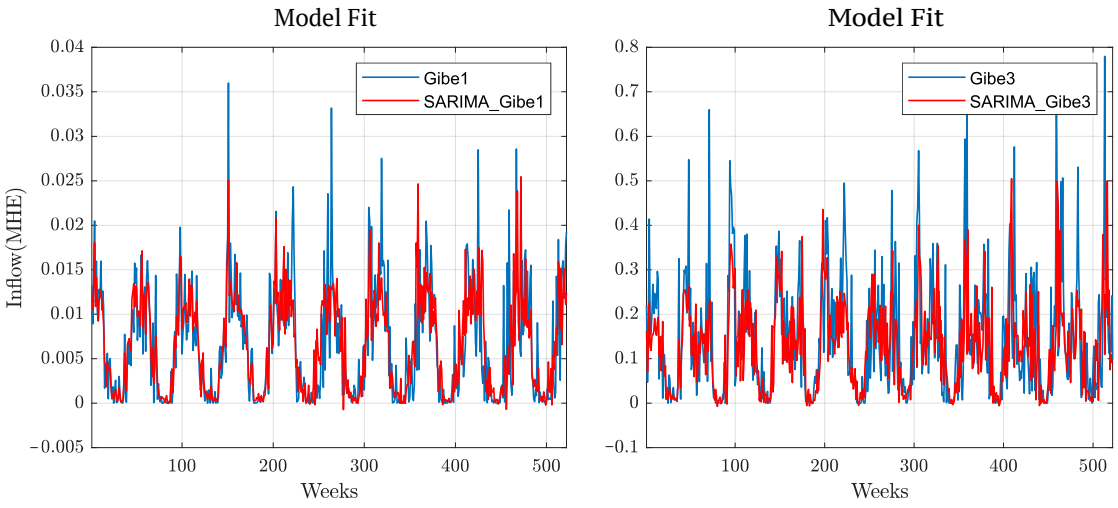

Figure 4.7: Model fit for Gibe-1 and Gibe-3 time series in weekly time resolution.

4.2.3 Residual diagnosis

After estimating the stochastic process, a residual diagnosis is performed in both time series to make sure the models fit with the historical series.

Daily time resolution

A residual diagnosis is performed first using a visual inspection of the ACF and histogram plots shown in Fig.4.8, which shows normally distributed and uncorrelated residuals. In addition to the visual inspection of the ACF plot, we run theLjung-box Q-test (LBQ)for autocorrelation of the Gibe-3 SARIMA model using the Matlab econometric modeler tool Version 5.1 (R2018b) with the test parameters of $Lags = 20$, Degree of freedom $(DOF) = 10$, and significance level $= 0.05$.

The null hypothesis is that the first m autocorrelations of the residuals of the SARIMA model are jointly zero.

$$H_0 : \rho_1 = \rho_2 = ... = \rho_m = 0$$

$$H_a : \rho_j \neq 0, j \in 1, ..., m$$

Table 4.1: Test results

	Null Rejected	P-Value	Test Statistic	Critical Value
1	false	0.27408	23.3047	31.4104

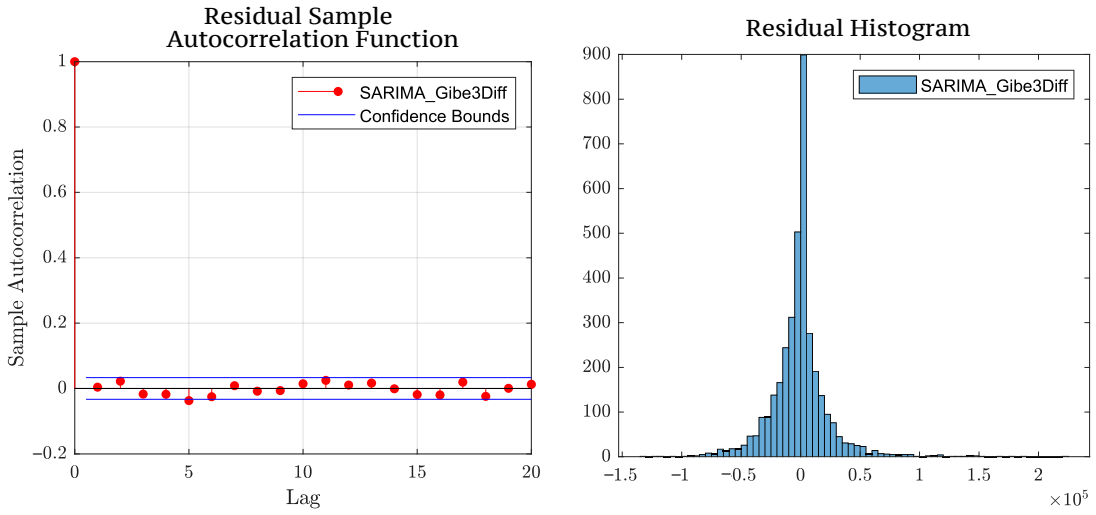

Figure 4.8: Residual diagnosis of differenced Gibe3 time series.

The test result in Table 4.1 shows that the null hypothesis is not rejected, indicating a good fit for the model. The estimation result for the SARIMA model of Gibe-3 Reservoir is

presented in Table 4.2.

Table 4.2: Model Estimation result for SARIMA(0,1,3)(0,1,2)[365] Model

Parameter	Value	StandardError	TStatistic	PValue
Constant	0	0		
MA{1}=θ_1	-1.403	0.045174	-31.0574	9.0611e-212
MA{2} =θ_2	0.28348	0.085036	3.3336	0.00085725
MA{3} =θ_3	0.1482	0.058094	2.551	0.010741
SMA{1}=Θ_{365}	-0.77234	0.064318	-12.0081	3.2218e-33
SMA{2}=Θ_{730}	0.014517	0.070344	0.20637	0.8365
Variance	3.0546e+9	3.1855e-12	9.5891e+21	0

Weekly time resolution

The residuals are diagnosed visually using ACF and histogram plots and using the LBQ test. The result from the visual inspection of the ACF and histogram plots of the residuals in Fig.4.9 indicates almost normally distributed residuals without correlation. Furthermore, the result of the null hypothesis in the LBQ test with the test parameter of $Lags = 20$, Degree of freedom $(DOF) = 10$, and significance level $= 0.05$ shows that the first m autocorrelations

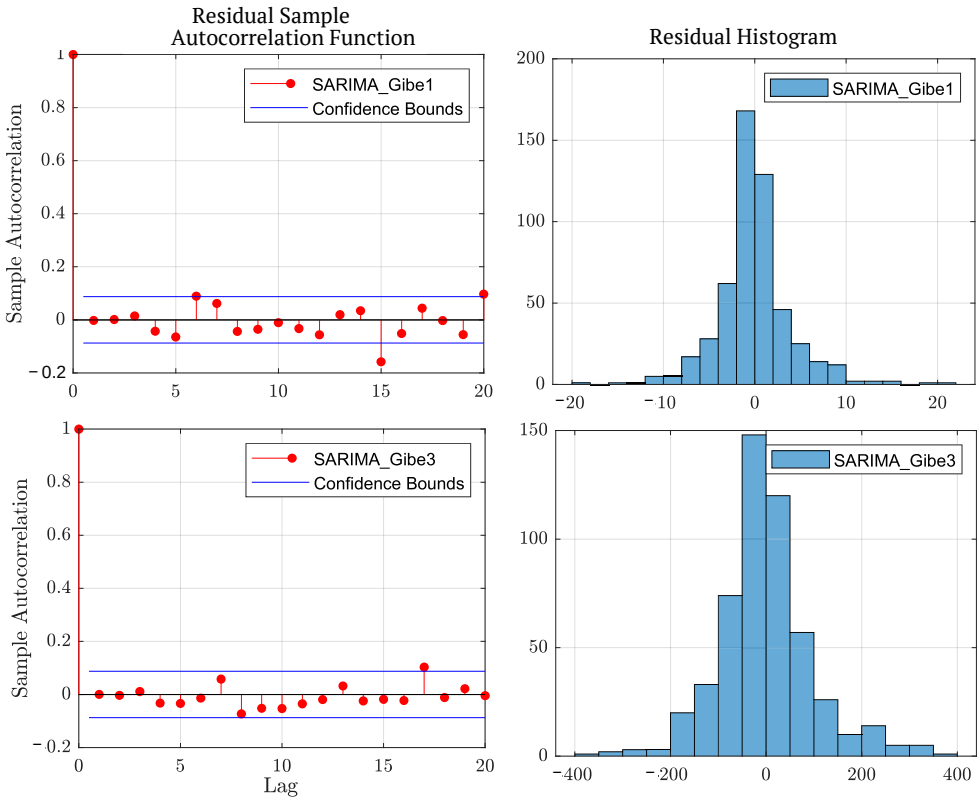

Figure 4.9: Residual diagnosis weekly time resolution.

of the residuals of the SARIMA model are jointly zero, and the hypothesis is not rejected for both Gibe 1 and Gibe 3; the same holds for the rest of the reservoirs. That means the model passes all the diagnosis checks, which indicates a good fit for the model.

4.2.4 Scenario Generation

To generate the sample realizations of random inflow scenarios from the estimated stochastic models, SARIMA models in our case, we apply the Monte Carlo Simulation Method using the synthetic time series and the inferred residuals as pre-sample data. This method enables us to generate as many different paths as we want for the length of observation time we require. In this thesis, fifty different paths for two years of observation are generated for both time resolutions.

Daily time resolution

The simulation result in Fig.4.10 on the left-hand side shows that the model captures the seasonal variation of the inflow series and follows the same pattern as the synthetic time series. It can be noted, though, that the simulation does not have the large peaks seen in the synthetic time series. Moreover, the simulation mean goes down to the negative value when the synthetic inflow is at its minimum; this means there are negative inflows during specific periods. These negative inflow results are mainly due to the assumption of a Gaussian distribution in the autoregressive integrated moving average (ARIMA) model estimation and the Monte Carlo sample values in the range of ($-\infty$ to ∞). In practice, the negative inflow would correspond to a situation where the evaporation is higher than the inflow of water, which is very rare in Ethiopia; at least, it is not visible in the synthetic series. Then, we do not want to have negative inflows in the randomly generated scenarios either. Therefore, we remove the negative values from the generated scenarios by truncating the values to zero. The right-hand side of Fig.4.10 shows the synthetic time series and the mean of truncated inflow scenarios; when we compare the two curves, the simulation mean tends to the positive throughout the time of simulation because the truncation process significantly affects the simulation mean.

We can conclude that the sample realizations of the random series generated from the daily time resolution are not realistic scenarios and would not transform the features in the synthetic series to a random, future scenario.

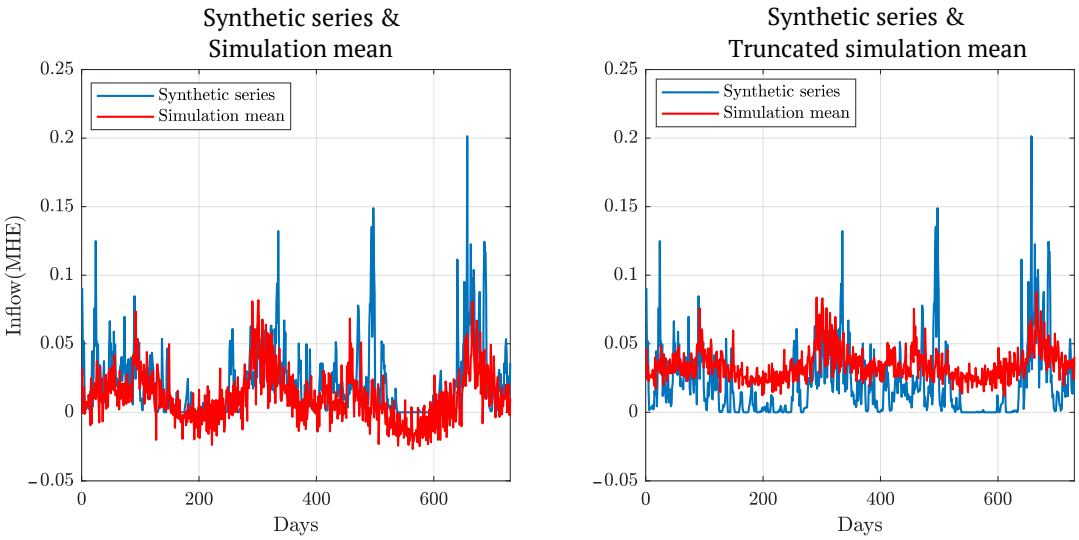

Figure 4.10: Simulation mean and synthetic historical series for Gibe 3 in daily time resolution.

Weekly time resolution

The simulation result in Fig.4.11 on the left-hand side shows that the simulation mean has an almost similar pattern to the synthetic series. There are two points where the mean becomes negative, indicating the presence of a negative inflow in the generated series. The figure on the right-hand side shows the synthetic series with the mean of the truncated inflow series; the result shows a slight upward shift in the simulation mean. However, the approximation effect is much less for the series in weekly time resolution.

When we compare the simulation mean of the two data sets, in Fig.4.10 and Fig.4.11, we can see that the model in the weekly time series best captures the behavior of the synthetic time series; moreover, the effect of the truncation is less visible in the weekly resolution. Therefore, we can conclude that the scenarios generated from the weekly resolution time series best capture the features in the synthetic historical series.

4.2.5 Evaluation of Generated Inflow Scenarios.

Random inflow scenarios could be used for long-term hydropower planning using stochastic models. Before we use the random inflow scenarios directly to stochastic models, we need to verify that the scenarios are useful as inputs for hydropower planning problems. The scenarios in the weekly time resolution are tested in the deterministic model presented in

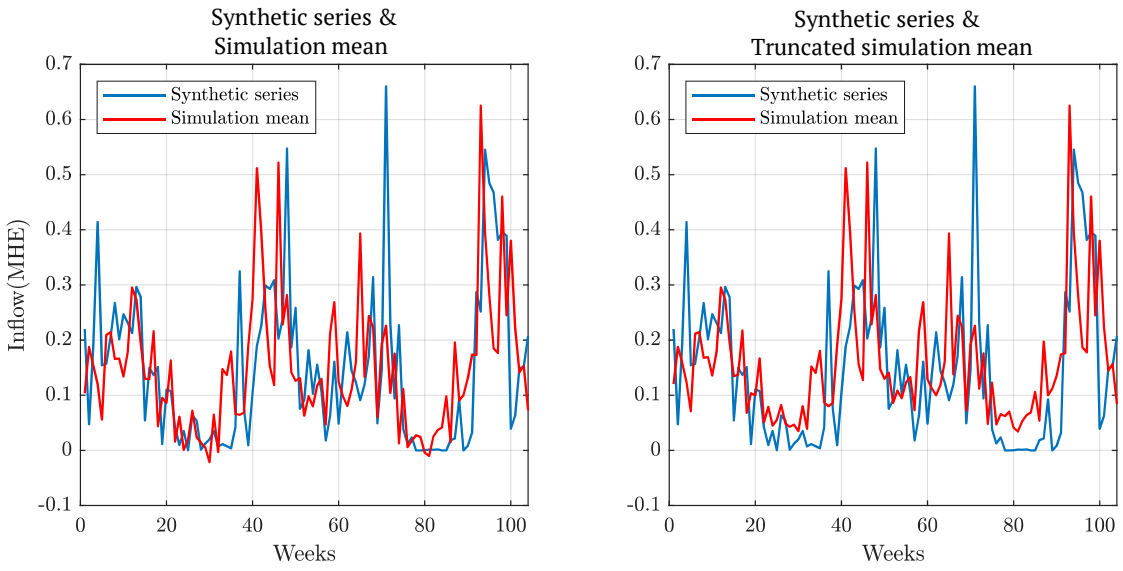

Figure 4.11: Simulation mean and synthetic historical series in weekly resolution.

section 4.1.

The deterministic simulation model is a model to maximizes the value of stored water and minimizes load shedding by utilizing the water stored in the rainy season throughout the dry season with optimized water management. The objective here is to simulate the model with the random inflow realizations and to see if we can get a reasonable generation scheduling, acceptable load shedding, realistic reservoir level patterns, and realistic spillage compared to the actual operation in the Ethiopian power system.

Fifty scenarios have been created using the model with weekly time resolution. In case-1, the inflow will be equal to the mean of all these scenarios; case-2 will use the scenario with the highest total inflow, and case-3 will use the scenario with the lowest total inflow. A load demand equal to the actual demand in 2018-2019 is considered for all the simulations. The simulation results from the three cases are compared to the actual planning of the Ethiopian power system in 2018-2019.

The three cases of inflow scenarios and the synthetic inflow in the 2018-2019 planning year in weekly time resolution are shown in Fig.4.12. The deterministic hydropower model uses a time resolution of one hour. Therefore, the inflows in weekly time resolution shown in Fig.4.12 are converted to hourly resolution so that any hour is assumed to be 1/168 of the corresponding weekly inflow. The simulation result of case 1 for the generation and load shedding is similar to the simulation result of the deterministic model in section 4.1. This

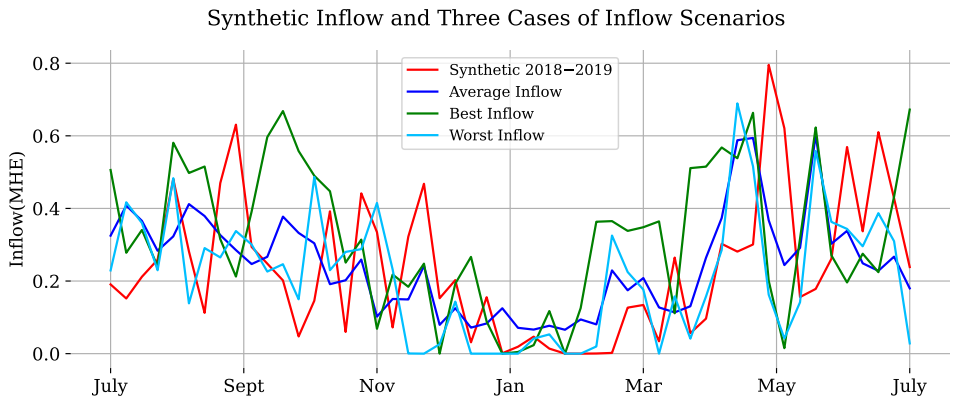

Figure 4.12: The three cases of inflow scenarios and synthetic inflow of 2018-2019.

shows that the average inflow in Case1 is realistic that we get realistic output.

We can also see in Fig.4.13 that the simulation result of the generation scheduling in the actual and simulated operation for ten days in April when we can see a load shedding in the actual operation and zero load shedding in the simulation.

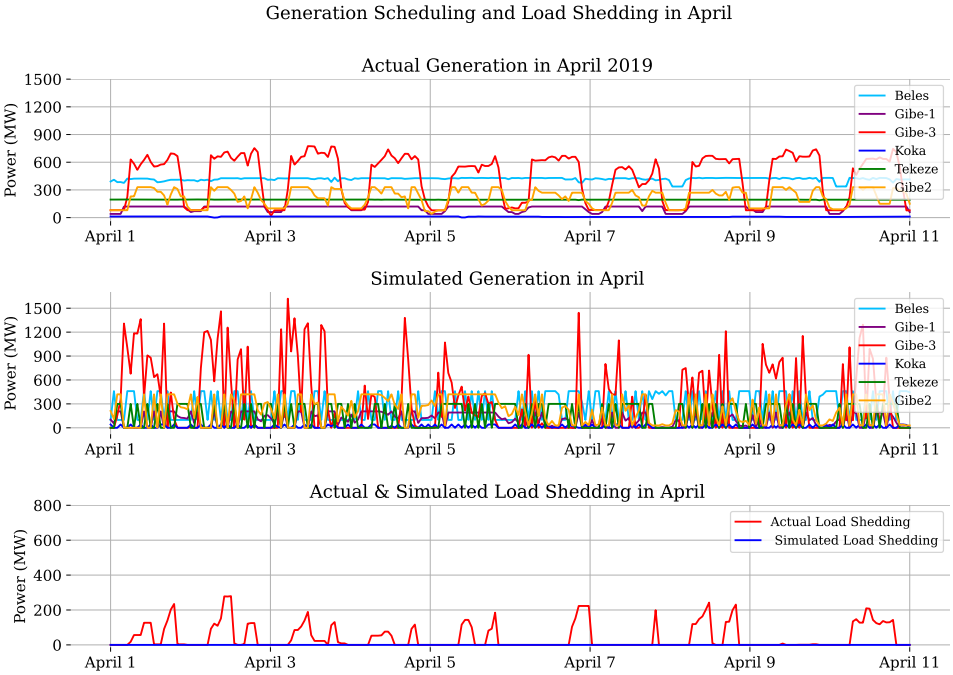

Figure 4.13: Actual and simulated load shedding and generation schedule for sample reservoirs in April.

The figure shows that the actual operation follows the same generation pattern each day, the

Gibe-3 reservoir supplies the variation in the load, and the smaller reservoirs have the same generation level; consequently, we see a lot of load shedding during this time of the planning year. However, the model is expected to perform better than the actual operation since it has the perfect information. Therefore, the model schedules the generation arbitrarily between the reservoirs in the simulation to minimize load shedding and maximize stored water.

In Fig.4.14, we can see sample reservoirs' start and final content for actual and simulated operation, which are at the same level for most reservoirs except the Gibe-3 reservoir. Let us compare the synthetic historical inflow and the inflow scenario. The inflow is slightly higher in the average scenario (12.17 million HE compared to 11.15 million HE in the synthetic scenario for 2018-2019). However, on the other hand, the amount of stored water is around 1.1 million HE higher in the simulated operation of the average scenario compared to the actual operation in 2018-2019. This indicates that the load shedding in 2018-2019 was not because there was insufficient water but because the water was not used efficiently. In practice, water must have been spilled during the earlier rainy seasons. Unfortunately, there are no records of spillage from Ethiopian hydropower plants. Therefore, it is not possible to verify this conclusion.

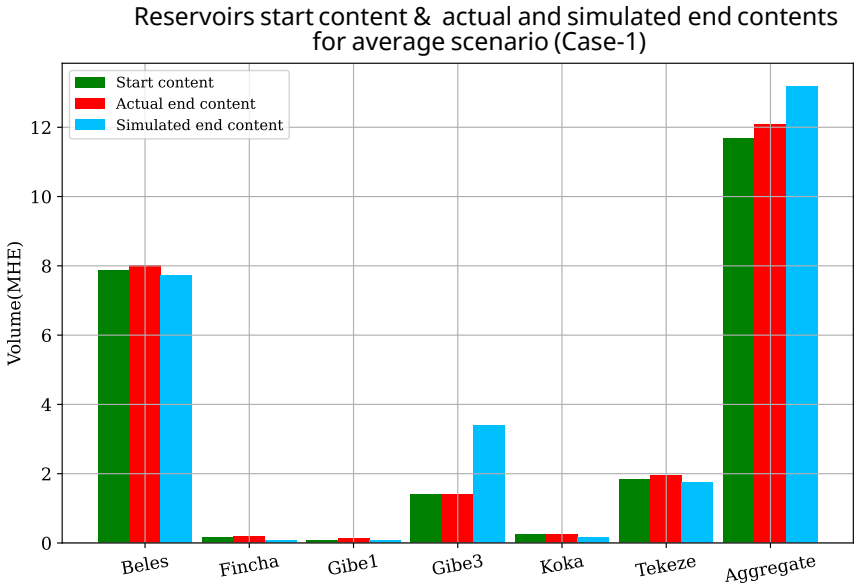

Figure 4.14: Start and final reservoir contents; for actual operation and simulation of case-1.

If the inflow scenarios were unrealistic, we could, for example, have periods with full reservoirs (due to inflow peaks) and spillage, or we could have periods with empty reservoirs

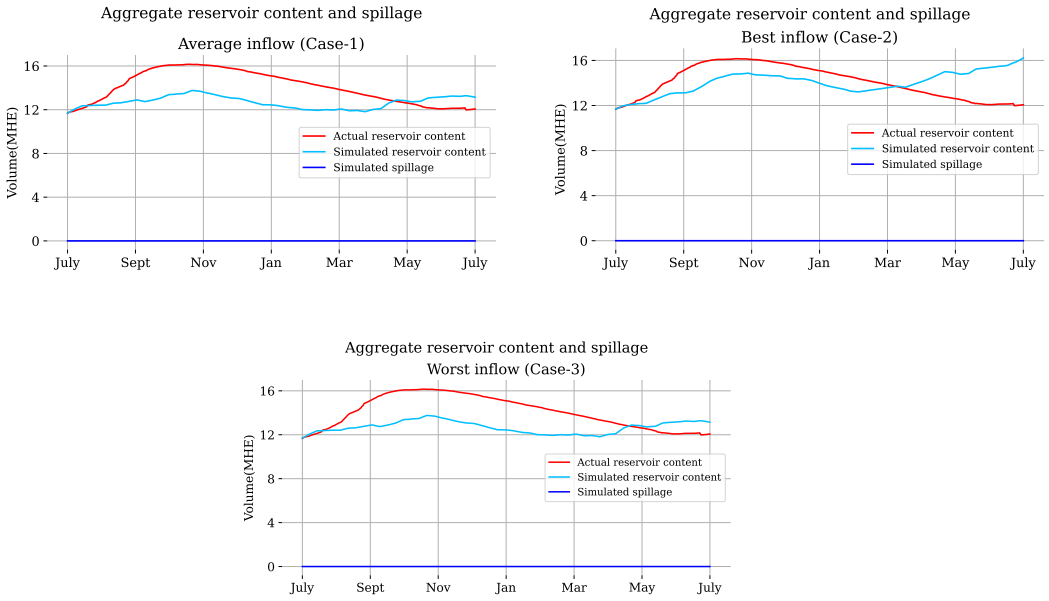

Figure 4.15: Actual reservoir content plus simulated reservoir contents and spillage for the tree cases.

and plenty of load shedding. However, no such problems are experienced in the simulation of all three cases, as presented in Fig.4.15. Therefore, we can conclude that the random inflow scenarios generated are good enough to get realistic results. From a long-term perspective, it would be more efficient to use planning tools taking into account forecasts rather than the existing rules of thumb or following historical generation trends.

4.3 Stochastic model

The stochastic planning model is developed using the random inflow scenarios generated in the previous section in a weekly time resolution. This model will allow us to use random scenarios for a range of possible outcomes in the future. The simulation result of the two-stage stochastic planning model in Fig.4.16 shows the generation, load shedding, reservoir content, and spillage for the 2018–2019 planning year load demand (hereinafter called current load). In all inflow scenarios, the system supplies the demand with zero load shedding, as shown on the left-hand side of the figure, with a range of possible reservoir content and spillage; the average value of reservoir content and spillage are shown in the right-hand side of the figure the with the blue curve. It would be interesting to see the performance of the model with an addition in the load level.

Fig.4.17 shows the model outputs with a 35% load level increase. The possible generation

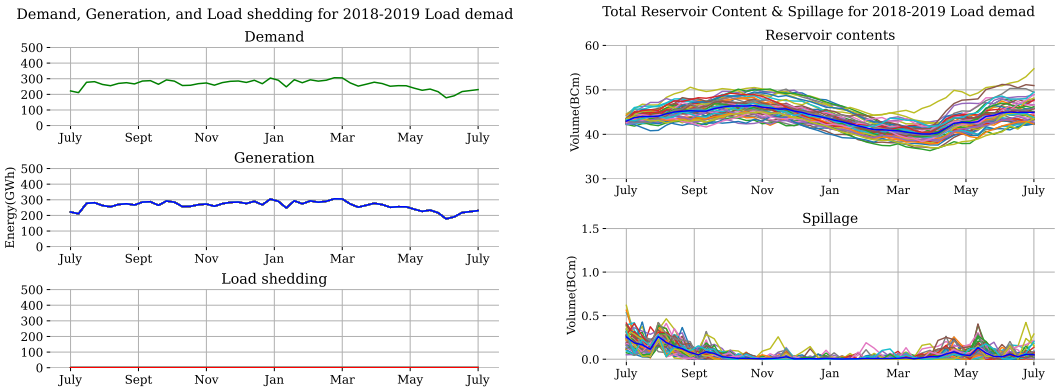

Figure 4.16: Model output for current load level in a weekly time resolution.

outputs and the corresponding load shedding for the different inflow scenarios can now be seen clearly. The average values are indicated with the bold blue curve for the generation and the bold red curve for the load-shedding. The reservoir content and spillage curves also show the range of possible outcomes, and more water is utilized as compared to the current load level.

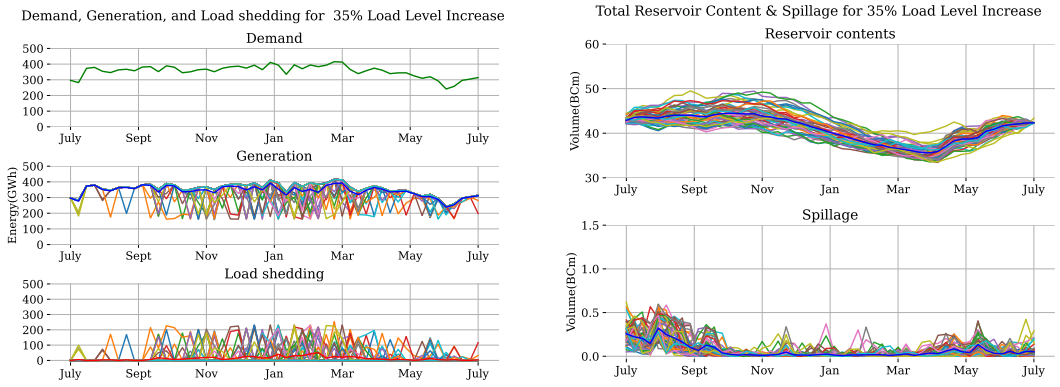

Figure 4.17: Model output for 35% load level increase in a weekly time resolution

The next figures in Fig.4.18 show the generation, load shedding, reservoir content, and spillage for the average, best, and worst inflow scenarios of the 35% load level increase.

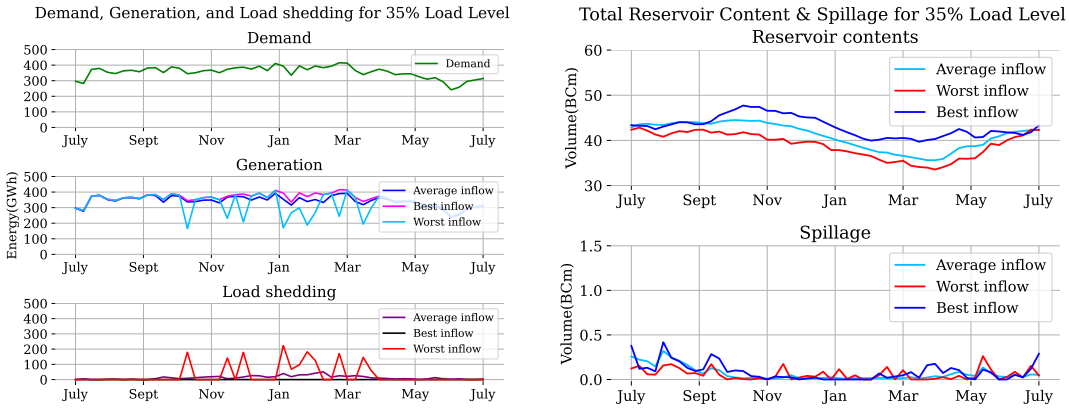

Figure 4.18: Model output of 35% load level increase for the average, best, and worst inflow scenarios in a weekly time resolution

4.3.1 Value of Stochastic Solution (VSS).

This section discusses the advantage of considering uncertainties in the planning model to account for unfavorable conditions instead of planning the generation considering average values, i.e., the advantage of doing stochastic models over deterministic models. The two-stage stochastic model is compared to the deterministic model. The load demand of the 2018–2019 planning year is used for both models. The 50 inflow scenarios are used in the stochastic simulation. The inflow for the deterministic model is set to be the average of these 50 scenarios. The models are further simulated for 35% and 50% load level increases with the same 50 inflow scenarios.

Table 4.3 shows the optimal values for the stochastic problem (RP), EEV, and the VSS for the different load level increases in the two-stage stochastic model. For the maximization problem, all the values of the VSS for the different load level increases are positive. This indicates solving the stochastic model is more profitable than the deterministic one, and it is worth considering the uncertainties in the inflow for the hydropower planning model.

Table 4.3: Value of stochastic solution (VSS) for a different load level increase

Load Level increase	Optimal values (MUSD)		Quality Metric
	Z^{RP}	Z^{EEV}	VSS
0%	1,598.42	1,520.88	77.54
35%	1,015.44	984.75	30.69
50%	134.08	120.86	13.82

4.3.2 Risk-Averse and Risk-Neutral stochastic Models

In stochastic models, it is common to consider risk measures for unfavorable scenarios. A model that incorporates risk measures for unfavorable scenarios into the objective function or as an additional set of constraints is called a risk-averse model and a model without these measures is called a risk-neutral model.

Risk-Neutral stochastic Model

The stochastic model developed in the previous section 4.4 can be considered as a risk-neutral stochastic model. In the risk-neutral problem, we do not consider the worst thing that can happen following different scenarios. However, we make a trade-off between the planning we are doing now and what we are going to do in the future, i.e., load shedding now or in the future, by introducing a higher penalty cost for load shedding weighted by a cost factor $C \in [0, \infty]$ and limiting the minimum reservoir content at the end of the planning period for all inflow scenarios (28).

To determine a reasonable penalty cost, the model is simulated for different values of C as shown in Table 4.4. In the optimization process, a reasonable value is assigned for the value

Table 4.4: Sensitivity analysis of cost of load shedding C/MWh.

$\lambda = \$50$	$C = \$200$	$C = \$500$	$C = \$750$	$C = \$1000$
Optimal value (M$)	1,213.65	1,015.44	852.83	690.22
Energy in Stored Water (TWh)	26.97	26.81	26.81	26.81
Load shedding(TWh)	0.67	0.65	0.65	0.65

of stored water based on the tariff set in the Ethiopian power system, which is $50/MWh. We simulate the model using different values of penalty cost to determine how high we should set the penalty cost for the model. As it can be seen from Table 4.4, the load shedding is higher for $C = \$200$/MWh, but it is the same for $C = \$500, \$750$, and $\$1000$/MWh; hence, no matter how high the penalty cost might be, the system cannot keep the load shedding less than 0.65 TWh. Therefore, the highest penalty cost that could be assigned for this model will be $C = \$500$/MWh.

Risk-Averse stochastic Model

The risk-averse model considers risk measures related to low reservoir content, high load shedding, and combining the two, i.e., the risk of low optimal value in some unfavorable

inflow scenarios. We have used the CVaR risk measure in three different cases using equations (33a -33c) to determine the risk measure with reasonable results. Case-a, when the risk measure considers only the value of stored water, constraint (33a); Case-b when the risk measure considers only the load shedding, constraint (33b); and Case-c when the risk measure considers all the objective functions, constraint (33c).

The model is simulated for different β values. The simulation results presented in Table 4.5 show that when the value of $\beta = 0$, the problem will be risk neutral; the values are the same for all three cases; when the value of β is different from zero, the model becomes risk-averse, and we will get different results for the different cases.

Table 4.5: Summery of CVaR risk measure with $\alpha = 0.8$ and different values of β

Risk-Averse $(\eta \geq \zeta - Z^{\omega})$	$C = 500$ **USD/MWh,** $\lambda = 50$ **USD/MWh**	$\beta = 0$	$\beta = 0.5$	$\beta = 0.75$	$\beta = 1$
Risk measures for stored water $(Z^{\omega} = Z_1^{\omega})$ (Case-a)	Optimal value with out the risk measure (M$)	1,015.44	1,005.50	865.93	- 6,872.34
	Energy in stored water (TWh)	26.81	26.88	27.75	37.05
	Load shedding (TWh)	0.65	0.68	1.04	17.45
	$\beta * CVaR$ (M$)	421.35	647.32	1,840.70	1,849.95
Risk measures for load shedding $(Z^{\omega} = -Z_2^{\omega})$ (Case-b)	Optimal value without the risk measure (M$)	1,015.44	1,015.44	1,015.44	883.27
	Energy in stored water (TWh)	26.81	26.81	26.81	26.16
	Load shedding (TWh)	0.65	0.65	0.65	0.85
	$\beta * CVaR$ (M$)	0.00	- 377.29	- 750.80	- 754.57
Risk measures for entire objective $(Z^{\omega} = Z_1^{\omega} - Z_2^{\omega})$ (Case-c)	Optimal value without the risk measure (M$)	1,015.44	1,015.44	1,015.44	639.04
	Energy in stored water (TWh)	26.81	26.81	26.81	24.94
	Load shedding (TWh)	0.65	0.65	0.65	1.22
	$\beta * CVaR$ (M$)	0.00	265.77	528.88	531.54

Case-a, when the risk measure considers the value of stored water only, as the value of β increases from zero to 0.5, the energy in stored water increases by 0.07 TWh, and load shedding increases by 0.03 TWh. This is an indication that water is used more efficiently since the increase in stored energy is larger than the increased load shedding. Comparing $\beta = 0$ to $\beta = 0.75$ shows that the energy in stored water increases by 0.94 TWh and load shedding increases by 0.39 TWh, which again means that we store more water in the future at the expense of a small amount of load shedding now. However, when we further increase

the value of β, we get a lot of load shedding, which leads to a very high penalty cost without an equivalent increase in the stored water, indicating inefficient water use.

Case-b, when the risk measure considers the load shedding only, as the value of β increases to 0.5 and to 0.75, there is no change in all the values; the change starts when $\beta = 1$, i.e., when we are a 100% risk-conscious, at this point, the energy in the stored water decreases by 0.65 TWh, and the load shedding increases by 0.20 TWh, which is less efficient than what we get in Case-a at $\beta = 0.5$.

Case-c, when the risk measure considers the entire objective function, as the value of β increases to 0.5 and to 0.75, there is no change in all the values; when $\beta = 1$, the energy in the stored water decreases by 1.87 TWh, and the load shedding increases by 0.57 TWh. which is less efficient than Case-b at $\beta = 1$ and Case-a at $\beta = 0.5$.

4.4 Rolling horizon framework

The rolling horizon framework helps to make periodic decisions and update the information in each rolling horizon, which minimizes the error in a prolonged forecast. The model rolls in a fixed horizon, with the first period updated in each roll. The rolling horizon framework is a simulation for real operation. In real operations, we do not make one plan at the beginning of the year and stick to that until the end of the year. Rather, we make a plan, watch what happens, and update the plan, watch what happens and update the plan again, and the process continues until the end of the planning period.

The different models have been evaluated in a weekly rolling horizon framework. This framework allows making immediate decisions for one week at a time and updating the actual information after each week. The update can also include an updated forecast for the remaining time horizon. However, this study will use the same 50 inflow scenarios for the rolling horizon.

The simulation results of the two risk-averse stochastic models are compared to those of the risk-neutral stochastic model and the deterministic model. Based on the results in section 4.3.2, the risk-averse model was tested for two risk measures: Case-a with $\beta = 0.5$ and Case-b with $\beta = 1.0$.

The objective of the comparison is to study how they manage load shedding when there is not enough hydropower generation available. In particular, the challenge is the trade-off

between load shedding now and in the future. In principle, we can avoid load shedding using all the water we have right now, but then, if we have a poor rainy season with low inflow next year, we may get into a massive problem supplying the demand next year. Therefore, we have to have some margins left if things get worse in the future. This is a challenge for the power system planners; they want to avoid massive load shedding events where they have to disconnect almost half the power system. This inevitably disconnects essential loads, leading to enormous problems for society, whereas, if we have smaller load shedding, we can do rotating load curtailments that affect residential areas, which may have a smaller societal impact. Hence, if load shedding is inevitable, it is preferable to have small levels of load shedding for longer time periods rather than massive load shedding during short periods. The overall objective is still to have as low load shedding as possible. Consequently, there are three criteria to evaluate for the different planning models:

- How large is the total load shedding during a year?
- How much water is saved for the future?
- How is the load shedding distributed within the year?

The four models are studied as four cases, with the deterministic model considered as Case-D, the risk-neutral stochastic model as Case-RN, the risk-averse model with risk measure of stored water at $\beta = 0.5$ as Case-RA-1, and the risk-averse model with risk measure of load shedding at $\beta = 1$ as Case-RA-2.

All the cases are simulated in a weekly rolling horizon framework using the synthetic historical inflow of 2018–2019 as the actual inflow to update the information after each one-week time step. The load demand of the 2018–2019 planning year is used as a current load demand. The system supplies the current load demand with zero load shedding in all the cases. Therefore, it would be interesting to see how the system performs in the four cases when the demand is getting higher without additional capacity. All the cases are simulated with load level increases of 35% and 50% from the current load to study the performance when the hydropower capacity is insufficient. The results are summarised in Table 4.6, Fig.4.19 and Fig.4.20. The two figures show a different pattern and distribution of the load shedding throughout the year for the different cases.

For the deterministic model (Case-D), Table-4.6 and Fig.4.20 show that for the 35% load level increase, the load shedding concentrates in the second half of the year with a total

Table 4.6: Summary of total and maximum load shedding, energy in stored and spilled water in (TWh) for the four cases.

	Load level increase ($D_t + \%D_t$)	Deterministic (Case-D)	Risk-neutral Stochastic (Case-RN)	Risk-averse Stochastic (Case-RA-1)	Risk-averse Stochastic (Case-RA-2)
Total L.sh	35%	1.17	0.82	0.77	1.32
(U_{tot})	50%	2.23	2.38	2.00	3.34
Maximum L.sh	35%	0.20	0.07	0.07	0.05
(U_{max})	50%	0.26	0.12	0.14	0.11
Energy	35%	28.29	28.35	28.30	28.48
Stored (TWh)	50%	28.26	28.28	28.21	28.48
Energy	35%	0.50	0.41	0.38	0.44
Spilled(TWh)	50%	0.26	0.37	0.35	0.41

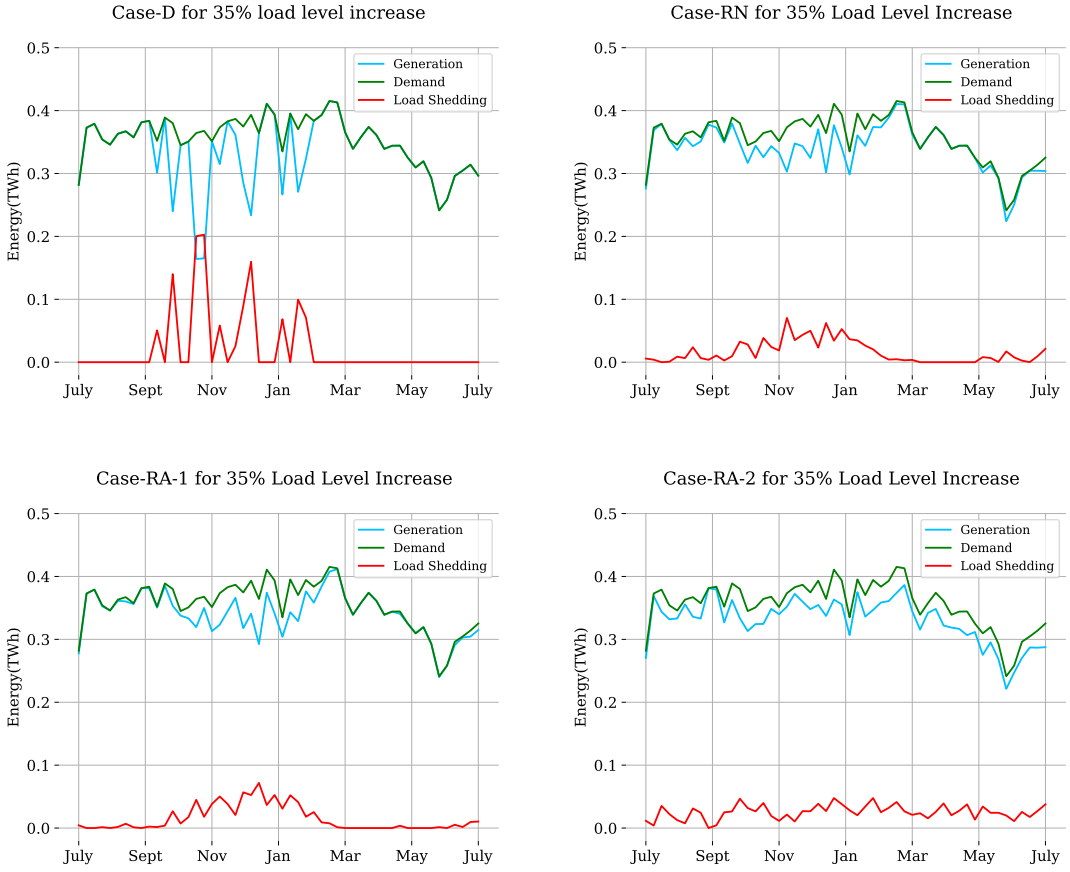

Figure 4.19: Generation, Demand, and Load shedding of 35% load level increase for the four cases.

of 1.17 TWh and a maximum of 0.20 TWh per week. When the load demand increases by 50%, as shown in Fig.4.21, we will see frequent massive load shedding periods starting

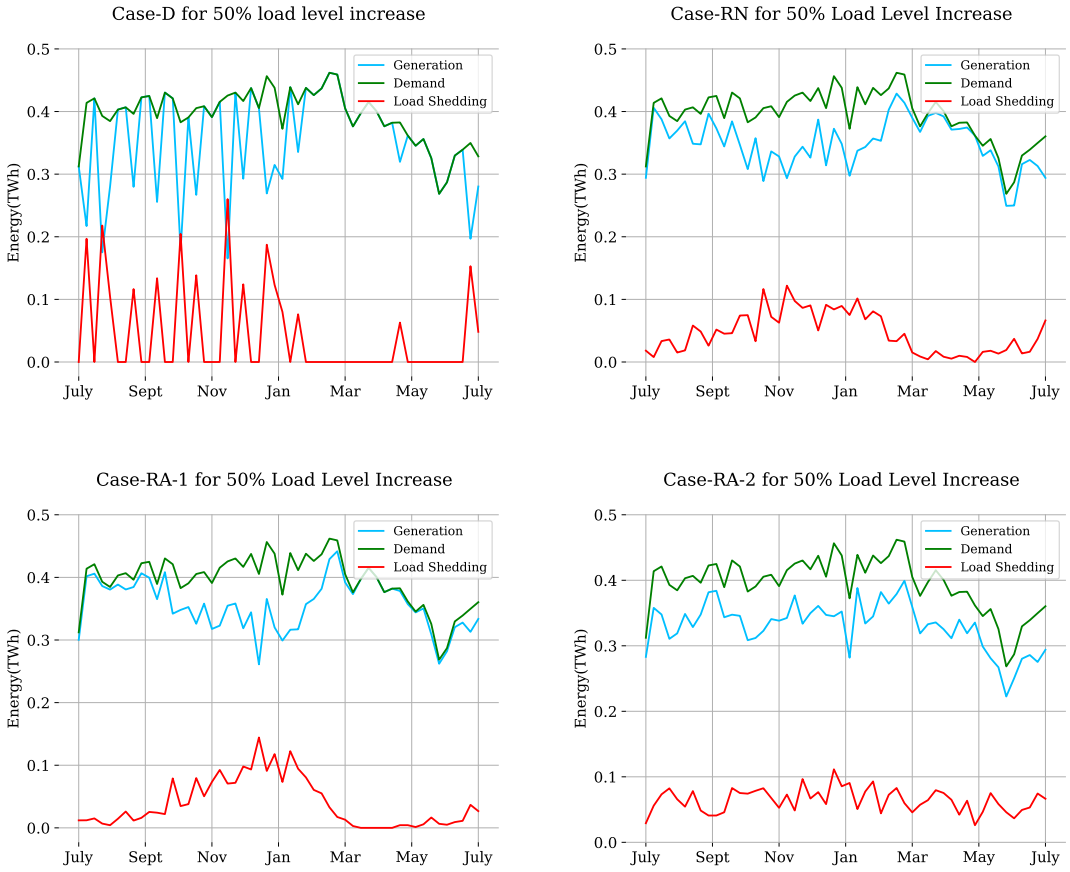

Figure 4.20: Generation, Demand and Load shedding of 50% load level increase, for the four cases.

from the beginning of the planning year and extending to January with a total of 2.23 TWh and a maximum of 0.26 TWh load shedding recorded at a time. Moreover, it stores the least energy for both 35% and 50% load level increase and spills the highest energy in the 35% load level increase. Therefore, Case-D performs poorly based on all the three criteria described.

The risk-neutral stochastic model (Case-RN) distributes the load shedding throughout the year with a total of 0.82 TWh and a maximum load shedding of 0.07 TWh recorded at a time for the 35% load level increase. The risk-neutral model performs better than the deterministic model regarding total and maximum load shedding and the amount of stored energy. As the load level increases by 50%, as shown in Fig.4.20, the total load shedding becomes higher than Case-D and Case-RA-1 but distributes the load shedding more evenly throughout the year, keeping the value below 0.12 TWh. In terms of stored energy, it

performs in between the two risk-averse models; it stores 0.02 TWh more energy than Case-D, 0.07 TWh more energy than Case-RA-1, and 0.20 TWh less energy than Case-RA-2. It spills 0.11 TWh more energy than Case-D, 0.02 TWh more energy than Case-RA-1, and 0.04TWh less energy than Case-RA.

For a 35% load increase, the first risk-averse stochastic model (Case-RA-1) keeps the load shedding below 0.07 TWh, the same as Case-RN, throughout the year with a total of 0.77 TWh, which is lower than all the other cases. It stores and spills less energy than the other two stochastic models. When the load demand increases by 50%, as shown in Fig.4.20, the total load shedding becomes 2.00 TWh, which is the lowest value of all the models. The load shedding is fairly evenly distributed over the year, with the maximum being 0.14 TWh, slightly higher than Case-RN and Case-RA-2. The model stores 0.07 TWh less energy than Case-RN and 0.27 TWh less energy than Case-RA-2. However, we get the advantage of lower load shedding at the expense of a little bit of lower stored energy at the end of the year compared to the other cases.

For a 35% load increase, the second risk-averse stochastic model (Case-RA-2) keeps the load shedding below 0.05 TWh throughout the year, which is lower than the other cases; however, the total load shedding is 1.32 TWh, which is the highest of all the cases. On the other hand, the model stores 0.20 TWh more energy than Case-D, 0.13 TWh more energy than Case-RN, and 0.18 TWh more energy than Case-RA-2. When the load demand increases by 50%, as shown in Fig.4.20, the system keeps the load shedding below 0.11 TWh with a total of 3.34 TWh, which is higher than all the cases. However, the model stores and spills more energy than the other cases at the end of the year; for example, it stores 0.20 TWh and spills 0.04TWh more energy than the Case-RN and stores 0.27 TWh and spills 0.07 TWh more energy than Case-RA-1.Therefore, the poor performance of this case in terms of total load shedding is because it stores and spills more energy than the other cases.

Fig.4.21 compares the distribution of load shedding in the four cases for the 50% load level increase. It is evident from the figure that the stochastic models are more efficient than the deterministic model, which indicates that it would be beneficial to consider uncertainty to avoid inefficient use of water and incidents of extensive load shedding. The stochastic models distribute the load throughout the year, i.e., small load shedding for an extended period instead of massive load shedding for a short period. The risk-neutral (Case-RN)

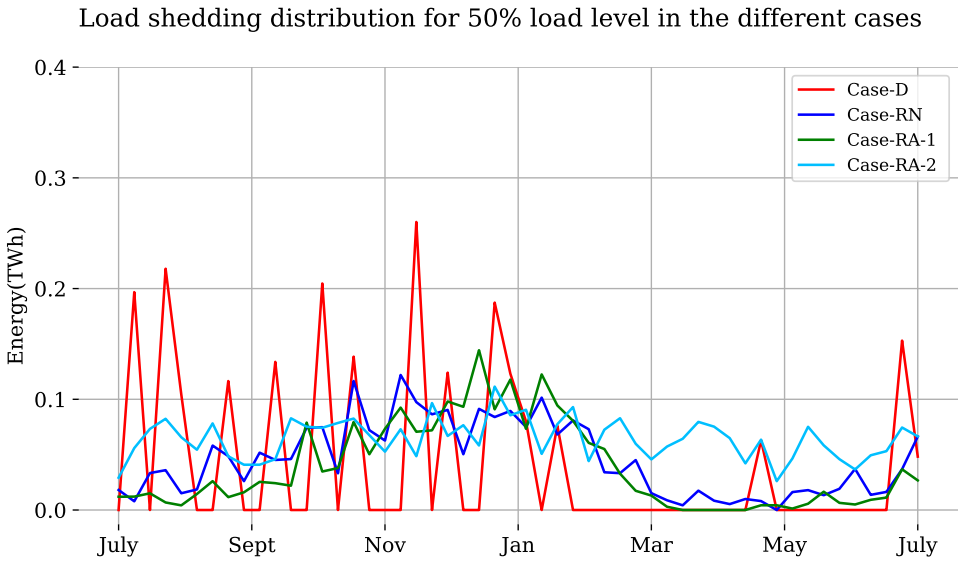

Figure 4.21: Load shedding distribution of the four cases for 50% load level increase

and the best risk-averse model (Case-RA-1) perform almost similarly, with the risk-averse being slightly better for this particular case. When we see the risk-averse (Case-RA-2), considering only the risk with ($\beta = 1$), we have higher load shedding, which leads to the spilling of more water at the end. Therefore, we believe that (Case-RA-1) could be the best model for the system. However, it needs further testing and fine-tuning of parameters such as the confidence level α and the risk factor β. In addition, we could get a different trade-off point for load shedding and stored water if we use actual forecasted inflow data to update the rolling week, if we use a load demand of a different year to run the simulation, or if we simulate the model for a more extended period than one year, etc.

5 Conclusion and future work

5.1 Conclusion

The total generation capacity in the Ethiopian power system is sufficient enough to cover the peak demand of the system. However, it is an energy-limited system because of the hydropower dominance. Therefore, it is very important to use the resources in the best way possible using appropriate planning tools. The absence of a suitable and appropriate generation planning tool makes the planning dependent on historical generation patterns. Consequently, it is common to see load shedding events, especially in the dry seasons of the year.

This thesis has developed and presented different long-term hydropower planning models, including deterministic and stochastic, risk-neutral, and risk-averse models for the Ethiopian power system. It further studies and tests the models in a rolling horizon framework for long-term operation. All the models are developed to utilize the water stored in the rainy season throughout the year with minimum load shedding and find an appropriate trade-off between using the available water now (risking future energy shortage) or starting load-shedding to a smaller or lesser extent.

The first model developed is the deterministic simulation model [C1]. It was shown that the Ethiopian hydropower system has a great deal of flexibility. In theory, most of the load shedding could be avoided both for current as well as a higher load demand. How much of this flexibility can be utilized in reality will depend on the inflow uncertainty, load forecasts, and trading with neighboring countries. Therefore, there is a need to develop long-term planning tools using stochastic models and appropriate forecasts.

To develop the stochastic models, we first need to identify the uncertain parameter and generate scenarios for this parameter, which is the inflow to the reservoir in the case of the Ethiopian power system. We have presented a method to develop a synthetic historical inflow time series by combining the hydropower generation data and satellite precipitation measurement. Identification of stochastic process and inflow scenario generation are also presented [J1]. With the proposed methods, we can generate two sets of synthetic historical time series with daily and weekly time resolutions from the limited available data. We have shown that existing methods can be applied to identify the stochastic process and generate realistic inflow scenarios for the Ethiopian power system, considering the limited

data available.

Monte Carlo simulation is used to generate the scenarios from the fitted stochastic models for both data sets. It is concluded that the time series with weekly resolution best captures the characteristics of the synthetic historical time series and can generate realistic random scenarios. The evaluation of the inflow scenarios indicates that they are good enough to generate reasonable results. These random inflow scenarios have been utilized to develop the stochastic models.

The stochastic planning model is tested for both risk-averse and risk-neutral versions. Three cases of risk considerations are compared to account for a reasonable risk measure for the risk-averse problem. The best solution is the tradeoff between the value of stored water and the cost of load shedding and considering risk measures for stored water. The second best solution is to consider risk measures only for the cost of load shedding. Therefore, the two cases are used to develop two risk-averse stochastic models. The models are then compared with the risk-neutral and the deterministic models in a rolling horizon framework for a one-year planning period [J2].

The rolling horizon framework helps to make periodic decisions and update the information in each rolling week. Moreover, it simulates the real operation. In reality, the long-term planning will be updated after every short-term operation. The model rolls in a fixed horizon, with the first period updated at each roll. The synthetic historical inflow of the 2018–2019 planning year is used as an actual inflow to update the rolling week inflow. Finally, we use a 35% and 50% load level increase to compare the performances of the models.

The results show that the stochastic models achieve the goal of not having a massive blackout; they distribute the load shedding throughout the year. The results clearly indicate that a stochastic planning model is preferable to a deterministic one. The risk-neutral (Case-RN) and the first best risk-averse (Case-RA-1) models seem to be the most promising planning tools to be used in the Ethiopian power system. The case study in this thesis only shows a small difference between the risk-neutral and risk-averse models, and it is not possible to draw any certain conclusion about which method is preferable. That is open for further interpretation and further testing.

Therefore, using any of these two stochastic models would be an improvement compared to the planning, which is mostly based on historical generation patterns. The long-term

stochastic rolling horizon models can be used to improve the utilization of hydropower and reduce and manage the load-shedding encountered randomly at any time of the year and the draining of reservoirs in the dry season. In addition, it can indicate the need for additional capacity in the system when the load demand increases above a certain level. Moreover, better planning tools can improve the utilization of hydropower to minimize generation costs and load shedding. The developed model can be applicable in most African and developing countries' power systems where similar deficiencies might be observed.

5.2 Future work

The long-term hydropower planning models presented in this thesis could be further developed by considering, for example, transmission limitations and more precise models for the efficiency of the hydropower plants. Moreover, to obtain more reliable results, the procedure for collecting and validating power system data in Ethiopia needs to be improved.

If Ethiopia is going to have a modern power system, a detailed hydrological model is something necessary, which is not in place currently. It is recommended to have a long-term objective to develop such a model. It could be future research work to compare the simplified model with what we could do if we had a detailed hydrological model. It is also recommended to consider temporal and spatial correlation in inflow for reservoirs in related locations and correlation between inflow and wind speed, as there is an expansion plan for VRES generation in the Ethiopian power system in the future.

To further improve the long-term stochastic hydropower planning model, it would be interesting to investigate and test the risk-averse model with CVaR risk measure with different confidence levels (α) and risk factor (β) values. To simulate the rolling horizon and test the models using a load profile of a different year or simulation of a more extended period than one year, to use actual inflow forecast information to update the rolling week, etc. These will help to get a better trade-off between load shedding this year and energy stored for the following year. Moreover, it would be interesting to apply the water value method [59] used in the Nordic power system. It could be worth looking at how it works if we apply it to the Ethiopian power system and evaluate its performance in the future.

The other recommendation for future work is to develop a simulation model using stochastic dual dynamic programming for the multi-year reservoirs like GERD, and further

consider energy trade to neighboring countries, renewable integration, and the possible electricity market that may emerge after the commissioning of the mega power projects under construction and the implementation of policies outlined in the third transformation plan.

References

[1] *Hydropower Special Market Report*. Tech. rep. IEA, 2021. DOI: 10.1787/07a7bac8-en.

[2] IHA. *Hydropower Status Report 2020*. Tech. rep. 2020, pp. 1–83. URL: https://www.hydropower.org/publications/2022-hydropower-status-report%20https://www.hydropower.org/sites/default/files/publications-docs/2019_hydropower_status_report_0.pdf.

[3] *Federal Democratic Republic of Ethiopia National Electrification Program 2.0*. Tech. rep.

[4] Ethiopian Electric Power. *Ethiopin Electric Power System Development*. Tech. rep. February. Addis Ababa, 2022.

[5] Naghizadeh, Ramezan Ali et al. "Modeling Hydro Power Plants and Tuning Hydro Governors as an Educational Guideline Article in International Review on Modelling and Simulations (IREMOS) · Modeling Hydro Power Plants and Tuning Hydro Governors as an Educational Guideline". In: *International Review on Modelling and Simulations (I.RE.MO.S.)* 5.4 (2012). ISSN: 1974-9821. URL: https://www.researchgate.net/publication/235675537.

[6] Singh, Vineet Kumar and Singal, S. K. *Operation of hydro power plants-a review*. Mar. 2017. DOI: 10.1016/j.rser.2016.11.169.

[7] Azad, Abdus Samad et al. *Optimization of the hydropower energy generation using Meta-Heuristic approaches: A review*. Nov. 2020. DOI: 10.1016/j.egyr.2020.08.009.

[8] Ahlfors, Charlotta and Amelin, Mikael. "Weekly planning of hydropower in systems with large volumes and varying power generation: A literature review". In: *2021 IEEE Madrid PowerTech, PowerTech 2021 - Conference Proceedings*. Institute of Electrical and Electronics Engineers Inc., June 2021. ISBN: 9781665435970. DOI: 10.1109/PowerTech46648.2021.9495058.

[9] Benedikt Hreinsson, Egill. "Operations modeling in the Iceland hydro dominated power system". In: *Proceedings of the Universities Power Engineering Conference* (2013), pp. 1–6. DOI: 10.1109/UPEC.2013.6714916.

[10] Hammid, Ali Thaeer et al. “A review of optimization algorithms in solving hydro generation scheduling problems”. In: *Energies* 13.11 (2020), pp. 1–21. ISSN: 19961073. DOI: 10.3390/en13112787.

[11] Gjelsvik, Anders, Mo, Birger, and Haugstad, Arne. “Long- and Medium-term Operations Planning and Stochastic Modelling in Hydro-dominated Power Systems Based on Stochastic Dual Dynamic Programming”. In: (2010), pp. 33–55. DOI: 10.1007/978-3-642-02493-1{_}2.

[12] Weiss, Olga et al. “Long-Term scheduling model of Swiss hydropower”. In: *International Conference on the European Energy Market, EEM* 2019-Septe (2019), pp. 1–5. ISSN: 21654093. DOI: 10.1109/EEM.2019.8916260.

[13] Hreinsson, Egill Benedikt. “Long term hydro scheduling with short term load duration and linear transmission constraints; Long term hydro scheduling with short term load duration and linear transmission constraints”. In: *2016 51st International Universities Power Engineering Conference (UPEC)* (2016). DOI: 10.1109/UPEC.2016.8114099.

[14] Scarcelli, Ricardo O. et al. “Aggregated inflows on stochastic dynamic programming for long term hydropower scheduling”. In: *2014 North American Power Symposium, NAPS 2014*. Institute of Electrical and Electronics Engineers Inc., Nov. 2014. ISBN: 9781479959044. DOI: 10.1109/NAPS.2014.6965473.

[15] Shang, Ling et al. “Long-, Medium-, and Short-Term Nested Optimized-Scheduling Model for Cascade Hydropower Plants: Development and Practical Application”. In: *Water (Switzerland)* 14.10 (May 2022). ISSN: 20734441. DOI: 10.3390/w14101586.

[16] Flatabø, Nils et al. “Short-term and Medium-term Generation Scheduling in the Norwegian Hydro System under a Competitive Power Market Structure”. In: *VIII SEPOPE, Brazilia, 2002* January (1998), pp. 1–18. URL: https://www.researchgate.net/publication/306446062.

[17] Oviedo-Sanabria, Ricci E. and González-Fernández, Reinaldo A. “Short-term operation planning of the Itaipu hydroelectric plant considering uncertainties”. In: *19th Power Systems Computation Conference, PSCC 2016* (2016), pp. 0–5. DOI: 10.1109/PSCC.2016.7540928.

[18] Guedes, Lucas S.M. et al. “A Unit Commitment Algorithm and a Compact MILP Model for Short-Term Hydro-Power Generation Scheduling”. In: *IEEE Transactions on Power Systems* 32.5 (2017), pp. 3381–3390. ISSN: 08858950. DOI: 10.1109/TPWRS.2016.2641390.

[19] Fosso, Olav Bjarte and Belsnes, Michael Martin. “Short-term hydro scheduling in a liberalized power system”. In: *2004 International Conference on Power System Technology, POWERCON 2004* 2.November (2004), pp. 1321–1326. DOI: 10.1109/icpst.2004.1460206.

[20] Vardanyan, Yelena and Amelin, Mikael. “The state-of-the-art of the short term hydro power planning with large amount of wind power in the system”. In: *2011 8th International Conference on the European Energy Market, EEM 11*. 2011, pp. 448–454. ISBN: 9781612842844. DOI: 10.1109/EEM.2011.5953053.

[21] Séguin, Sara et al. “Stochastic short-term hydropower planning with inflow scenario trees”. In: *European Journal of Operational Research* 259.3 (June 2017), pp. 1156–1168. ISSN: 03772217. DOI: 10.1016/j.ejor.2016.11.028.

[22] Côté, Pascal and Leconte, Robert. “Comparison of Stochastic Optimization Algorithms for Hydropower Reservoir Operation with Ensemble Streamflow Prediction”. In: *Journal of Water Resources Planning and Management* 142.2 (2016), p. 04015046. ISSN: 0733-9496. DOI: 10.1061/(asce)wr.1943-5452.0000575.

[23] Baslis, Costas G. and Bakirtzis, Anastasios G. “Mid-term stochastic scheduling of a price-maker hydro producer with pumped storage”. In: *IEEE Transactions on Power Systems* 26.4 (Nov. 2011), pp. 1856–1865. ISSN: 08858950. DOI: 10.1109/TPWRS.2011.2119335.

[24] Vardanyan, Yelena and Amelin, Mikael. “A sensitivity analysis of short-term hydropower planning using stochastic programming”. In: *IEEE Power and Energy Society General Meeting*. 2012, pp. 1–7. ISBN: 9781467327275. DOI: 10.1109/PESGM.2012.6344769.

[25] Fleten, Stein Erik and Kristoffersen, Trine Krogh. “Stochastic programming for optimizing bidding strategies of a Nordic hydropower producer”. In: *European Journal of Operational Research* 181.2 (Sept. 2007), pp. 916–928. ISSN: 03772217. DOI: 10.1016/j.ejor.2006.08.023.

[26] Quintana, V. H. and Chikhani, A. Y. “A Stochastic Model for Mid-Term Operation Planning of Hydro-Thermal Systems with Random Reservoir Inflows”. In: *IEEE Transactions on Power Apparatus and Systems* PAS-100.3 (1981), pp. 1119–1127. ISSN: 00189510. DOI: 10.1109/TPAS.1981.316578.

[27] Daniel, Edsel B. “Watershed Modeling and its Applications: A State-of-the-Art Review”. In: *The Open Hydrology Journal* 5.1 (2011), pp. 26–50. ISSN: 18743781. DOI: 10.2174/1874378101105010026.

[28] Leavesley, George H. et al. “Precipitation-Runoff Modeling System.” In: 1981, pp. 263–264.

[29] Daniel, Edsel B et al. *Watershed Modeling Using GIS Technology: A Critical Review*. Tech. rep. 2. 2010.

[30] Moon, J, Srinivasan, R, and Jacobs, J H. “STREAM FLOW ESTIMATION USING SPATIALLY DISTRIBUTED RAINFALL IN THE TRINITY RIVER BASIN, TEXAS”. In: *Transactions of the ASAE* 47.5 (), pp. 1445–1451.

[31] Obeysekera, J. T.B. and Salas, J. D. “Modeling of aggregated hydrologic time series”. In: *Journal of Hydrology* 86.3-4 (1986), pp. 197–219. ISSN: 00221694. DOI: 10.1016/0022-1694(86)90165-4.

[32] Stokelj, T., Paravan, D., and Golob, R. “Short and mid term hydro power plant reservoir inflow forecasting”. In: *PowerCon 2000 - 2000 International Conference on Power System Technology, Proceedings*. Vol. 2. Institute of Electrical and Electronics Engineers Inc., 2000, pp. 1107–1112. ISBN: 0780363388. DOI: 10.1109/ICPST.2000.897175.

[33] Sharma, Ashish and O’Neill, Robert. “A nonparametric approach for representing interannual dependence in monthly streamflow sequences”. In: *Water Resources Research* 38.7 (July 2002), pp. 5–1. ISSN: 00431397. DOI: 10.1029/2001WR000953.

[34] Jimenez, C, Mcleod, A I, and Hipel, K W. “Stochastic Hydrology and Hydraulics Kalman filter estimation for periodic autoregressive-moving average models”. In: *Stochastic Hydrology and Hydraulics*. Vol. 3. Springer-Verlag, 1989, pp. 227–240.

[35] Pereira, Guilherme and Veiga, Alvaro. “PAR(p)-vine copula based model for stochastic streamflow scenario generation”. In: *Stochastic Environmental Research and Risk Assessment* 32.3 (2018), pp. 833–842. ISSN: 14363259. DOI: 10.1007/s00477-017-1411-2.

[36] Wang, Wenzhuo et al. “A stochastic simulation model for monthly river flow in dry season”. In: *Water (Switzerland)* 10.11 (2018). ISSN: 20734441. DOI: 10.3390/w10111654.

[37] De Almeida Pereira, Guilherme Armando and Souza, Reinaldo Castro. “Long Memory Models to Generate Synthetic Hydrological Series”. In: *Mathematical Problems in Engineering* 2014 (2014). ISSN: 15635147. DOI: 10.1155/2014/823046.

[38] Rodilla, Pablo et al. “Hydro resource management, risk aversion and equilibrium in an incomplete electricity market setting”. In: *Energy Economics* 51 (Sept. 2015), pp. 365–382. ISSN: 01409883. DOI: 10.1016/j.eneco.2015.07.002.

[39] Çavuş, Özlem, Kocaman, Ayse Selin, and Yılmaz, Özlem. “A risk-averse approach for the planning of a hybrid energy system with conventional hydropower”. In: *Computers and Operations Research* 126 (Feb. 2021). ISSN: 03050548. DOI: 10.1016/j.cor.2020.105092.

[40] Shapiro, Alexander et al. “Risk neutral and risk averse Stochastic Dual Dynamic Programming method”. In: *European Journal of Operational Research* 224.2 (2013), pp. 375–391. ISSN: 03772217. DOI: 10.1016/j.ejor.2012.08.022.

[41] Costley, Mitch et al. “A rolling-horizon unit commitment framework with flexible periodicity”. In: *International Journal of Electrical Power and Energy Systems* 90 (Sept. 2017), pp. 280–291. ISSN: 01420615. DOI: 10.1016/j.ijepes.2017.01.026.

[42] Sethi, Suresh and Sorger, Gerhard. “A Theory of Rolling Horizon Decision Making”. In: *Annals of Operations Research* 29 (1991), pp. 387–416.

[43] Devine, Mel T. and Bertsch, Valentin. “Examining the benefits of load shedding strategies using a rolling-horizon stochastic mixed complementarity equilibrium model”. In: *European Journal of Operational Research* 267.2 (June 2018), pp. 643–658. ISSN: 03772217. DOI: 10.1016/j.ejor.2017.11.041.

[44] Devine, Mel T., Gabriel, Steven A., and Moryadee, Seksun. “A rolling horizon approach for stochastic mixed complementarity problems with endogenous learning: Application to natural gas markets”. In: *Computers and Operations Research* 68 (Apr. 2016), pp. 1–15. ISSN: 03050548. DOI: 10.1016/j.cor.2015.10.013.

[45] Bischi, Aldo et al. “A rolling-horizon optimization algorithm for the long term operational scheduling of cogeneration systems”. In: *Energy* 184 (Oct. 2019), pp. 73–90. ISSN: 03605442. DOI: 10.1016/j.energy.2017.12.022.

[46] Beraldi, Patrizia et al. “Short-term electricity procurement: A rolling horizon stochastic programming approach”. In: *Applied Mathematical Modelling* 35.8 (Aug. 2011), pp. 3980–3990. ISSN: 0307-904X. DOI: 10.1016/J.APM.2011.02.002.

[47] Berhanu, Belete, Seleshi, Yilma, and Melesse, Assefa M. “Surface water and groundwater resources of Ethiopia: Potentials and challenges of water resources development”. In: *Nile River Basin: Ecohydrological Challenges, Climate Change and Hydropolitics*. Vol. 9783319027. Springer International Publishing, Nov. 2014, pp. 97–117. DOI: 10.1007/978-3-319-02720-3{_}6.

[48] Seleshi Bekele Awulachew et al. *Water Resources and Irrigation Development in Ethiopia.Colombo, Sri Lanka.International Water Management Institute.Working Paper 123*. 2007, p. 78. ISBN: 9789290906803.

[49] Conway, Declan. “The climate and hydrology of the Upper Blue Nile river”. In: *Geographical Journal* 166.1 (2000), pp. 49–62. ISSN: 00167398. DOI: 10.1111/j.1475-4959.2000.tb00006.x.

[50] Söder, Lennart and Amelin, Mikael. *Efficient Operation and Planning of Power Systems*. Tech. rep.

[51] Joshi, Anshul and Lakhanpal, Rahul T A - T T -. *Learning Julia : build high-performance applications for scientific computing*. eng. Birmingham, UK, 2017. DOI: LK-https://worldcat.org/title/1018480533. URL: https://search.ebscohost.com/login.aspx?direct=true&scope=site&db=nlebk&db=nlabk&AN=1641409.

[52] John R. BIRGE. “The Value of The Stochastic Solution In Stochastic Linear Programs with Fixed Recourse”. In: *Mathematical Programming* 24 (1982), pp. 314–325.

[53] Conejo, Antonio J, Carrión, Miguel, and Morales, Juan M. “Risk management”. In: *Decision Making Under Uncertainty in Electricity Markets*. NY, USA: Springer, 2010. Chap. 4, pp. 121–152. DOI: 10.1007/978-1-4419-7421-1.

[54] Song, Meng and Amelin, Mikael. “Price-Maker Bidding in Day-Ahead Electricity Market for a Retailer with Flexible Demands”. In: *IEEE Transactions on Power Systems* 33.2 (Mar. 2018), pp. 1948–1958. ISSN: 08858950. DOI: 10.1109/TPWRS.2017.2741000.

[55] Resources, NASA Prediction of Worldwide Energy. *POWER Data Access Viewer*. 2018. URL: https://power.larc.nasa.gov/data-access-viewer/.

[56] *Analyze Time Series Data Using Econometric Modeler - MATLAB & Simulink - MathWorks Nordic*. URL: https://se.mathworks.com/help/econ/econometric-modeler-overview.html.

[57] Box, George E. P., Jenkins, Gwilym M., and Reinsel, Gregory C. *Time Series Analysis*. Wiley Series in Probability and Statistics. Wiley, June 2008, pp. 1–746. ISBN: 9780470272848. DOI: 10.1002/9781118619193. URL: https://onlinelibrary.wiley.com/doi/book/10.1002/9781118619193.

[58] By Rob J Hyndman and George Athanasopoulos. *3.3 Residual diagnostics | Forecasting: Principles and Practice (2nd ed)*. May 2018. URL: https://otexts.com/fpp2/residuals.html.

[59] Wangensteen, Ivar. *Power system economics: the Nordic electricity market*. Trondheim SE -: Tapir Academic Press, 2006. DOI: LK-https://worldcat.org/title/915439030.

Appendices

Appendix

A Publicaion -I

Deterministic Hydropower Simulation Model for Ethiopia

Firehiwot Girma Dires
Sch.of Electrical and Computer Engineering
Addis Ababa institute of technology
Addis Ababa, Ethiopia
Email: dires@kth.se

Mikael Amelin
Dept. of Electrical Engineering
KTH Royal Institute of Technology
Stockholm, Sweden
Email: amelin@kth.se

Getachew Bekele
Sch.of Electrical and Computer Engineering
Addis Ababa institute of technology
Addis Ababa, Ethiopia
Email: getachew.bekele@aait.edu.et

2021 IEEE Madrid PowerTech | 978-1-6654-3597-0/21/$31.00 ©2021 IEEE | DOI: 10.1109/PowerTech46648.2021.9494862

***Abstract*—This paper presents a long-term deterministic linear simulation model for the Ethiopian hydropower system, intending to utilize the water stored in the rainy season throughout the year with minimum load shedding. Two cases are simulated and compared to historical data. The base case represents current load levels, and the second case represents a load level increase. The results show that the Ethiopian hydropower system has a great deal of flexibility to be operated in a more efficient way to minimize load shedding. The results also show that the system can support a 50% load increase with minimum load shedding, mostly when the load demand exceeds the total generating capacity. The contribution of this paper is to apply a standard hydropower model for Ethiopia to estimate the potential of the Ethiopian hydropower system to avoid or minimize load shedding with improved generation and operation planning.**

***Index Terms*—Hydroelectric power generation, power system planning, power system reliability, optimization**

I. Introduction

Ethiopia is a country located in the horn of Africa between latitudes of 3.8°N to 14.5°N and longitudes of 33°E to 48°E. The total area of Ethiopia is around 1.12 Mkm^2 with a varied topology ranging from the lowest point of 120.00 m below sea level and the highest point about 4620.00 m above sea level [1]. The country is endowed with a substantial amount of water body which is divided into twelve basins, eight of which are river basins, one lake basin, and the remaining three are dry basins as shown in Fig. 1, [2]. Seasonal rainfall in Ethiopia is driven mainly by the migration of the Intertropical Convergence Zone (ITCZ), tropical upper easterlies, and local convergence in the Red Sea coastal region [3]. There are four different seasons in Ethiopia; small rain *Belg* (April to June), heavy rain *Kiremt* (July to September), small rain *Tseday* (October to December), and dry season *Bega* (January to March).

Hydropower constitutes 90% of the country's electricity generation, with an overall national potential of as much as 45 GW [4]. To harness this considerable national potential, the government is working on further expansion of hydropower capacity with mega projects like the Grand Ethiopian Renaissance Dam (GERD) with an installed capacity of approximately 6 GW, which will be the largest hydroelectric power plant in Africa, and $Koysha$ hydropower plant with an installed capacity of 2.16 GW. Moreover, Ethiopia is following the green resilience policy and has a plan of becoming a middle-income county by 2025, as stipulated in its Growth and Transformation Plan (GTP-II) [5]. The government of Ethiopia launched the first National Electrification Program (NEP-1) in November 2017 that represents the action plan for achieving universal electricity access nationwide by 2025, 65% of access provision targeted with grid solutions and 35% with off-grid technologies (solar off-grid and mini-grids). The NEP-1 document has been updated to NEP-2 by 2019 to reflect the government's commitment to revise the electrification program based on implementation progress and improved analytics [6]. To ensure timely provision of reliable and sufficient electricity access and to address the ambitious plans, the power sector should undergo thorough modernization.

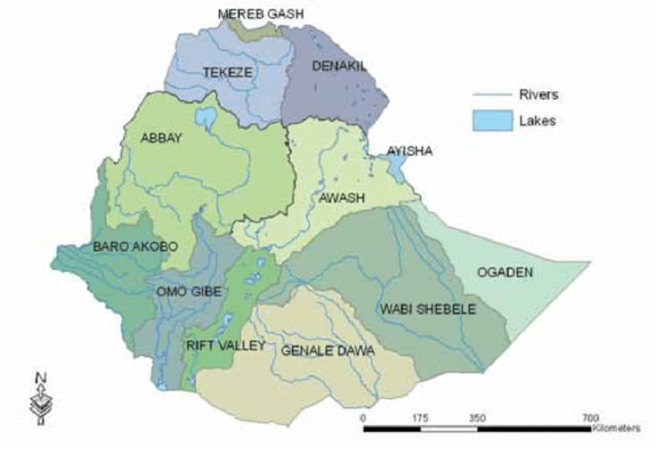

Fig. 1. Ethiopia River Basin Map

There are 13 existing larger hydropower plants, 3 wind power plants, and 1 waste-to-energy plant, which are fully engaged in the power generation as shown in Table I. All these power plants are owned, administrated, and operated by the Government.

978-1-6654-3597-0/21/$31.00 ©2021 IEEE

B Publicaion - II

water

MDPI

Article

Inflow Scenario Generation for the Ethiopian Hydropower System

Firehiwot Girma Dires [1,*,†], Mikael Amelin [2] and Getachew Bekele [1]

[1] School of Electrical and Computer Engineering, Addis Ababa Institute of Technology, Addis Ababa 385, Ethiopia
[2] School of Electrical Engineering and Computer Science, KTH Royal Institute of Technology, 10044 Stockholm, Sweden
* Correspondence: dires@kth.se; Tel.: +251-911238282
† Current address: Division of Electric Power and Energy Systems, KTH Royal Institute of Technology, Teknikringen 33, SE-10044 Stockholm, Sweden.

Abstract: In a hydropower system, inflow is an uncertain stochastic process that depends on the meteorology of the reservoir's location. To properly utilize the stored water in reservoirs, it is necessary to have a good forecast or a historical inflow record. In the absence of these two pieces of information, which is the case in Ethiopia and most African countries, the derivation of the synthetic historical inflow series with the appropriate time resolution will be a solution. This paper presents a method of developing synthetic historical inflow time series and techniques to identify the stochastic process that mimics the behavior of the time series and generates inflow scenarios. The methodology was applied to the Ethiopian power system. The time series were analyzed using statistical methods, and the stochastic process that mimics the inflow patterns in Ethiopia was identified. The Monte Carlo simulation was used to generate sample realizations of random scenarios from the identified stochastic process. Then, three cases of inflow scenarios were tested in a deterministic simulation model of the Ethiopian hydropower system and compared with the actual operation. The results show that the generated inflow scenarios give a realistic output of generation scheduling and reasonable reservoir content based on the actual operation.

Keywords: inflow scenarios; synthetic historical inflow series; time series analysis; stochastic process; scenario generation; hydropower; planning model

Citation: Dires, F.G.; Amelin, M.; Bekele, G. Inflow Scenario Generation for the Ethiopian Hydropower System. *Water* **2023**, *15*, 500. https://doi.org/10.3390/w15030500

Academic Editor: Helena M. Ramos

Received: 25 November 2022
Revised: 20 January 2023
Accepted: 24 January 2023
Published: 27 January 2023

1. Introduction

The generation and operation of hydropower plants are highly dependent on weather conditions in the particular location of the reservoirs. To efficiently utilize hydropower, it is, therefore, necessary to have an inflow forecast. Prior knowledge about the reservoir inflow would help manage the water resource properly throughout the year. Otherwise, in case of a low inflow year, the water in the reservoirs might be used up before the next rainy season, and the reservoirs will be empty. Consequently, there will be a lot of load shedding until the reservoirs fill up again, which can also affect the start content of the reservoirs for the next planning period. On the other hand, in case of an unexpectedly high inflow year, we may end up spilling much water, and reservoirs could also be flooded.

In Ethiopia and many other countries in East Africa, hydropower is the dominant source of electric power. According to the international hydropower association (IHA) 2022 hydropower status report, Africa's energy generation by hydropower is 146 TWh in 2021, 21% of this generation being from Eastern African countries, of which 45% is from Ethiopia [1]. Most of the inflow is during the rainy season, July to September (*Kiremt*).

The water in the rainy season is stored in large reservoirs to be distributed over the remaining part of the year until the next rainy season comes again. Therefore, hydropower

C Publicaion - III

energies

MDPI

Article

Long-Term Hydropower Planning for Ethiopia: A Rolling Horizon Stochastic Programming Approach with Uncertain Inflow

Firehiwot Girma Dires [1,*], Mikael Amelin [2] and Getachew Bekele [1]

[1] School of Electrical and Computer Engineering, Addis Ababa Institute of Technology, Addis Ababa 385, Ethiopia; getachew.bekele@aait.edu.et
[2] School of Electrical Engineering and Computer Science, KTH Royal Institute of Technology, SE-10044 Stockholm, Sweden; amelin@kth.se
* Correspondence: dires@kth.se; Tel.: +251-91-123-8282

Abstract: All long-term hydropower planning problems require a forecast of the inflow during the planning period. However, it is challenging to accurately forecast inflows for a year or more. Therefore, it is common to use stochastic models considering the uncertainties of the inflow. This paper compares deterministic and stochastic models in a weekly rolling horizon framework considering inflow uncertainty. The stochastic model is tested in both a risk-neutral and a risk-averse version. The rolling horizon framework helps make periodic decisions and update the information in each rolling week, which minimizes the errors in prolonged forecasts. The models aim to utilize the water stored in the rainy season throughout the year with minimum load shedding while storing as much water as possible at the end of the planning horizon. The Conditional Value at Risk ($CVaR$) risk measure is used to develop the risk-averse stochastic model. Three different risk measures are investigated to choose the risk measure that yields the best outcome in the risk-averse problem, and the two best measures are compared to a deterministic and risk-neutral model in a weekly rolling horizon framework. The results show that the risk-neutral and best risk-averse models perform almost equally and are better than the deterministic model. Hence, using a stochastic model would be an improvement to the actual planning performed in the Ethiopian and other African countries' power systems.

Keywords: stochastic model; rolling horizon; risk-averse model; uncertain inflow; hydropower; planning model

Citation: Dires, F.G.; Amelin, M.; Bekele, G. Long-Term Hydropower Planning for Ethiopia: A Rolling Horizon Stochastic Programming Approach with Uncertain Inflow. *Energies* **2023**, *16*, 7399. https://doi.org/10.3390/en16217399

Academic Editor: Massimiliano Renzi

Received: 15 September 2023
Revised: 25 October 2023
Accepted: 30 October 2023
Published: 2 November 2023

1. Introduction

Many hydropower plants have large reservoirs, which allow water to be stored for an extended period of time. This water is used when the demand is high or other generation sources are scarce in the system. In many cases, there are a few short periods with substantial inflow each year. The task of long-term hydropower planning is to decide during which periods this water should be used. In a country like Ethiopia, where hydropower plants dominate power generation, the challenge is to decide how to use the inflow from the rainy season while considering the uncertainty of future inflow. Hydropower planning will, therefore, have to find an appropriate trade-off between using the available water now (risking future energy shortages) or starting load shedding to a smaller extent now. Therefore, all long-term planning problems require a forecast of the inflow during the planning period. However, it is challenging to accurately forecast the inflow to hydropower reservoirs with a reasonable time resolution (preferably not longer than one week) for one year or more. Therefore, it is common to use stochastic planning models, where the planning is based on several possible scenarios.

D Time series analysis in weekly time resolutions.

Econometric Modeler Analysis

Summary of results from the Econometric Modeler App

Econometrics Toolbox Version 5.1 (R2018b)

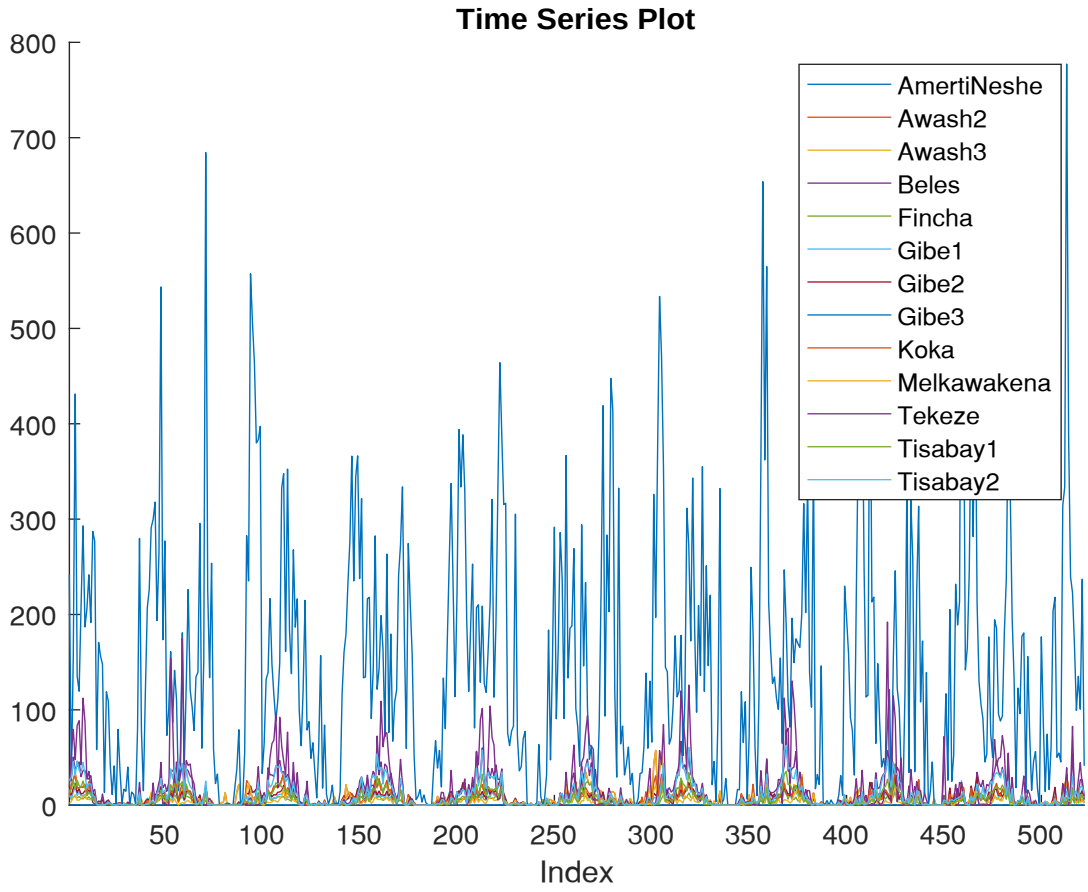

Figure 1.2. Time Series Plot of AmertiNeshe, Awash2, Awash3, Beles, Fincha, Gibe1, Gibe2, Gibe3, Koka, Melkawakena, Tekeze, Tisabay1, Tisabay2

1. Time Series: AmertiNeshe

1.1. Time Series Plot

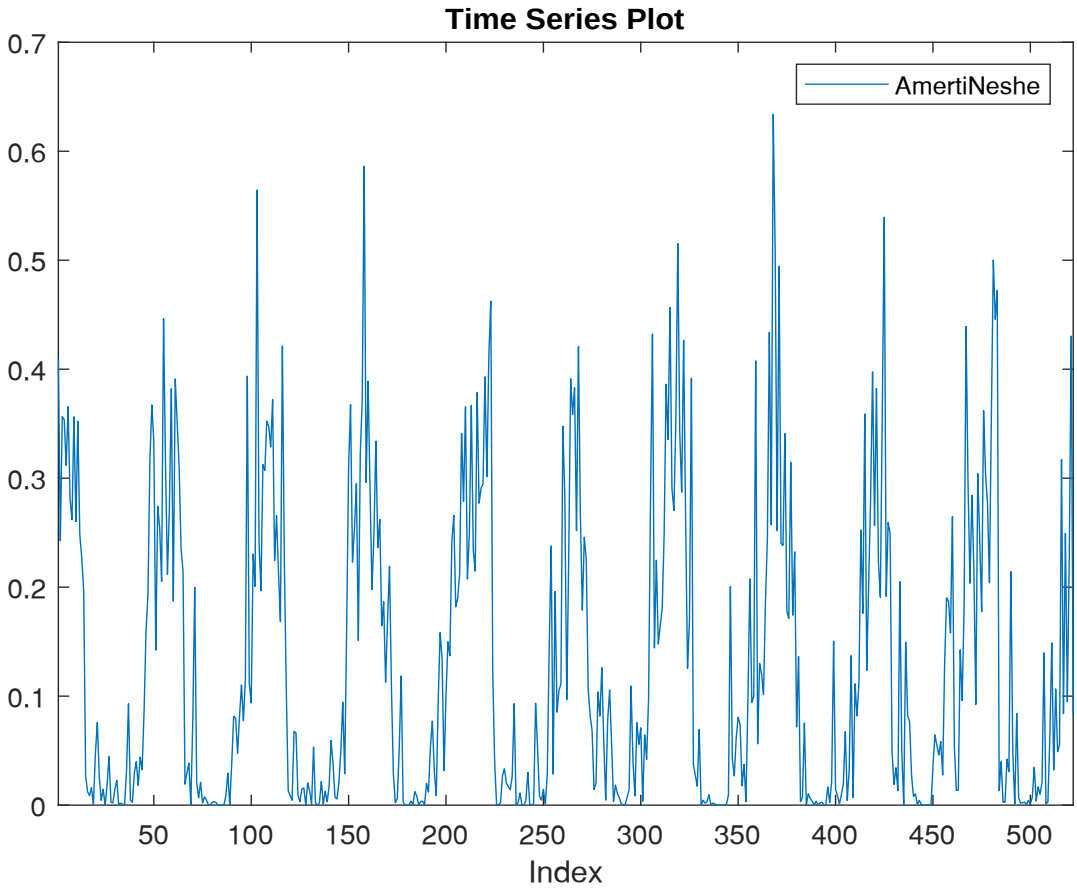

Figure 1.1. Time Series Plot of AmertiNeshe

4. Time Series: Beles

4.1. Time Series Plot

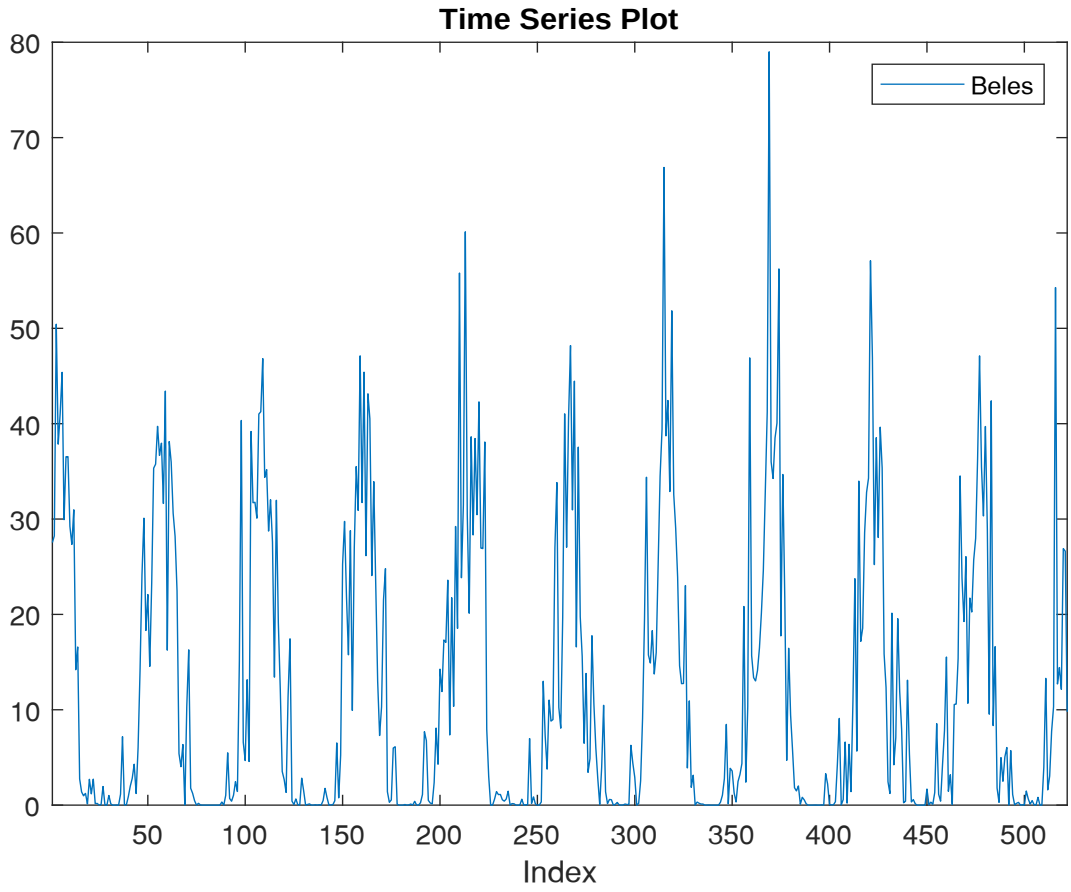

Figure 4.1. Time Series Plot of Beles

5. Time Series: Fincha

5.1. Time Series Plot

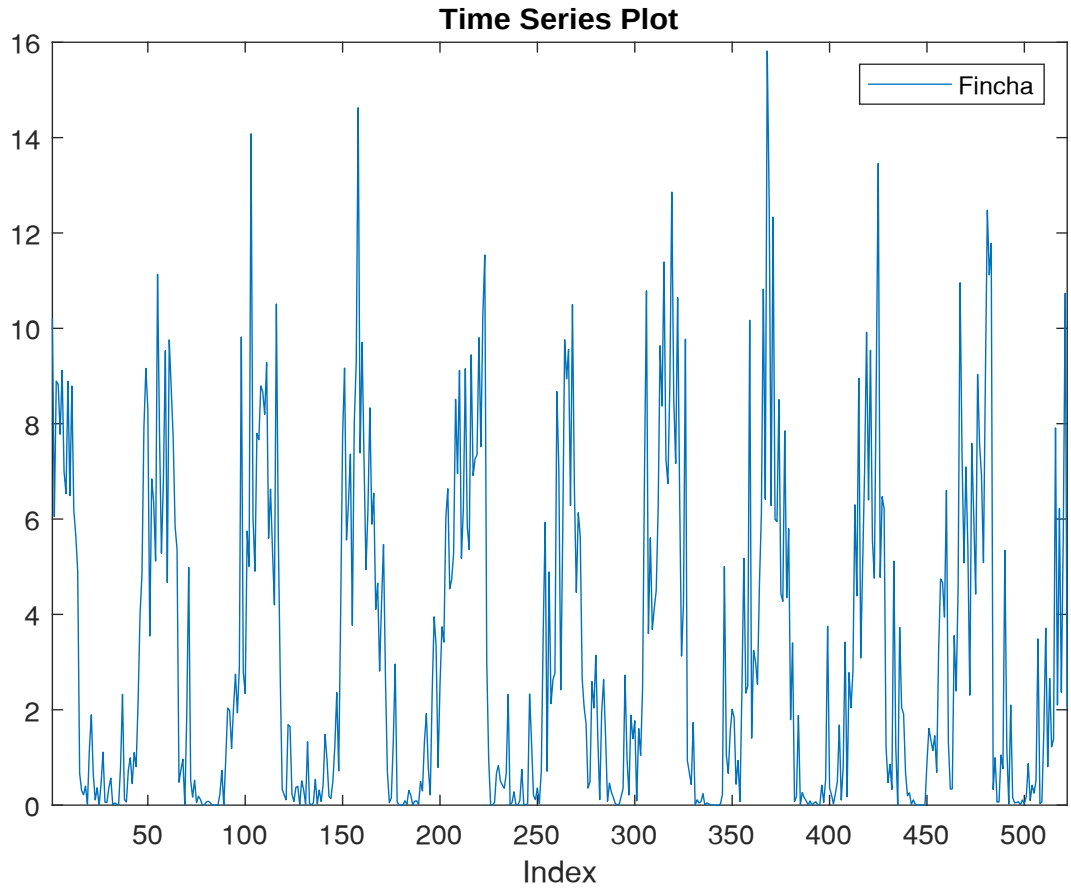

Figure 5.1. Time Series Plot of Fincha

6. Time Series: Gibe1

6.1. Time Series Plot

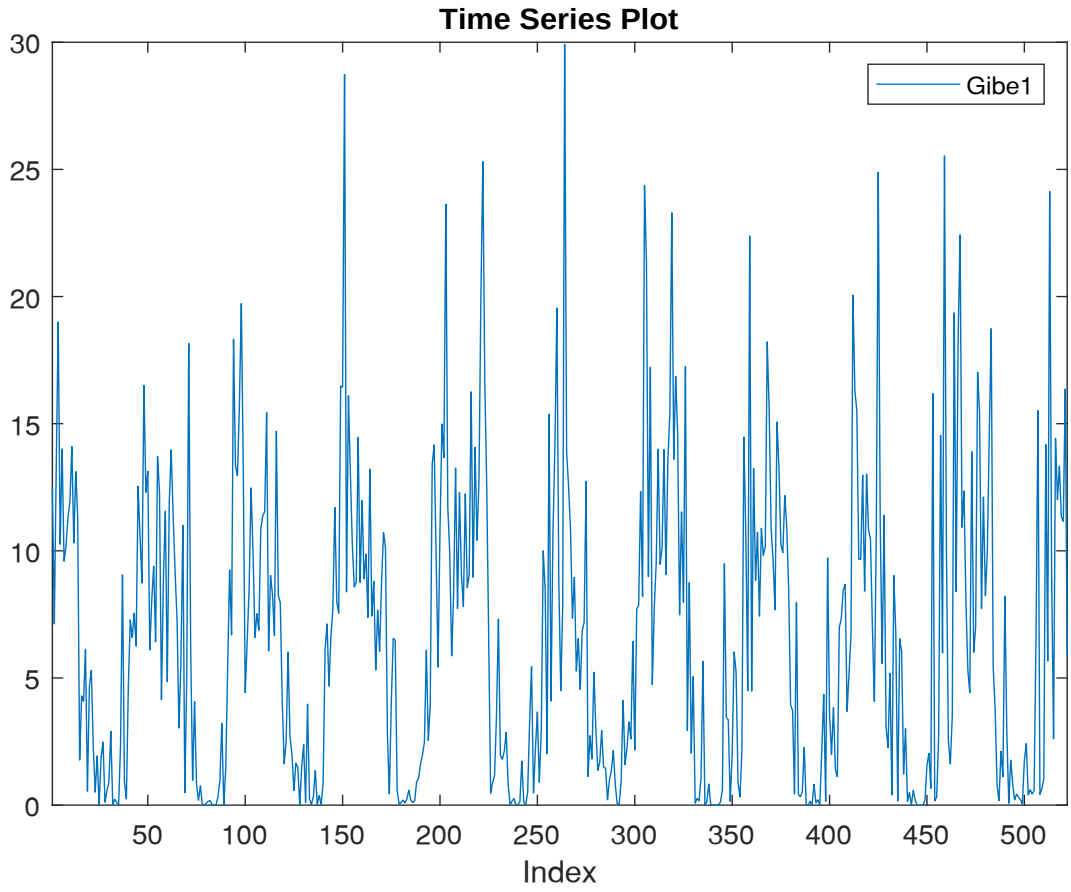

Figure 6.1. Time Series Plot of Gibe1

7. Time Series: Gibe2

7.1. Time Series Plot

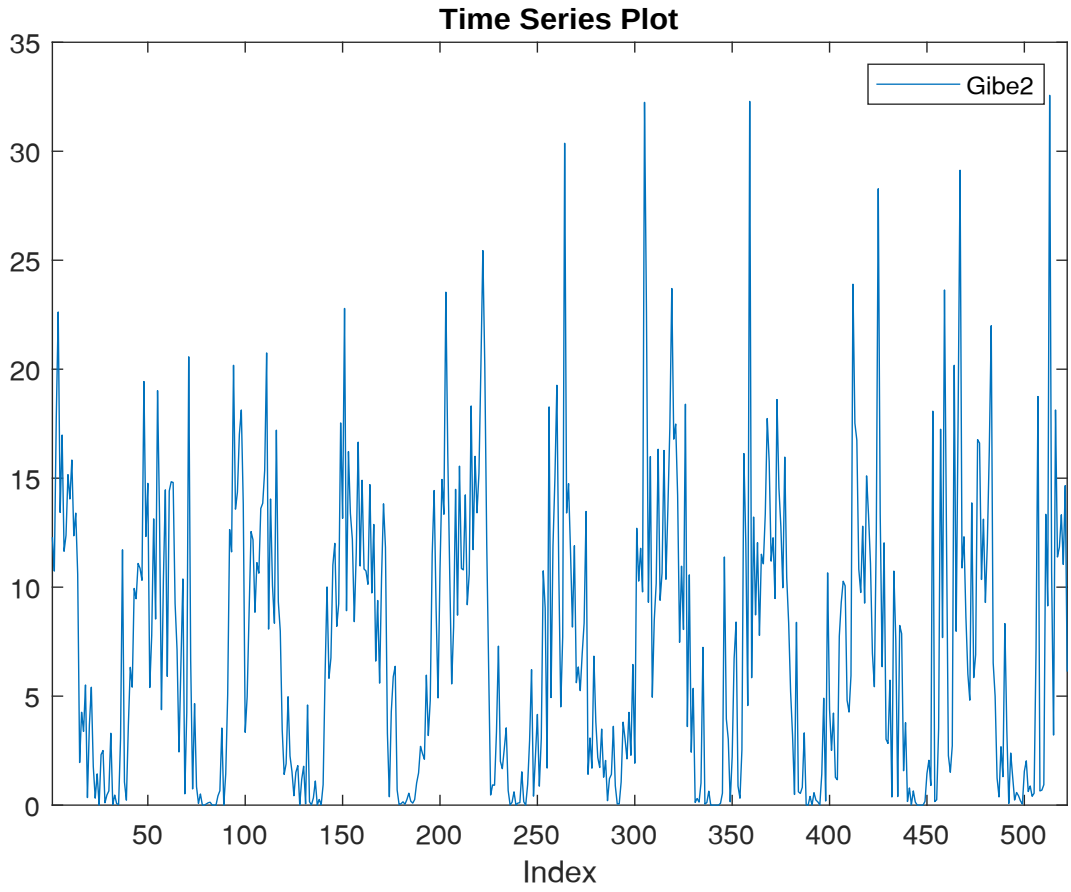

Figure 7.1. Time Series Plot of Gibe2

8. Time Series: Gibe3

8.1. Time Series Plot

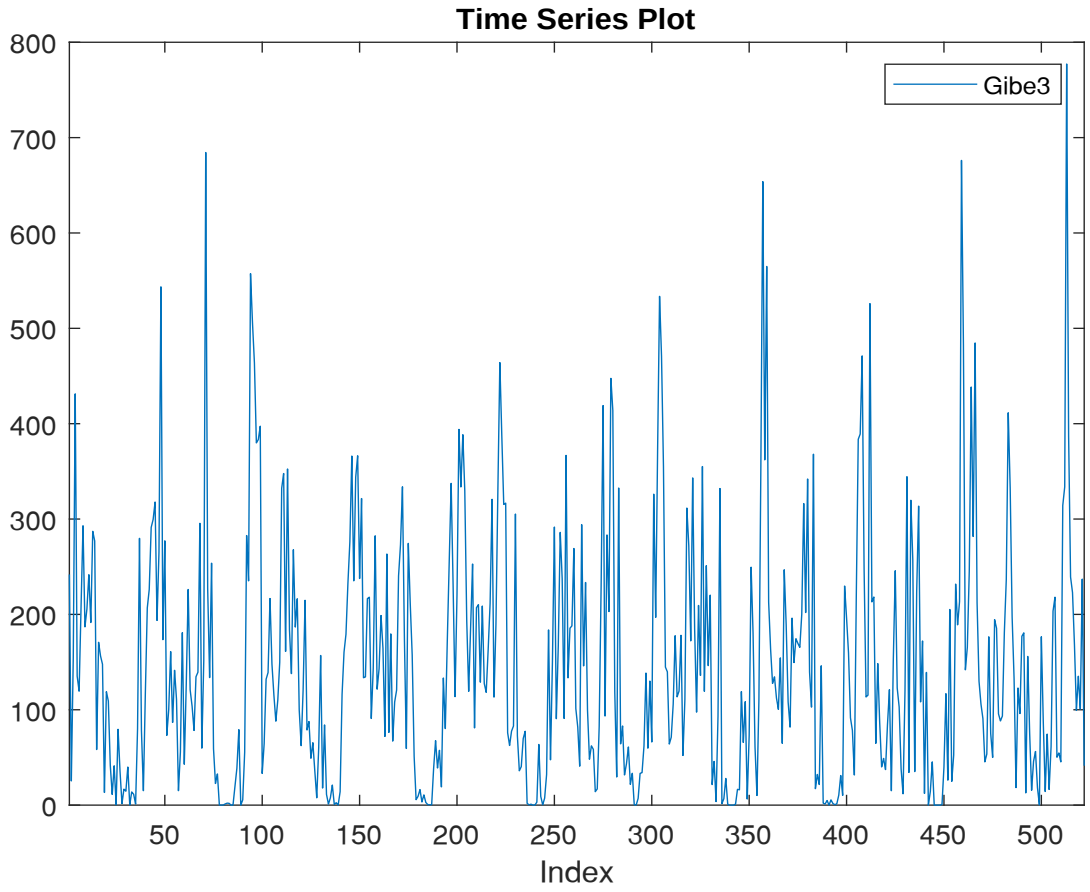

Figure 8.1. Time Series Plot of Gibe3

9. Time Series: Koka

9.1. Time Series Plot

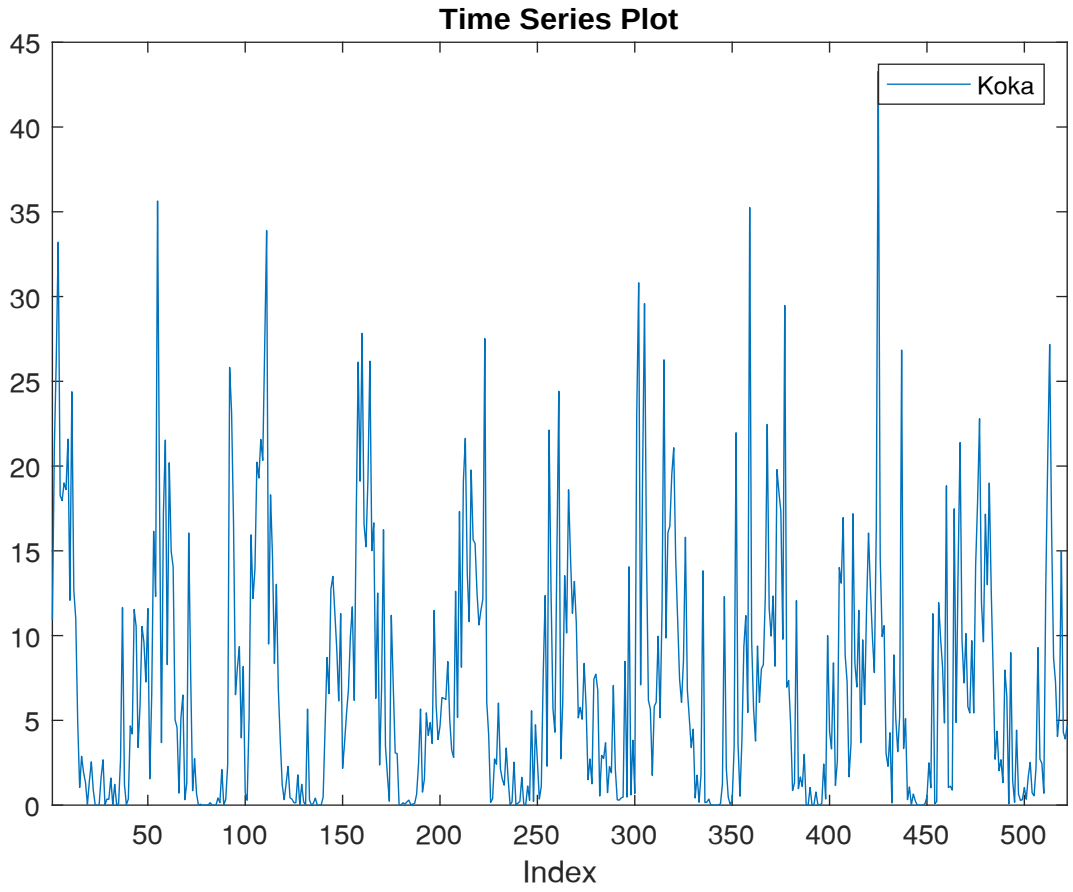

Figure 9.1. Time Series Plot of Koka

10. Time Series: Melkawakena

10.1. Time Series Plot

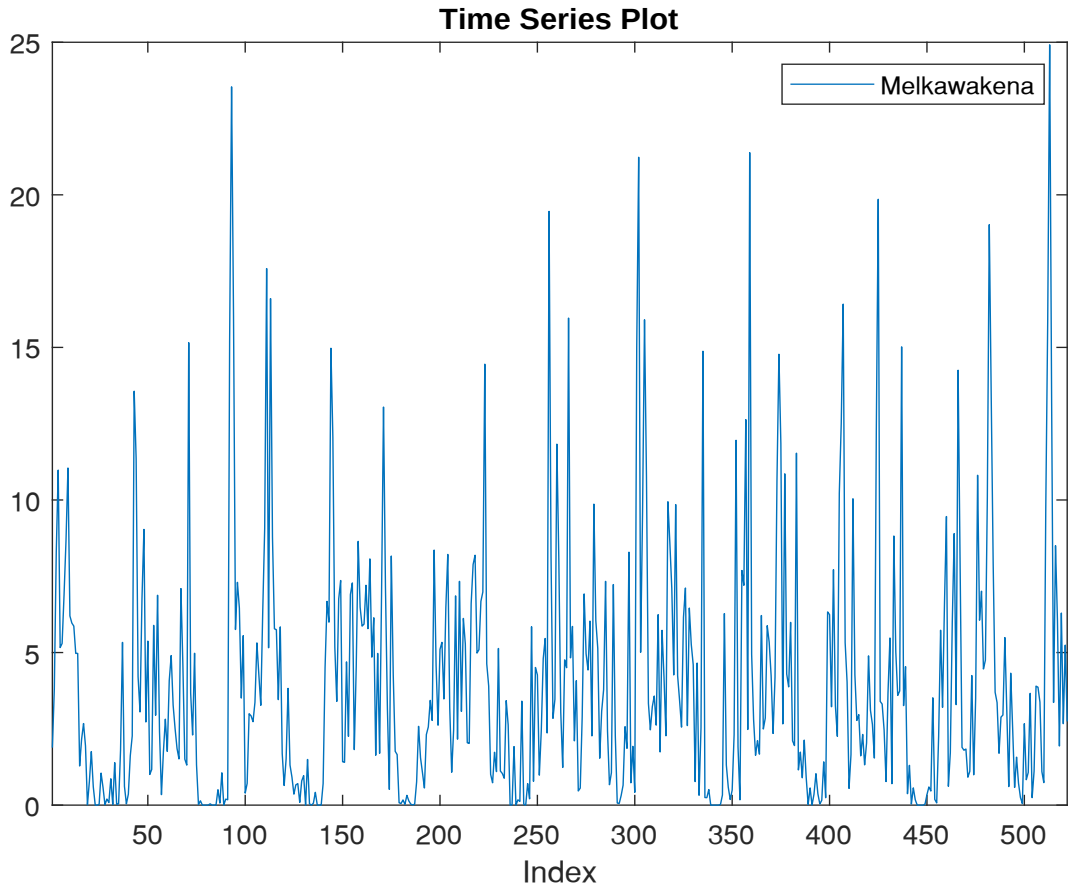

Figure 10.1. Time Series Plot of Melkawakena

11. Time Series: Tekeze

11.1. Time Series Plot

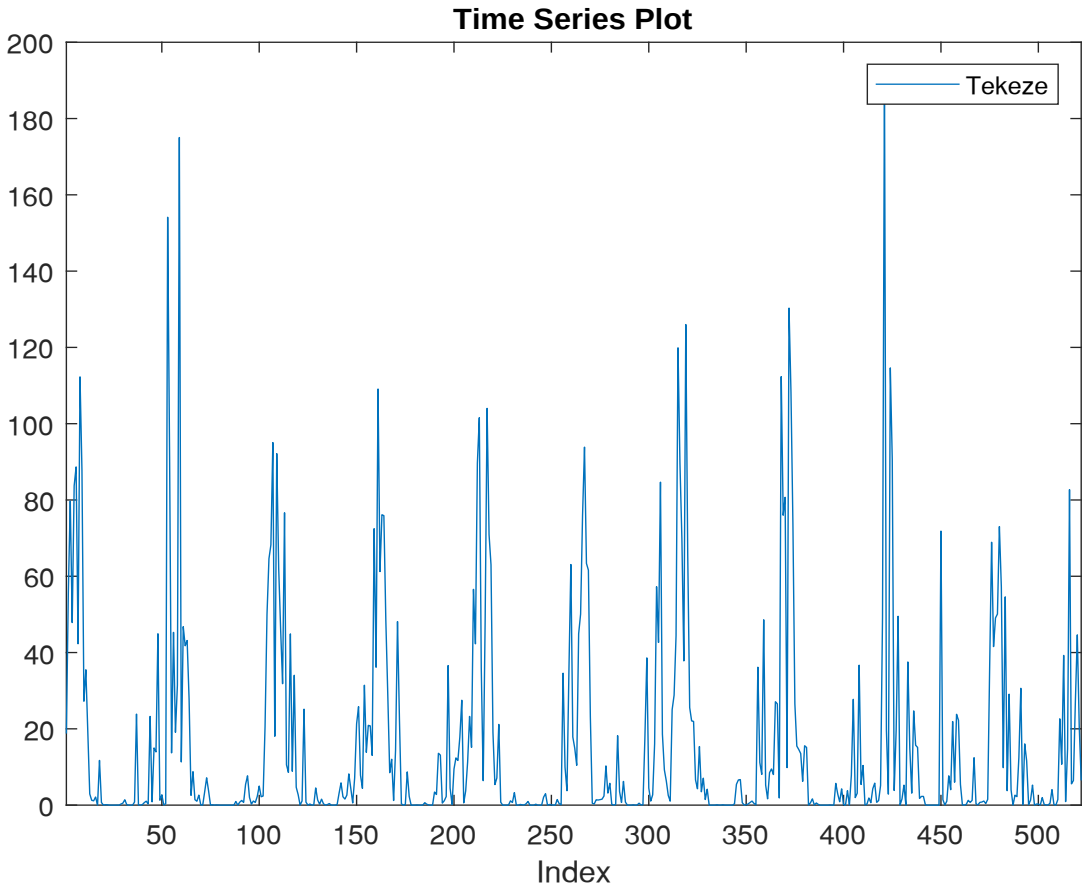

Figure 11.1. Time Series Plot of Tekeze

12. Time Series: Tisabay1

12.1. Time Series Plot

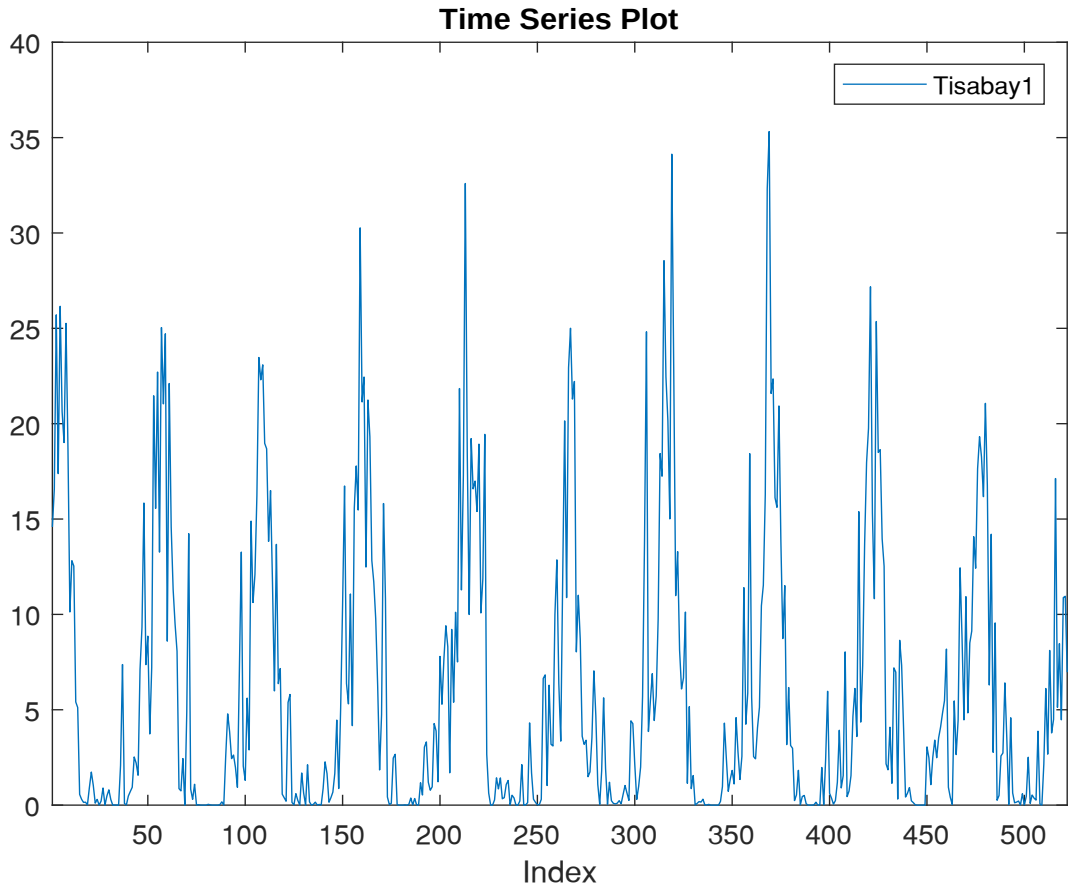

Figure 12.1. Time Series Plot of Tisabay1

13. Time Series: Tisabay2

13.1. Time Series Plot

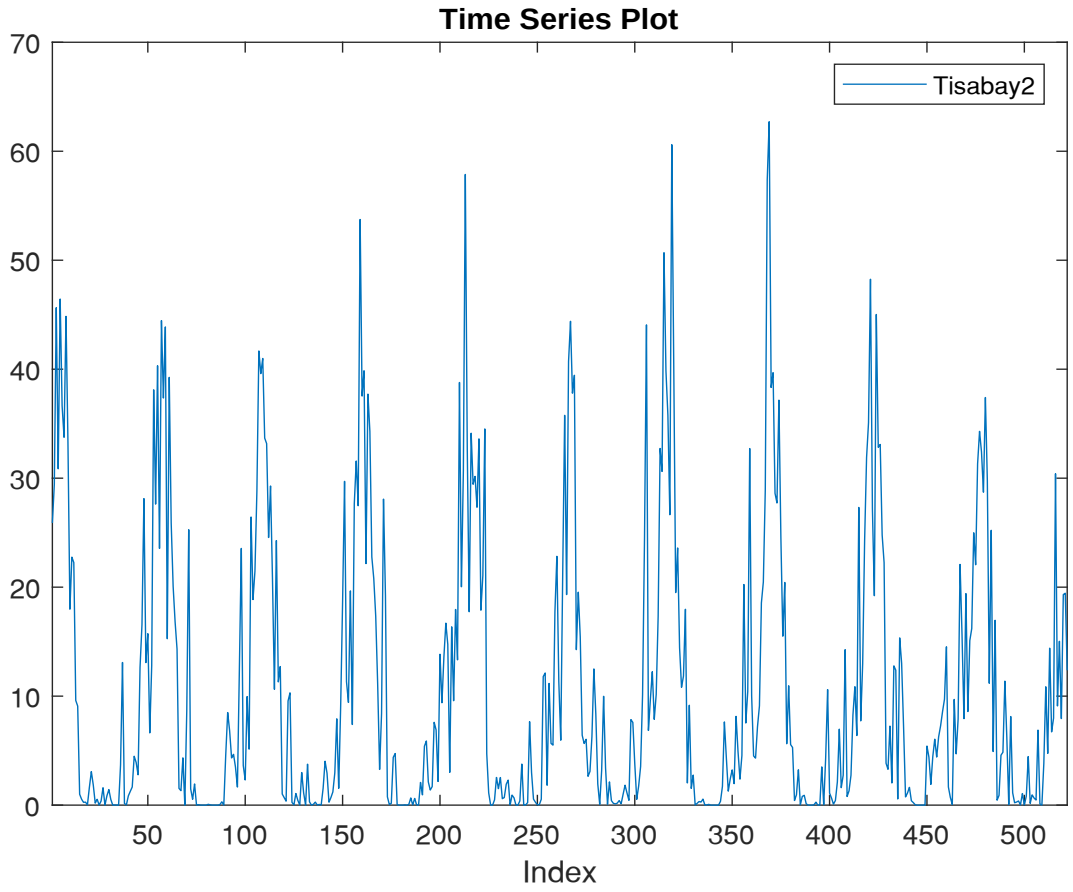

Figure 13.1. Time Series Plot of Tisabay2

Econometric Modeler Analysis

Summary of results from the Econometric Modeler App

Econometrics Toolbox Version 5.1 (R2018b)

31-Aug-2022

1. ARIMA(3,0,0) Model Seasonally Integrated with Seasonal AR(156) (Gaussian Distribution) (SARIMA_AmertiNesheW)

Seasonal ARIMA model of time series AmertiNesheW with the following equation:

$$(1 - \phi_1 L - \phi_2 L^2 - \phi_3 L^3)(1 - \Phi_{52} L^{52} - \Phi_{104} L^{104} - \Phi_{156} L^{156})(1 - L^{52}) y_t \ = \ \varepsilon_t$$

1.1. Model Estimation

Table 1.1. Estimation Results

Parameter	Value	StandardError	TStatistic	PValue
Constant	0	0		
AR{1}	0.29315	0.032144	9.1198	7.5233e-20
AR{2}	-0.01498	0.032942	-0.45473	0.6493
AR{3}	0.046147	0.035175	1.3119	0.18955
SAR{52}	-0.83806	0.029629	-28.2851	5.2774e-176
SAR{104}	-0.7891	0.035988	-21.9267	1.4462e-106
SAR{156}	-0.71502	0.026571	-26.9104	1.6617e-159
Variance	0.0065587	0.00026926	24.3581	4.7635e-131

Table 1.2. Goodness of Fit

AIC	-1128.7051
BIC	-1102.5265

1. ARIMA(3,0,0) Model Seasonally Integrated with Seasonal AR(156) (Gaussian Distribution) (SARIMA_AmertiNesheW)

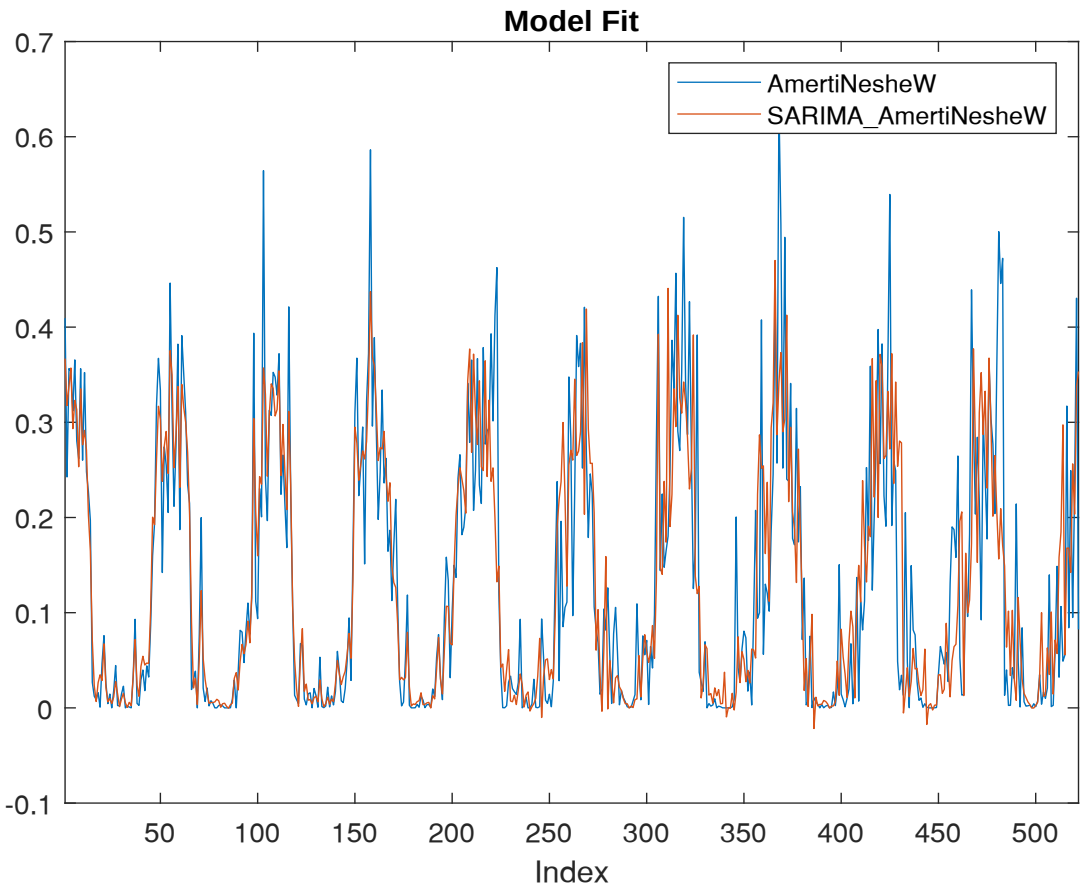

Figure 1.1. Plot the fit of model SARIMA_AmertiNesheW time series AmertiNesheW

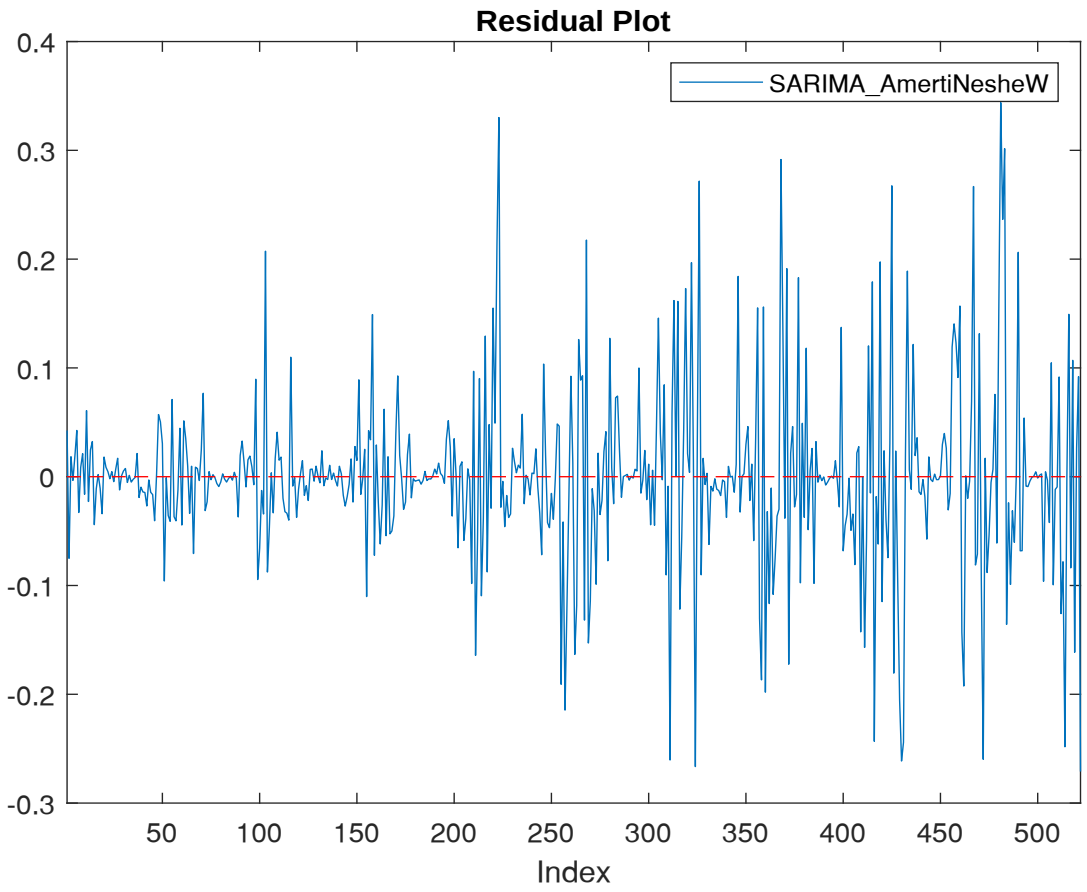

Figure 1.2. Plot of the residuals of model SARIMA_AmertiNesheW

1.2. Residual Sample Autocorrelation Function

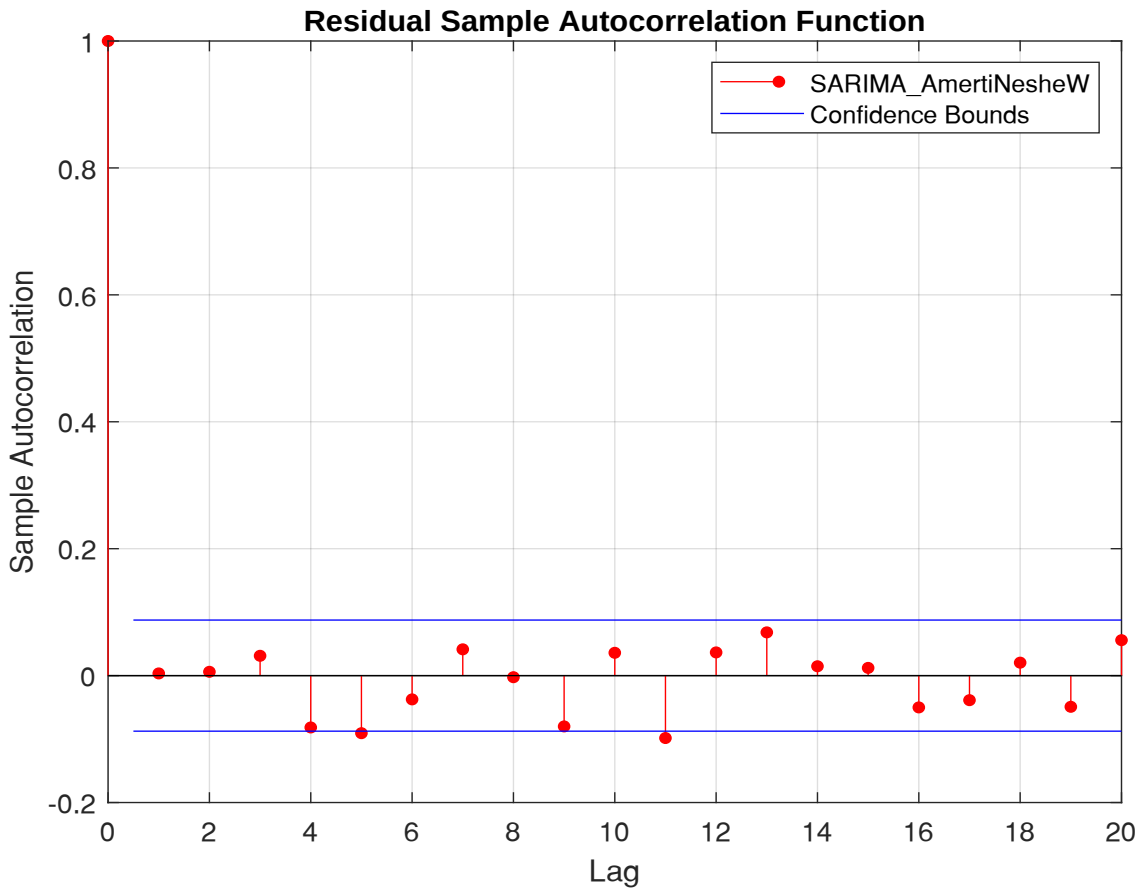

Figure 1.3. Sample autocorrelation function of the residuals of SARIMA_AmertiNesheW

1.3. Ljung-Box Q-Test

Null Hypothesis: The first m autocorrelations of the residuals of SARIMA_AmertiNesheW are jointly 0

$$H_0 : \rho_1 = \rho_2 = ... = \rho_m = 0$$

$$H_a : \rho_j \neq 0, \ j \in 1, ..., m$$

Table 1.3. Test Parameters

	Lags	DOF	Significance Level
1	20	20	0.05

Table 1.4. Test Results

	Null Rejected	P-Value	Test Statistic	Critical Value
1	false	0.10518	28.1811	31.4104

1. ARIMA(3,0,0) Model Seasonally Integrated with Seasonal AR(156) (Gaussian Distribution) (SARIMA_BELES_W)

Seasonal ARIMA model of time series BELES_W with the following equation:

$$(1 - \phi_1 L - \phi_2 L^2 - \phi_3 L^3)(1 - \Phi_{52} L^{52} - \Phi_{104} L^{104} - \Phi_{156} L^{156})(1 - L^{52}) y_t \ = \ \varepsilon_t$$

1.1. Model Estimation

Table 1.1. Estimation Results

Parameter	Value	StandardError	TStatistic	PValue
Constant	0	0		
AR{1}	0.10383	0.028406	3.6551	0.00025703
AR{2}	0.065045	0.031899	2.0391	0.041443
AR{3}	0.020992	0.031174	0.6734	0.5007
SAR{52}	-1	0.030975	-32.2841	1.1686e-228
SAR{104}	-0.95092	0.03172	-29.9788	1.852e-197
SAR{156}	-0.66471	0.028636	-23.2121	3.4392e-119
Variance	54.2411	1.845	29.3986	5.7157e-190

Table 1.2. Goodness of Fit

AIC	3579.947
BIC	3606.1256

1. ARIMA(3,0,0) Model Seasonally Integrated with Seasonal AR(156) (Gaussian Distribution) (SARIMA_BELES_W)

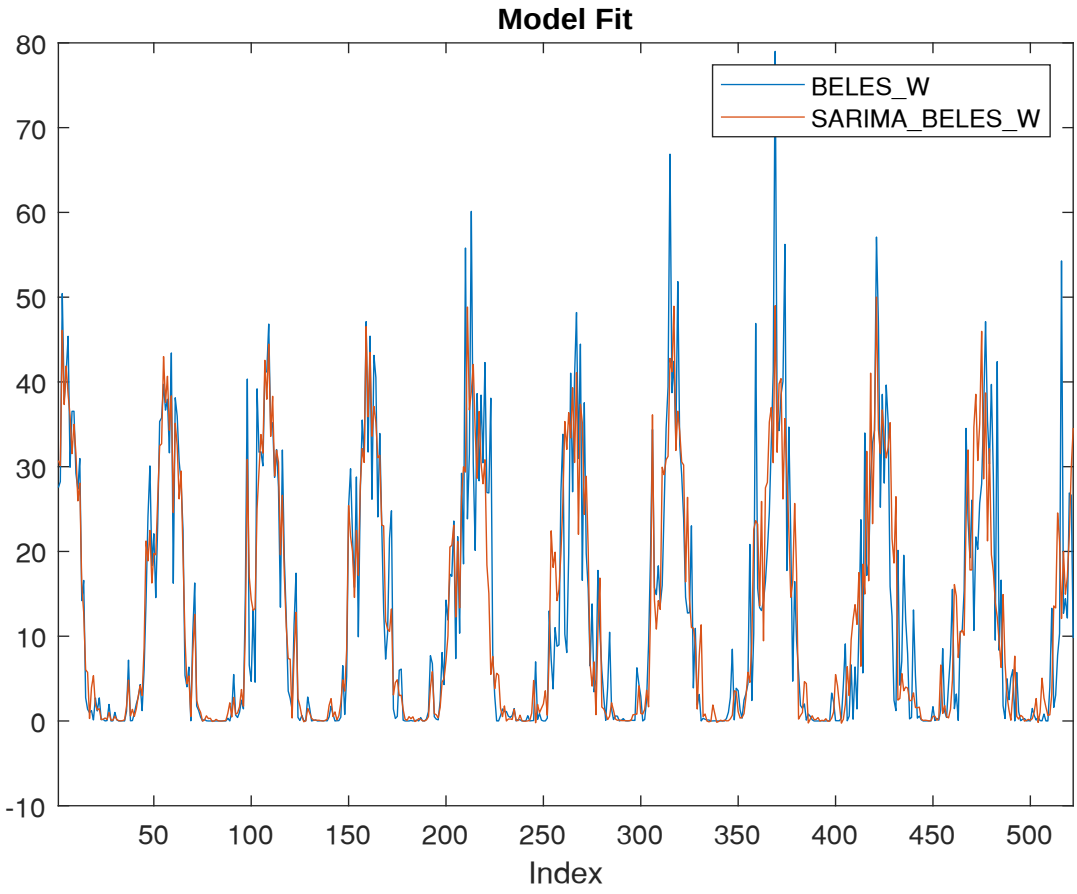

Figure 1.1. Plot the fit of model SARIMA_BELES_W time series BELES_W

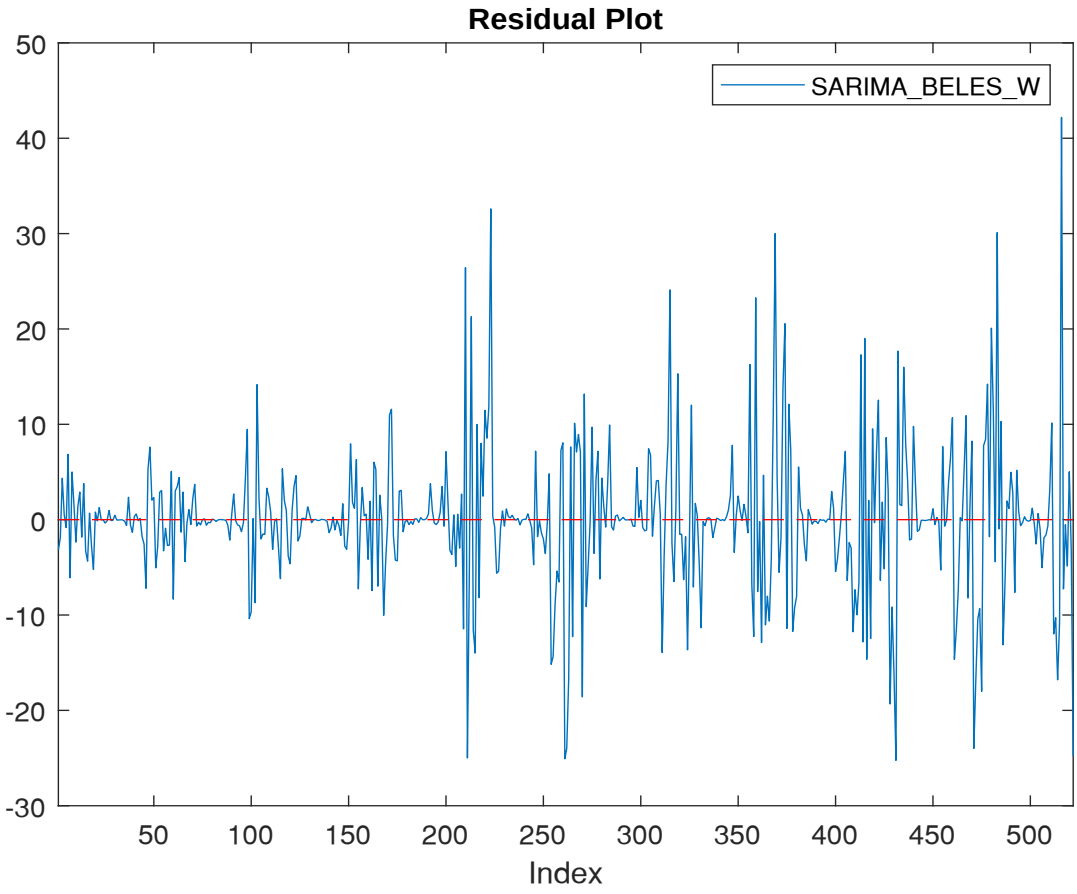

Figure 1.2. Plot of the residuals of model SARIMA_BELES_W

1.2. Residual Histogram

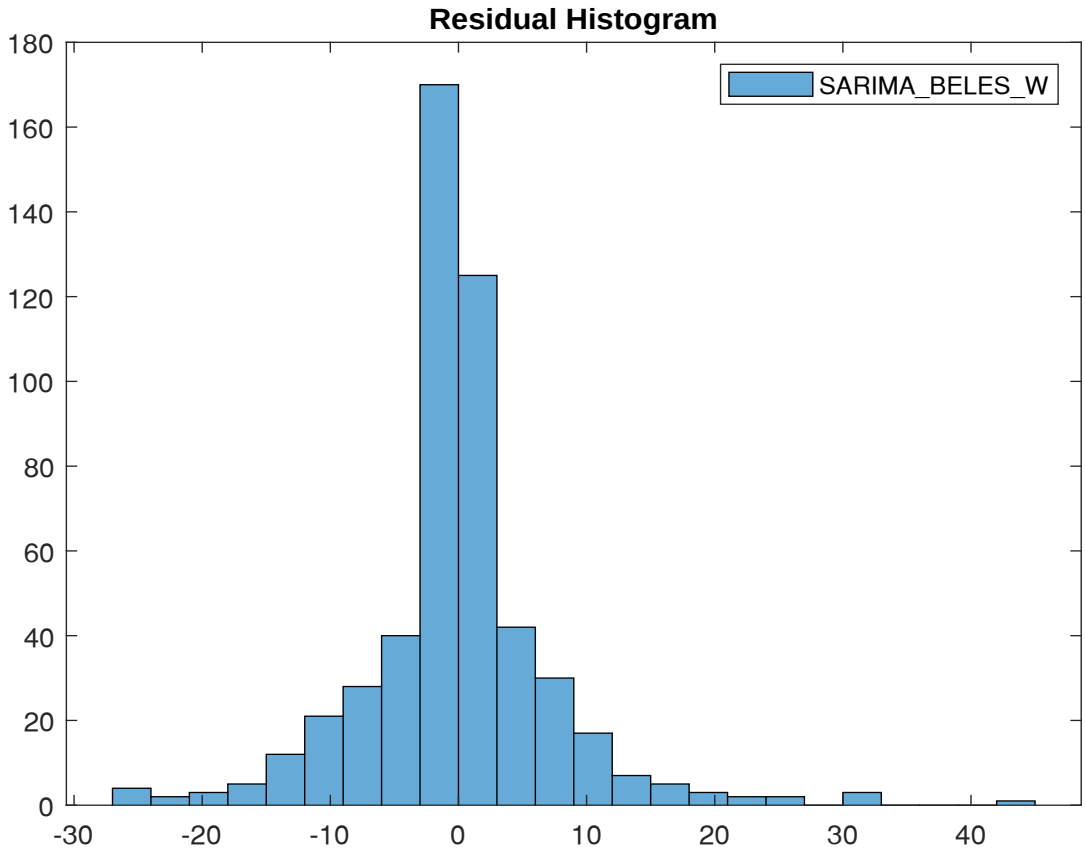

Figure 1.3. A histogram of the residuals of model SARIMA_BELES_W.

1.3. Residual Sample Autocorrelation Function

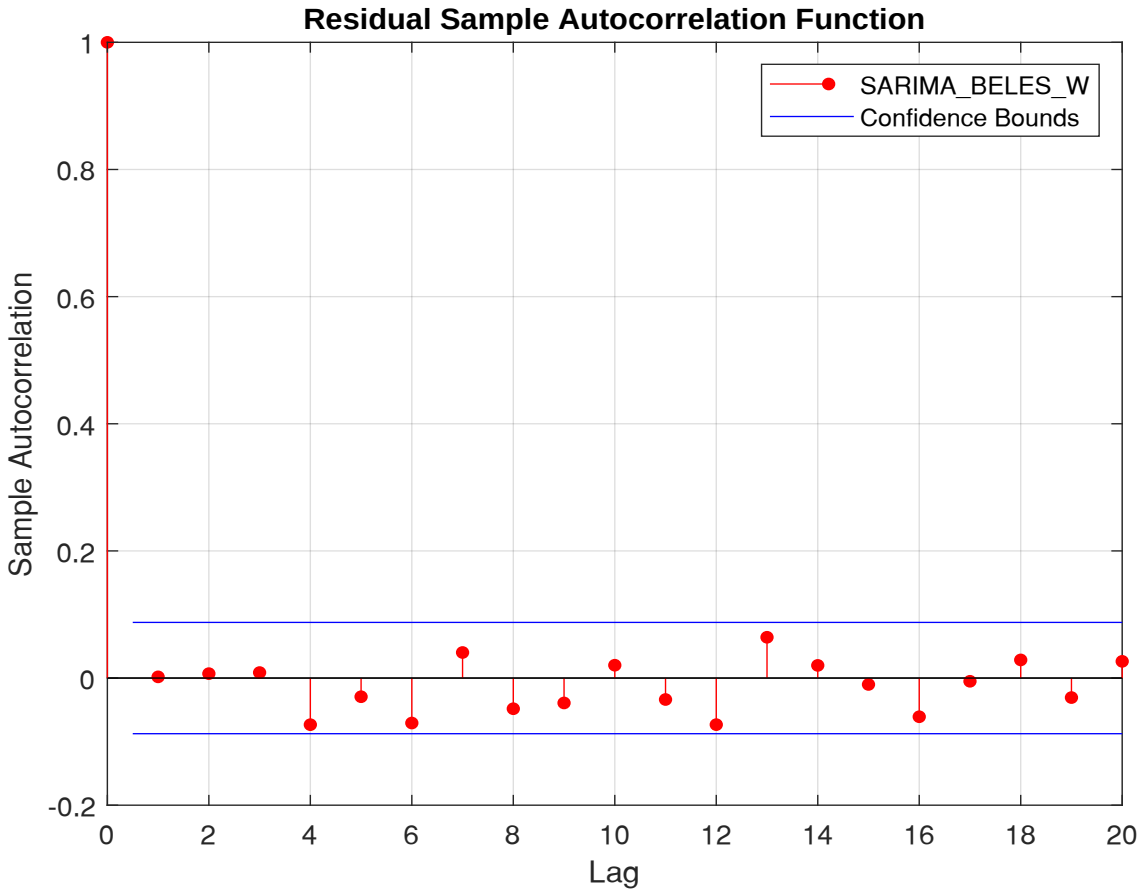

Figure 1.4. Sample autocorrelation function of the residuals of SARIMA_BELES_W

1.4. Ljung-Box Q-Test

Null Hypothesis: The first m autocorrelations of the residuals of SARIMA_BELES_W are jointly 0

$$H_0 : \rho_1 = \rho_2 = ... = \rho_m = 0$$

$$H_a : \rho_j \neq 0, \ j \in 1, ..., m$$

Table 1.3. Test Parameters

	Lags	DOF	Significance Level
1	20	20	0.05

Table 1.4. Test Results

	Null Rejected	P-Value	Test Statistic	Critical Value
1	false	0.5566	18.4681	31.4104

1. ARIMA(3,0,0) Model Seasonally Integrated with Seasonal AR(156) (Gaussian Distribution) (SARIMA_FinchaW)

Seasonal ARIMA model of time series FinchaW with the following equation:

$$(1 - \phi_1 L - \phi_2 L^2 - \phi_3 L^3)(1 - \Phi_{52} L^{52} - \Phi_{104} L^{104} - \Phi_{156} L^{156})(1 - L^{52}) y_t \ = \ \varepsilon_t$$

1.1. Model Estimation

Table 1.1. Estimation Results

Parameter	Value	StandardError	TStatistic	PValue
Constant	0	0		
AR{1}	0.29315	0.032144	9.1198	7.5233e-20
AR{2}	-0.01498	0.032942	-0.45474	0.64929
AR{3}	0.046147	0.035175	1.3119	0.18955
SAR{52}	-0.83806	0.029629	-28.285	5.2819e-176
SAR{104}	-0.7891	0.035988	-21.9266	1.447e-106
SAR{156}	-0.71502	0.026571	-26.9103	1.6629e-159
Variance	4.0821	0.16759	24.358	4.7699e-131

Table 1.2. Goodness of Fit

AIC	2229.6252
BIC	2255.8037

1. ARIMA(3,0,0) Model Seasonally Integrated with Seasonal AR(156) (Gaussian Distribution) (SARIMA_FinchaW)

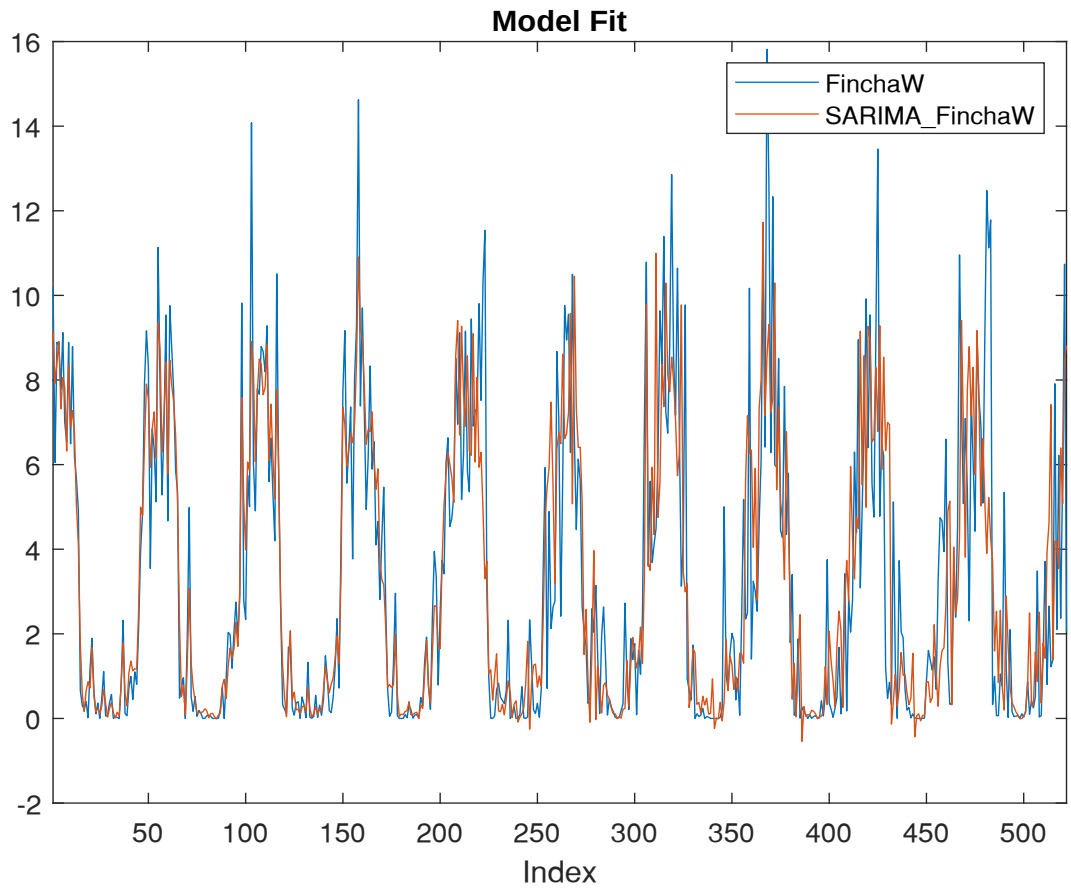

Figure 1.1. Plot the fit of model SARIMA_FinchaW time series FinchaW

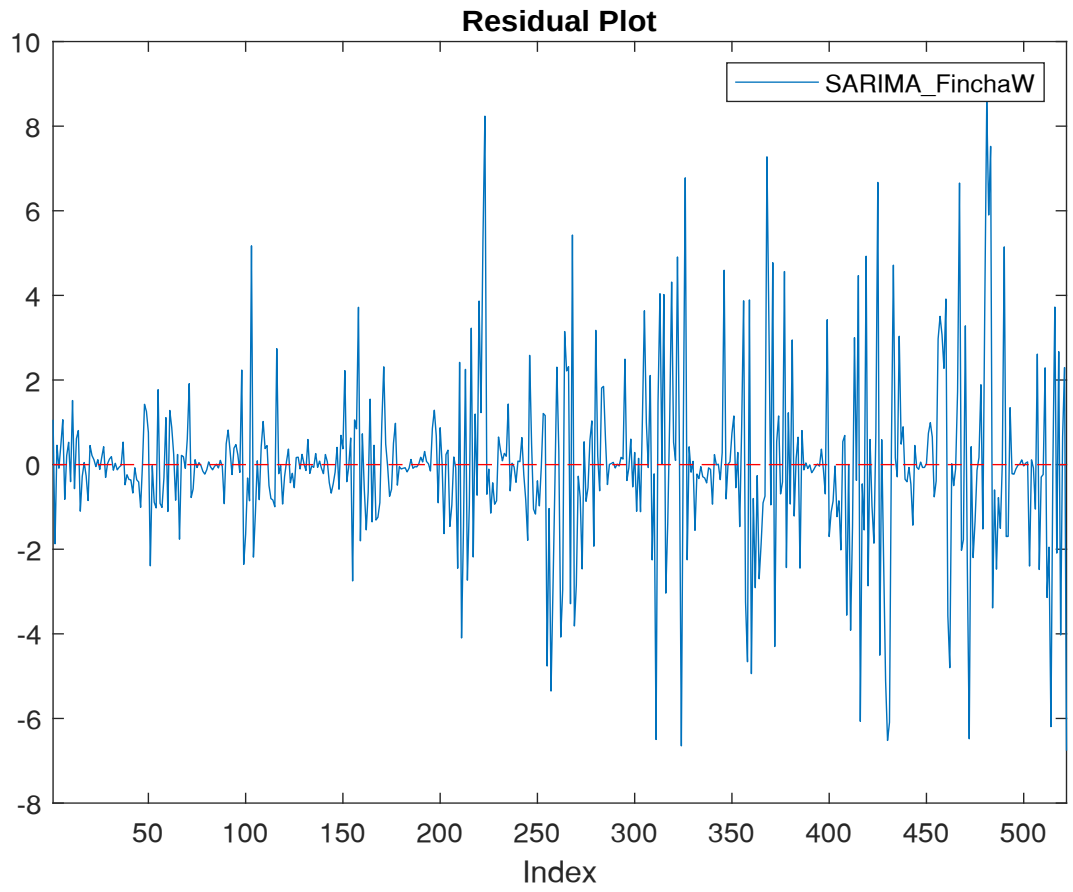

Figure 1.2. Plot of the residuals of model SARIMA_FinchaW

1.2. Residual Sample Autocorrelation Function

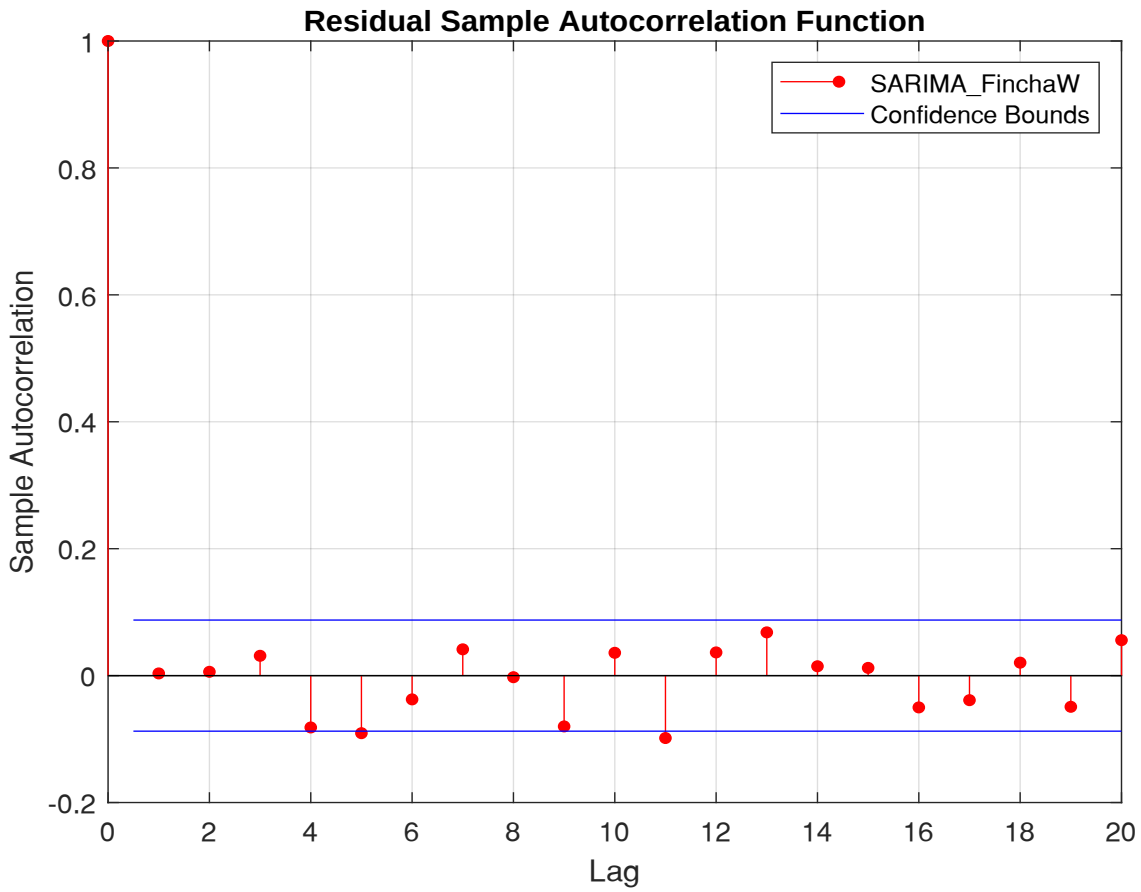

Figure 1.3. Sample autocorrelation function of the residuals of SARIMA_FinchaW

1.3. Ljung-Box Q-Test

Null Hypothesis: The first m autocorrelations of the residuals of SARIMA_FinchaW are jointly 0

$$H_0 : \rho_1 = \rho_2 = ... = \rho_m = 0$$

$$H_a : \rho_j \neq 0, \ j \in 1, ..., m$$

Table 1.3. Test Parameters

	Lags	DOF	Significance Level
1	20	20	0.05

Table 1.4. Test Results

	Null Rejected	P-Value	Test Statistic	Critical Value
1	false	0.10518	28.1811	31.4104

1. ARIMA(1,0,0) Model Seasonally Integrated with Seasonal AR(52) (Gaussian Distribution) (SARIMA_MelkawakenaW)

Seasonal ARIMA model of time series MelkawakenaW with the following equation:

$$(1 - \phi_1 L)(1 - \Phi_{52} L^{52})(1 - L^{52}) y_t = \varepsilon_t$$

1.1. Model Estimation

Table 1.1. Estimation Results

Parameter	Value	StandardError	TStatistic	PValue
Constant	0	0		
AR{1}	0.26728	0.030493	8.7654	1.8603e-18
SAR{52}	-0.65141	0.023637	-27.5585	3.5021e-167
Variance	16.1787	0.59435	27.2208	3.6857e-163

Table 1.2. Goodness of Fit

AIC	2940.4619
BIC	2952.5612

1. ARIMA(1,0,0) Model Seasonally Integrated with Seasonal AR(52) (Gaussian Distribution) (SARIMA_MelkawakenaW)

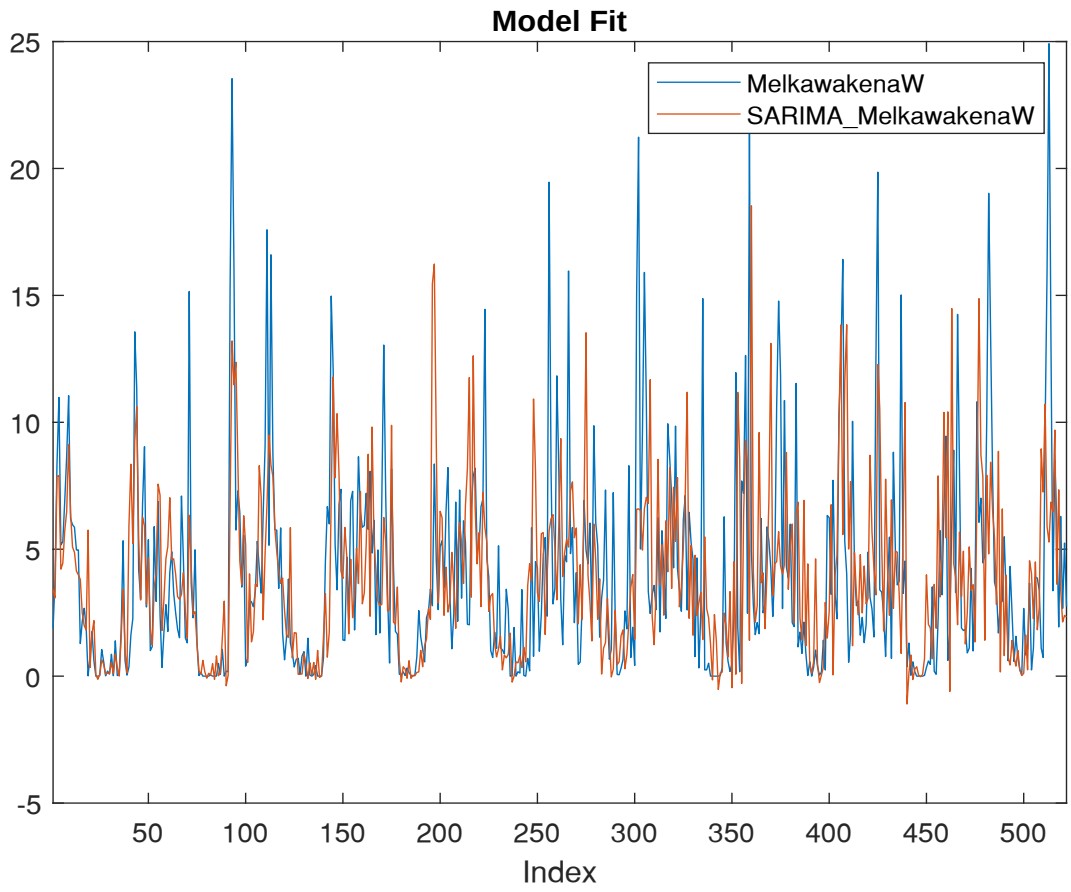

Figure 1.1. Plot the fit of model SARIMA_MelkawakenaW time series MelkawakenaW

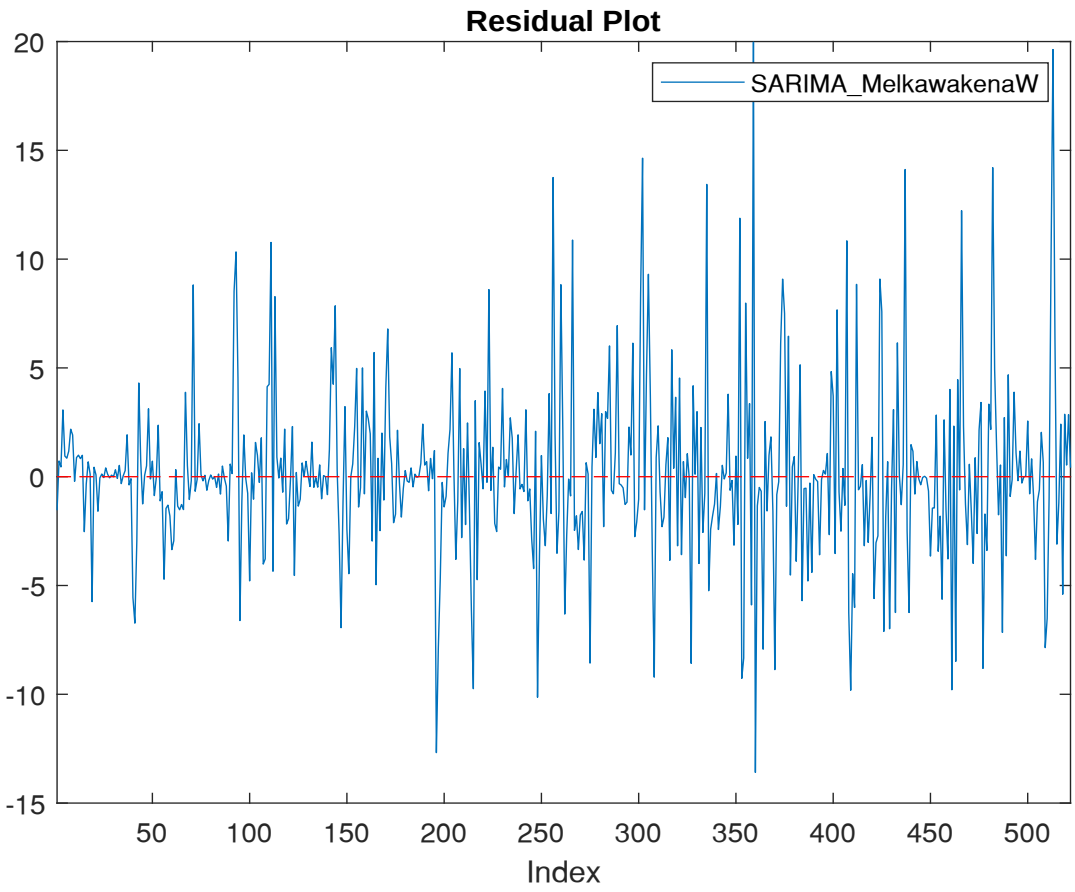

Figure 1.2. Plot of the residuals of model SARIMA_MelkawakenaW

1.2. Residual Sample Autocorrelation Function

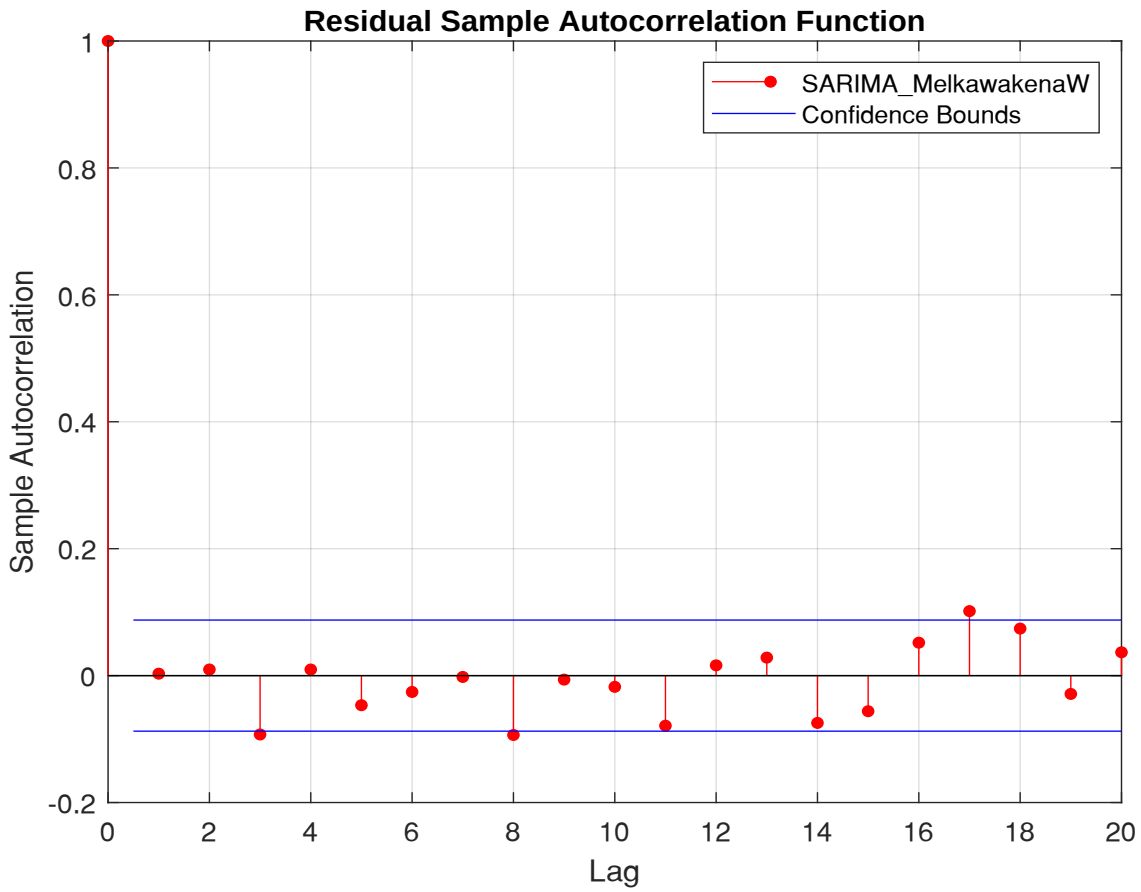

Figure 1.3. Sample autocorrelation function of the residuals of SARIMA_MelkawakenaW

1.3. Ljung-Box Q-Test

Null Hypothesis: The first m autocorrelations of the residuals of SARIMA_MelkawakenaW are jointly 0

$$H_0 : \rho_1 = \rho_2 = ... = \rho_m = 0$$

$$H_a : \rho_j \neq 0, \ j \in 1, ..., m$$

Table 1.3. Test Parameters

	Lags	DOF	Significance Level
1	20	20	0.05

Table 1.4. Test Results

	Null Rejected	P-Value	Test Statistic	Critical Value
1	false	0.057749	30.81	31.4104

1. ARIMA(3,0,0) Model Seasonally Integrated with Seasonal AR(156) (Gaussian Distribution) (SARIMA_Tisabay1W)

Seasonal ARIMA model of time series Tisabay1W with the following equation:

$$(1 - \phi_1 L - \phi_2 L^2 - \phi_3 L^3)(1 - \Phi_{52} L^{52} - \Phi_{104} L^{104} - \Phi_{156} L^{156})(1 - L^{52}) y_t \ = \ \varepsilon_t$$

1.1. Model Estimation

Table 1.1. Estimation Results

Parameter	Value	StandardError	TStatistic	PValue
Constant	0	0		
AR{1}	0.258	0.029646	8.7027	3.2403e-18
AR{2}	0.0064359	0.029796	0.216	0.82899
AR{3}	0.0038954	0.031012	0.12561	0.90004
SAR{52}	-0.89061	0.026043	-34.1976	2.6234e-256
SAR{104}	-0.86957	0.029698	-29.2801	1.8587e-188
SAR{156}	-0.69197	0.025333	-27.3148	2.8294e-164
Variance	13.4064	0.52478	25.5466	5.9822e-144

Table 1.2. Goodness of Fit

AIC	2850.3438
BIC	2876.5224

1. ARIMA(3,0,0) Model Seasonally Integrated with Seasonal AR(156) (Gaussian Distribution) (SARIMA_Tisabay1W)

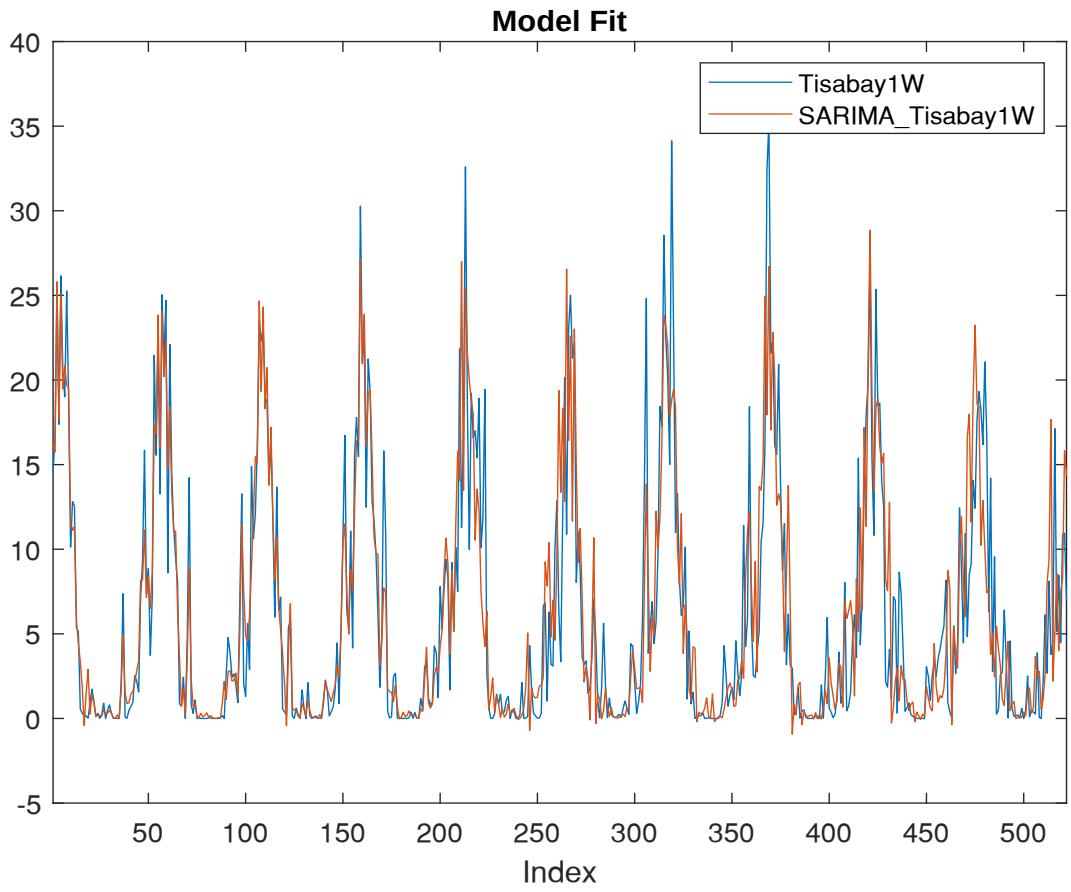

Figure 1.1. Plot the fit of model SARIMA_Tisabay1W time series Tisabay1W

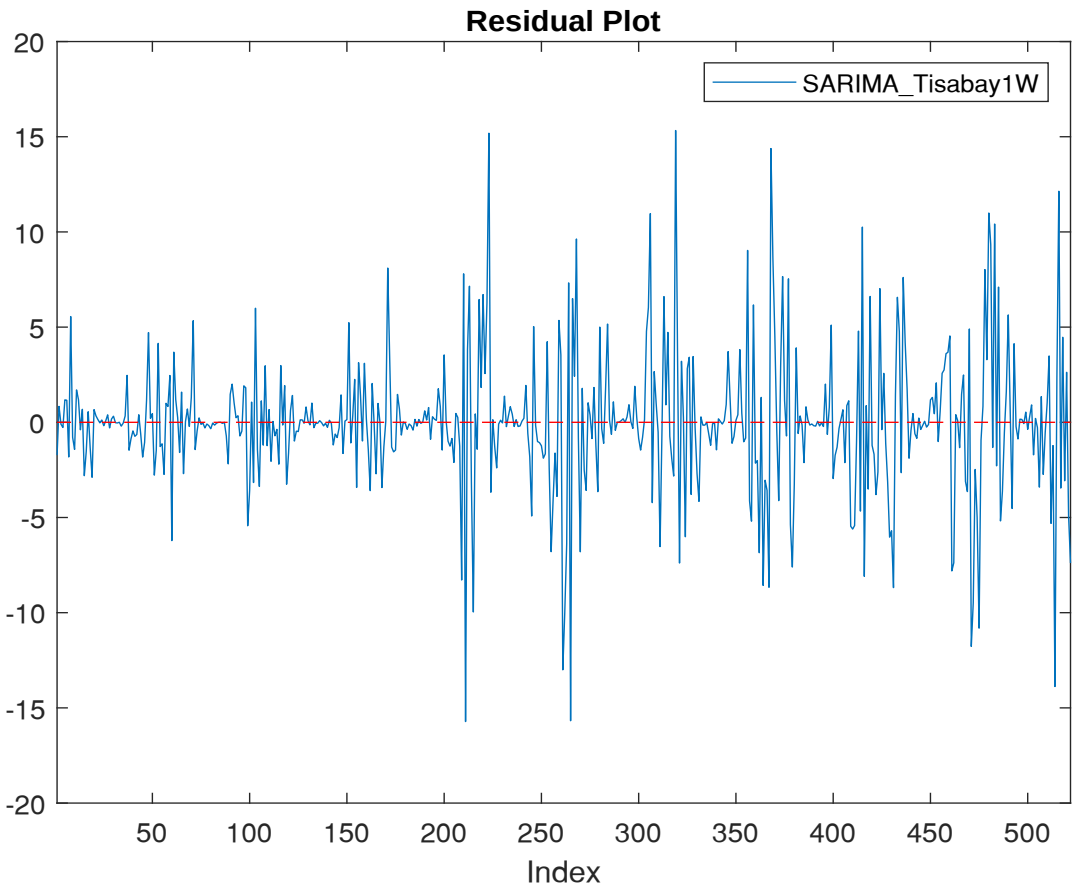

Figure 1.2. Plot of the residuals of model SARIMA_Tisabay1W

1.2. Residual Sample Autocorrelation Function

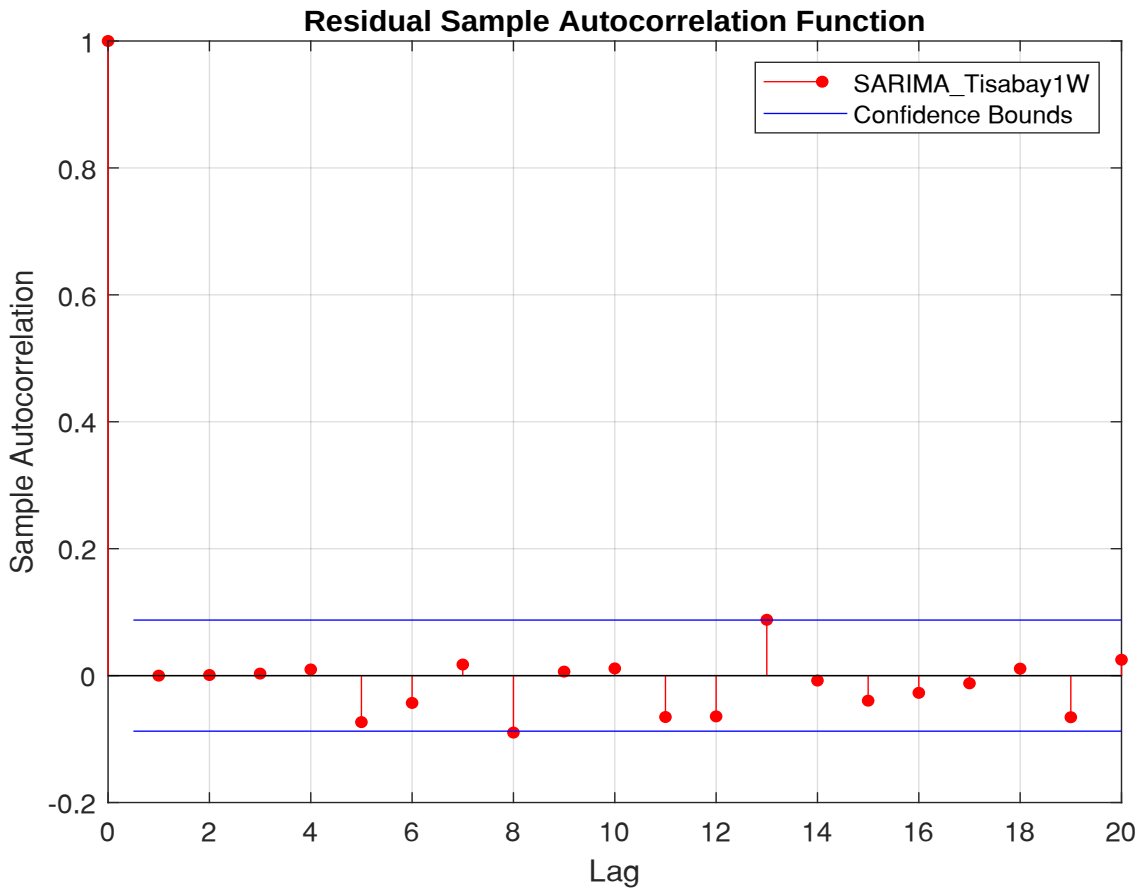

Figure 1.3. Sample autocorrelation function of the residuals of SARIMA_Tisabay1W

1.3. Ljung-Box Q-Test

Null Hypothesis: The first m autocorrelations of the residuals of SARIMA_Tisabay1W are jointly 0

$$H_0 : \rho_1 = \rho_2 = ... = \rho_m = 0$$

$$H_a : \rho_j \neq 0, \ j \in 1, ..., m$$

Table 1.3. Test Parameters

	Lags	DOF	Significance Level
1	20	20	0.05

Table 1.4. Test Results

	Null Rejected	P-Value	Test Statistic	Critical Value
1	false	0.38726	21.1688	31.4104

1. ARIMA(3,0,0) Model Seasonally Integrated with Seasonal AR(156) (Gaussian Distribution) (SARIMA_TekezeW)

Seasonal ARIMA model of time series TekezeW with the following equation:

$$(1 - \phi_1 L - \phi_2 L^2 - \phi_3 L^3)(1 - \Phi_{52} L^{52} - \Phi_{104} L^{104} - \Phi_{156} L^{156})(1 - L^{52}) y_t \ = \ \varepsilon_t$$

1.1. Model Estimation

Table 1.1. Estimation Results

Parameter	Value	StandardError	TStatistic	PValue
Constant	0	0		
AR{1}	0.16034	0.024292	6.6007	4.093e-11
AR{2}	-0.034357	0.026781	-1.2829	0.19953
AR{3}	0.056074	0.028728	1.9519	0.050951
SAR{52}	-0.94945	0.02429	-39.0882	0
SAR{104}	-0.88807	0.024902	-35.663	1.4805e-278
SAR{156}	-0.74842	0.01665	-44.9499	0
Variance	382.0442	12.275	31.1237	1.1503e-212

Table 1.2. Goodness of Fit

AIC	4598.942
BIC	4625.1206

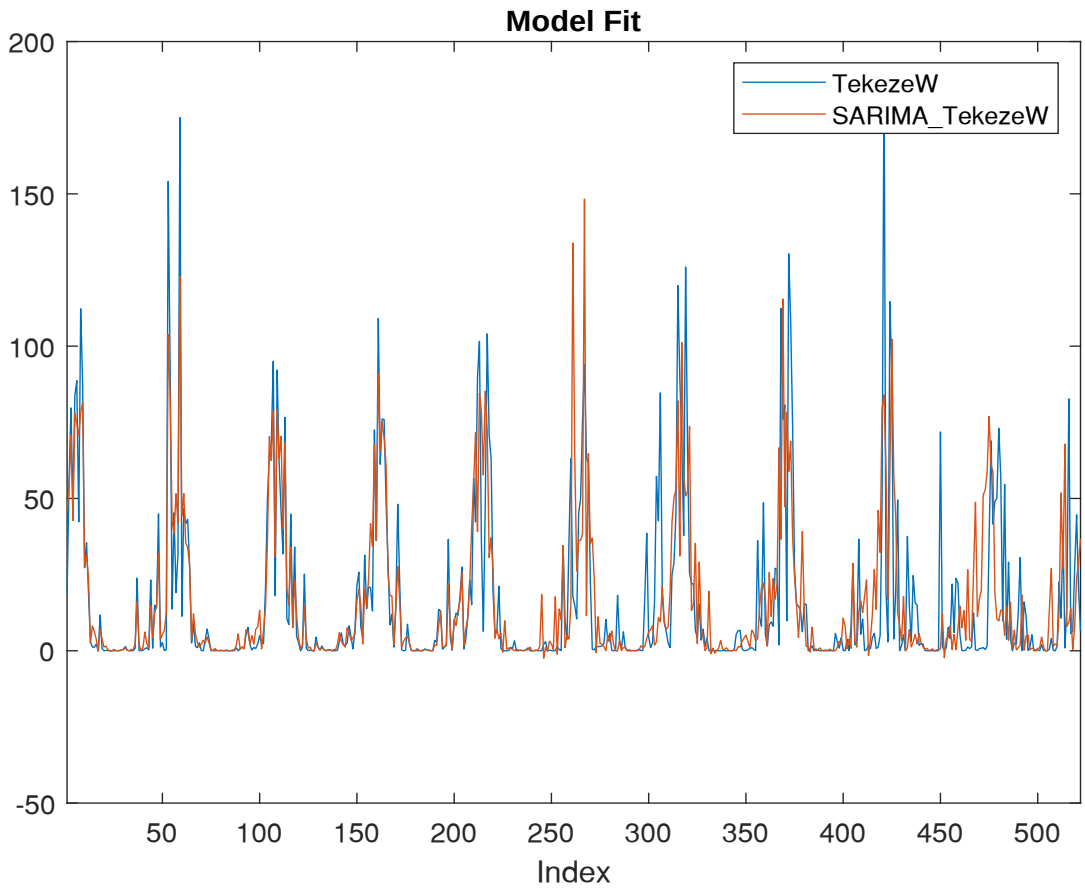

Figure 1.1. Plot the fit of model SARIMA_TekezeW time series TekezeW

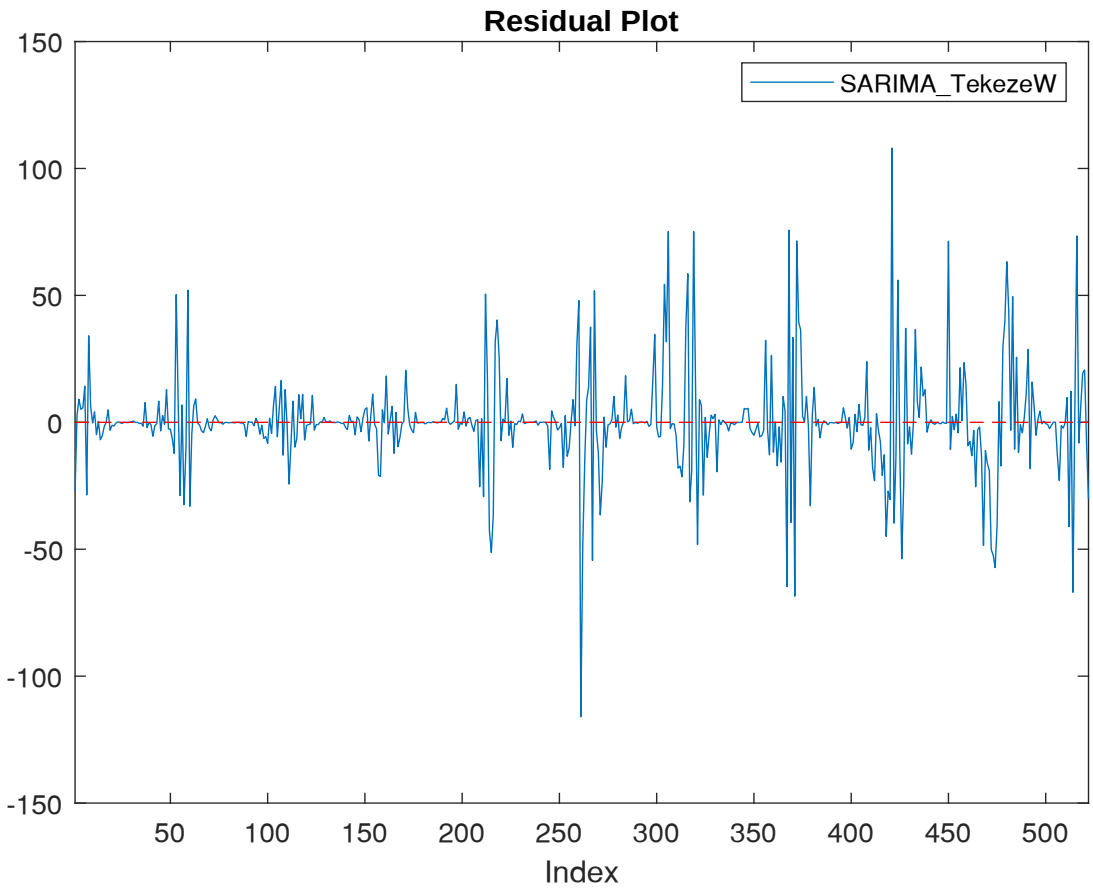

Figure 1.2. Plot of the residuals of model SARIMA_TekezeW

1.2. Residual Sample Autocorrelation Function

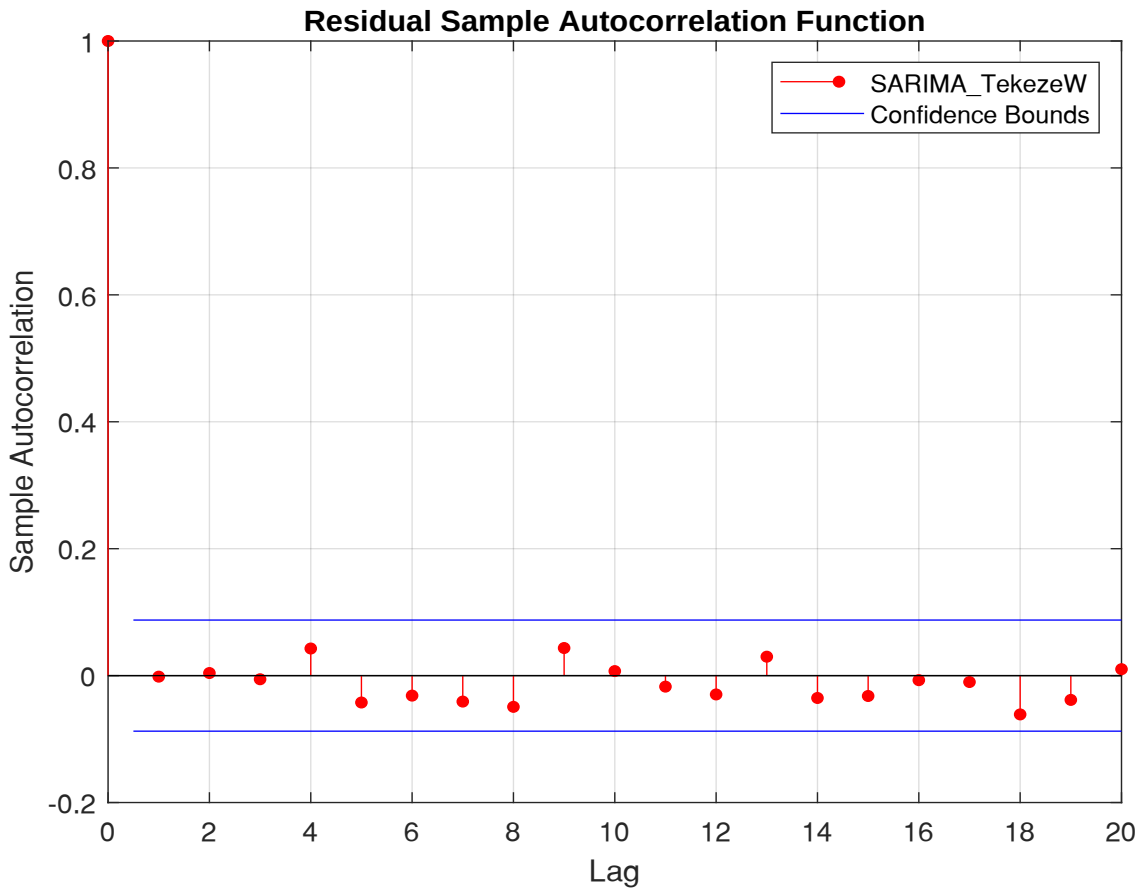

Figure 1.3. Sample autocorrelation function of the residuals of SARIMA_TekezeW

1.3. Ljung-Box Q-Test

Null Hypothesis: The first m autocorrelations of the residuals of SARIMA_TekezeW are jointly 0

$$H_0 : \rho_1 = \rho_2 = ... = \rho_m = 0$$

$$H_a : \rho_j \neq 0, \ j \in 1, ..., m$$

Table 1.3. Test Parameters

	Lags	DOF	Significance Level
1	20	20	0.05

Table 1.4. Test Results

	Null Rejected	P-Value	Test Statistic	Critical Value
1	false	0.94664	10.984	31.4104

1. ARIMA(3,0,0) Model Seasonally Integrated with Seasonal AR(156) (Gaussian Distribution) (SARIMA_KokaW)

Seasonal ARIMA model of time series KokaW with the following equation:

$$(1 - \phi_1 L - \phi_2 L^2 - \phi_3 L^3)(1 - \Phi_{52} L^{52} - \Phi_{104} L^{104} - \Phi_{156} L^{156})(1 - L^{52}) y_t \ = \ \varepsilon_t$$

1.1. Model Estimation

Table 1.1. Estimation Results

Parameter	Value	StandardError	TStatistic	PValue
Constant	0	0		
AR{1}	0.191	0.038523	4.9582	7.1158e-07
AR{2}	-0.03658	0.037759	-0.96876	0.33266
AR{3}	0.01844	0.043483	0.42408	0.67151
SAR{52}	-0.8793	0.036744	-23.9308	1.4659e-126
SAR{104}	-0.7847	0.037407	-20.9773	1.0565e-97
SAR{156}	-0.62204	0.030492	-20.4003	1.6632e-92
Variance	29.7521	1.0264	28.9877	9.3896e-185

Table 1.2. Goodness of Fit

AIC	3266.4654
BIC	3292.644

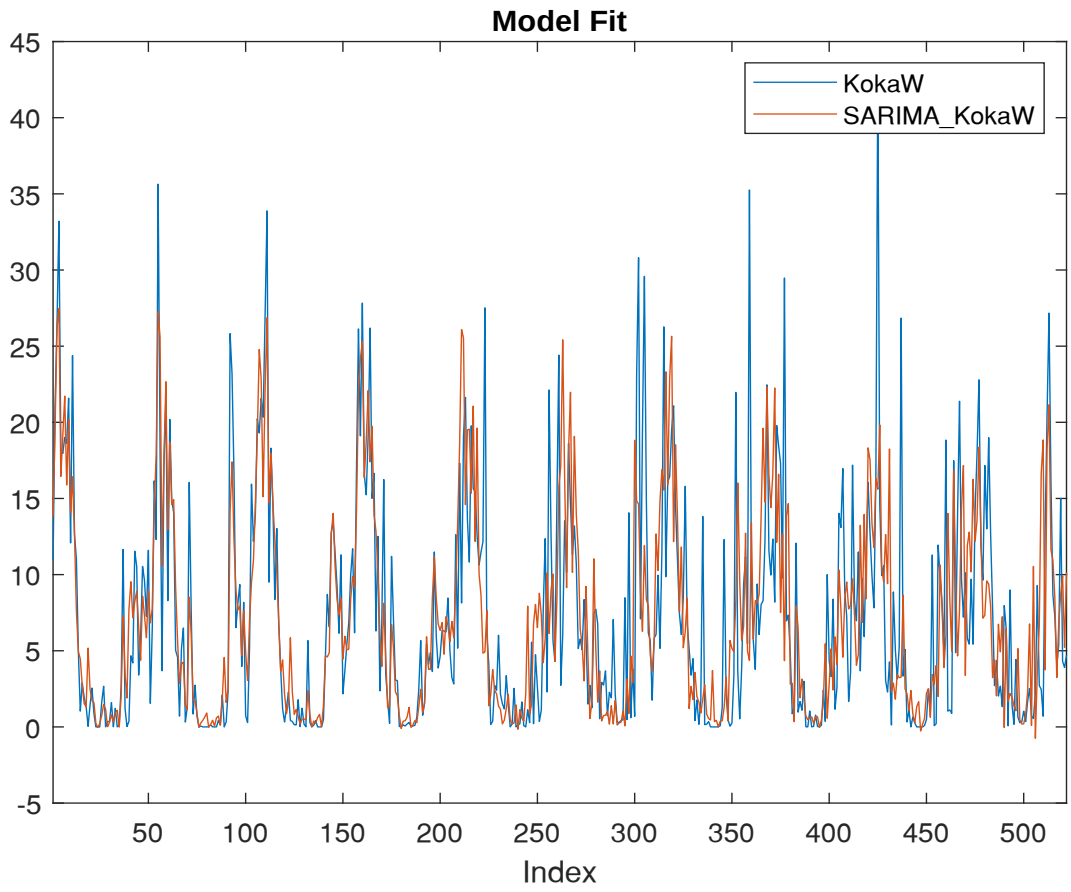

Figure 1.1. Plot the fit of model SARIMA_KokaW time series KokaW

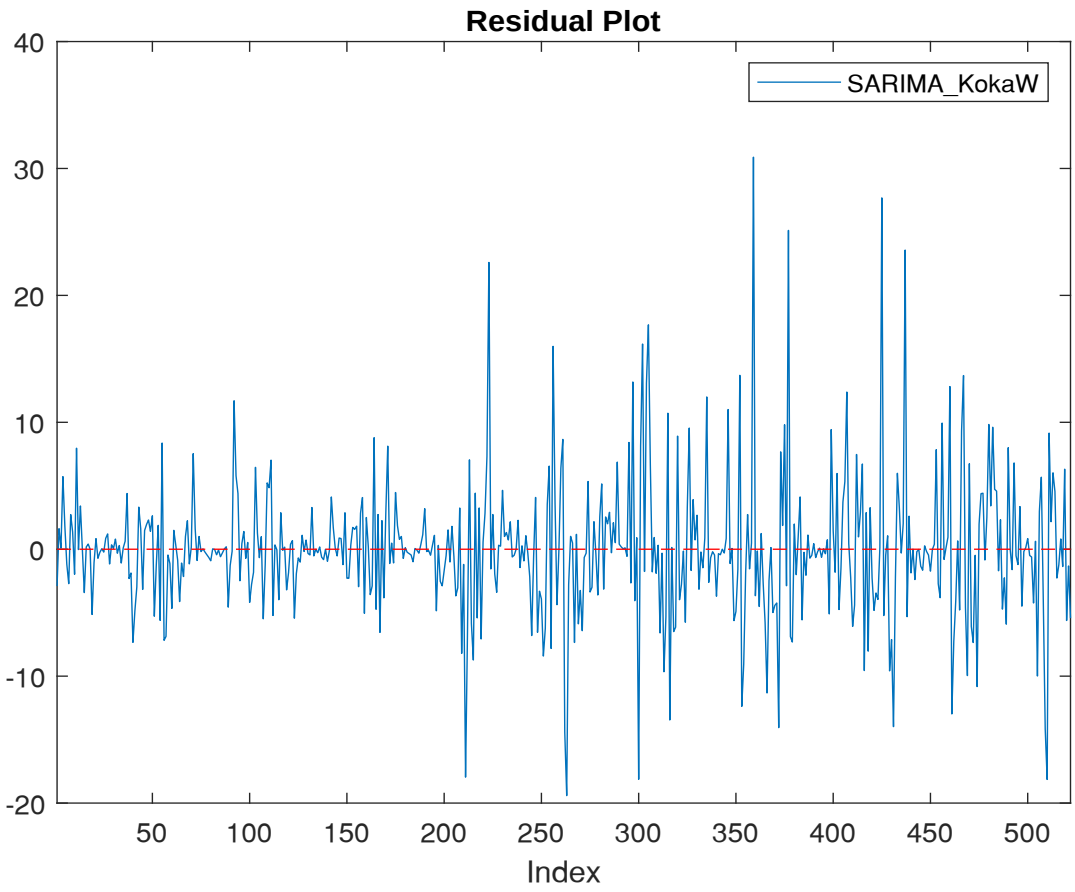

Figure 1.2. Plot of the residuals of model SARIMA_KokaW

1.2. Residual Sample Autocorrelation Function

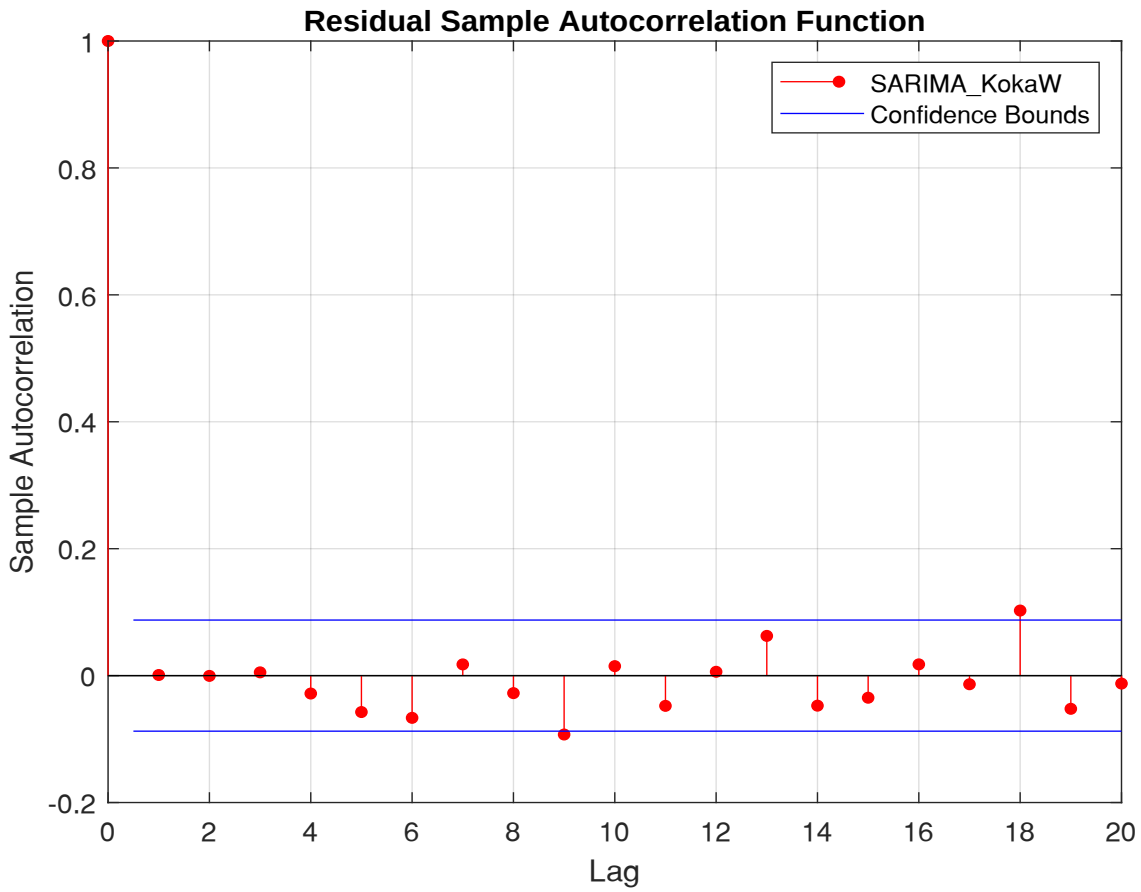

Figure 1.3. Sample autocorrelation function of the residuals of SARIMA_KokaW

1.3. Ljung-Box Q-Test

Null Hypothesis: The first m autocorrelations of the residuals of SARIMA_KokaW are jointly 0

$$H_0 : \rho_1 = \rho_2 = ... = \rho_m = 0$$

$$H_a : \rho_j \neq 0,\ j \in 1, ..., m$$

Table 1.3. Test Parameters

	Lags	DOF	Significance Level
1	20	20	0.05

Table 1.4. Test Results

	Null Rejected	P-Value	Test Statistic	Critical Value
1	false	0.31078	22.5625	31.4104